

KADIR HAS UNIVERSITY
GRADUATE SCHOOL OF SCIENCE AND ENGINEERING



IN SILICO DESIGN AND MODELING OF COUMARIN
DERIVATIVES AS SELECTIVE MONOAMINE OXIDASE A
INHIBITORS

GRADUATE THESIS

DİLARA KARAMAN

May, 2014

Dilara Karaman

M.S. Thesis

2014

IN SILICO DESIGN AND MODELING OF COUMARIN
DERIVATIVES AS SELECTIVE MONOAMINE OXIDASE A
INHIBITORS

DİLARA KARAMAN

Submitted to the Graduate School of Science and Engineering in partial fulfillment
of the requirements for the degree of
Master of Science
In
COMPUTATIONAL BIOLOGY AND BIOINFORMATICS

KADIR HAS UNIVERSITY
May, 2014

KADIR HAS UNIVERSITY
GRADUATE SCHOOL OF SCIENCE AND ENGINEERING

IN SILICO DESIGN AND MODELING OF COUMARIN
DERIVATIVES AS SELECTIVE MONOAMINE OXIDASE A
INHIBITORS

DİLARA KARAMAN

APPROVED BY:

Prof.Dr. Kemal Yelekçi(Advisor)



Prof. Dr. Safiye Sağ Erdem



Asst. Prof. Dr. Hatice Bahar Şahin



APPROVAL DATE: 22/May/2014

IN SILICO DESIGN AND MODELING OF COUMARIN DERIVATIVES AS SELECTIVE MONOAMINE OXIDASE A INHIBITORS

Abstract

Selective and reversible inhibition of Monoamine Oxidase (MAO) isoenzymes has an important place in treatment of various neurological disorders. Out of the two isoforms of Monoamine Oxidase enzymes, inhibition of MAO-A have been giving positive results in treatment of depression, and inhibition of MAO-B in cure of Parkinson's disease. The difference in treatment is due to the fact that these two enzymes have different substrate specificities.

In this study, 125 different coumarin derivatives were designed by adding 5 different side groups to 3rd, 5th, 7th positions of coumarin nucleus. These coumarin derivatives were tested in terms of affinity to MAO enzymes by using computational methods in silico. Using AutoDock4.2 docking software's results, we have found that most of these derivatives had affinity for both MAO-A and MAO-B enzymes at nanomolar and micromolar levels. At the same time we have seen that the coumarin derivatives had more inhibition properties with MAO-A. Binding properties of each the best five derivatives for MAO-A and MAO-B were examined comprehensively by using Accelrys Discovery Studio software. According to these results, M123 ligand might be the best coumarin derivative in the 125 ligands, because M123 ligand was the best second inhibitor and the most selective inhibitor. Other results from this study showed that, while using phenyl as side group increased the selectivity, using of phenyl and bromine increased the affinity to MAO-B but also decreased the selectivity. This study demonstrates that coumarin derivatives having particular phenyl at 7th position are effective at the MAO-A inhibition and coumarin derivatives that will be improved in this direction may be candidates in treatment of depression.

Key words: modelling, coumarin, monoamine oxidase, in silico design

KUMARİN TÜREVLERİNİN SEÇİCİ VE GERİ DÖNEBİLİR MONOAMİN OKSİDAZ-A İNHİBİTÖRLERİ OLARAK TASARLANMASI VE MODELLENMESİ

Özet

Monoamin oksidaz (MAO) izoenzimlerinin seçici ve geri dönebilir inhibisyonu, çeşitli nörolojik hastalıkların tedavisinde önemli bir yere sahiptir. Monoamin oksidaz enzimlerinin iki izoformu içinde MAO-A inhibisyonu depresyonun tedavisinde, MAO-B inhibisyonu ise Parkinson hastalığının tedavisinde olumlu sonuçlar vermektedir. Bu iki enzim farklı substrat özgünlüklerine sahiptir.

Bu çalışmada, kumarin çekirdeğinin 3'üncü, 5'inci ve 7'nci pozisyonlarına 5 farklı yan grup eklenerek 125 farklı kumarin türevi tasarlandı. Bu türevler hesaplamalı yöntemler ile *in silico* ortamda MAO enzimlerine uygunlukları açısından test edildiler. AutoDock4.2 programının sonuçlarına göre bu türevlerin çoğu hem MAO-A hem de MAO-B enzimlerine nanomolar ve mikromolar düzeyde afiniteye sahip olduğu gözlemlendi. Aynı zamanda bu kumarin türevlerinin MAO-A ile daha iyi inhibisyon özelliklerine sahip olduğu görüldü. En iyi beşer ligandın MAO-A ve MAO-B ile bağlanma özellikleri Accelrys Discovery Studio programı kullanılarak detaylı şekilde incelendi. Bu sonuçlara göre M123 ligandı bu 125 ligand içinde en iyi kumarin türevi olabilir çünkü M123 ligandı MAO-A için en iyi ikinci inhibitör ve en seçici inhibitördü. Bu çalışmadan çıkan diğer sonuçlar da düşünüldüğünde yan grup olarak fenil kullanılması seçiciliği arttırırken, fenil ve brom kullanılması MAO-B'ye ilgiyi arttırıyor ancak seçicilik de azalıyor. Bu çalışma, kumarin türevlerinin özellikle 7. pozisyonda fenil bulunması durumunda MAO-A inhibisyonunda etkili olduğu ve bu yönde geliştirilecek kumarin türevlerinin depresyon tedavisinde kullanılmaya aday olabileceğini göstermektedir.

Anahtar kelimeler: modelleme, kumarin, monoamine oksidaz, *in silico* tasarım

Acknowledgement

Firstly, thanks to my golden advisor Prof. Dr. Kemal Yelekçi who inoculated hope into me when I had lost all my belief on occurring of this thesis and he leaded me perfectly. It was a perfect light for me his correctness and assiduity. Apparently he improved this study facility in Kadir Has University to us by supporting materially.

I'm full of gratitude for great helping of Serkan Altuntaş, who is second advisor and my teachers and my friends for their unforgettable helps during lessons.

I'm very thankful to Dr. Hatice Bahar Şahin and Prof. Dr. Safiye Sağ Erdem for their valuable helps and fastidious reviews with a great attention and self-sacrifice.

Thanks to the remarkable person provided us to continue studying in Kadir Has University, Kadir Has University's esteemed General Secretary Fügen Çamlıdere who helped us immensely in our difficult times, gave tremendous support both in terms of emotional with continual encouragement and as material by giving fellowship, additionally a computer me to write this thesis and even meal opportunity in the University refectory. I believe that she is the most important supporter for all students in Kadir Has University.

Endless thanks to Meryem Yıldırım for her love and support.

To Prof. Dr. Metin Aktaş

Table of Contents

Abstract	i
Özet	ii
Acknowledgements	iii
Dedication	iv
Table of Contents	v
List of Tables	viii
List of Figures	ix
List of Abbreviations	xiii
1 Monoamine Oxidase Enzymes	1
1.1 Introduction.....	1
1.2 Related Disorders.....	2
1.3 General Structure of Monoamine Oxidase Enzymes.....	4
1.4 Structural Properties of MAO Isoenzymes.....	6
1.5 Effects of MAO Isoenzymes on Neurotransmitters.....	9
1.6 Amine Catalysis Reaction of MAO Isoenzymes.....	10
1.7 Monoamine Oxidase Inhibitors.....	11
2 Properties of Human Monoamine Oxidase Genes	14
2.1 Introduction.....	14
2.2 <i>MAOA</i> Gene.....	15
2.2.1 Positional Properties of <i>MAOA</i> Gene.....	15
2.2.2 Expression of <i>MAOA</i> Gene.....	16
2.2.3 Disorders Related to <i>MAOA</i> Gene.....	18
2.3 <i>MAOB</i> Gene.....	19
2.3.1 Positional Properties of <i>MAOB</i> Gene.....	19
2.3.2 Expression of <i>MAOB</i> Gene.....	21
2.3.3 <i>MAOB</i> Gene Related Disorders.....	23

3	Coumarin Derivatives	24
3.1	The Potential Behind of Vanilla Smell.....	24
3.2	Chemical and Structural Properties of Coumarin	25
3.3	Toxic Effects of Coumarin.....	26
3.4	Founding of Coumarins in Natural Products and Artificial Synthesis.....	27
3.5	Classification of Coumarin Derivatives.....	29
3.6	Effects of Coumarin Derivatives on MAO Enzymes.....	31
3.7	Other Medical Effects of Coumarin Derivatives.....	33
	3.7.1 Antioxidant Activity.....	33
	3.7.2 Anti-inflammatory Effects of Coumarins.....	34
	3.7.3 Roles of Coumarin in Treatment of High Protein Edema...34	
	3.7.4 Anti-tumor Activity.....	35
	3.7.5 Coumarin in Leukemia.....	35
	3.7.6 Chromone and Coumestan Derivatives	
4	Material and Methods	36
4.1	Introduction.....	36
4.2	Preparation of Ligands.....	37
4.3	Preparation of Proteins	38
4.4	Docking Study of Coumarin Derivatives with MAO-A and MAO-B.....	39
4.5	Molecular Modeling.....	59
4.6	Molecular Mechanics.....	59
4.7	The Environment in the Molecular Modeling.....	60
4.8	Application Areas.....	61
4.9	AutoDock 4.2.....	61
4.10	Equations.....	62
5	Results and Discussion	64
5.1	Introduction.....	64
5.2	Docking Results	71
5.3	Evaluation of M029 Ligand with MAO-A Enzyme.....	75
5.4	Evaluation of M029 Binding Properties for MAO-B.....	77
5.5	Evaluation of M109 Ligand with MAO-A Enzyme.....	79
5.6	Evaluation of M109 Ligand with MAO-B Enzyme.....	82

5.7	Evaluation of Binding Properties between Compound M115 and MAO-A Enzyme	84
5.8	Evaluation of M115 and MAO-B Binding Properties.....	86
5.9	Evaluation of M118 Ligand and MAO-A Enzyme Binding Properties.....	88
5.10	Evaluation of M118 Ligand Position in the MAO-B Enzyme....	90
5.11	Evaluation of Ligand M123 and MAO-A Enzyme Binding Properties.....	93
5.12	Evaluation of Compound M123 and MAO-B Binding Properties.....	95
5.13	Evaluation of M106 Ligand with MAO-B Enzyme Complex....	97
5.14	Evaluation of M061 Ligand with MAO-B Enzyme Active Site..	99
5.15	Evaluation of M101 Ligand and MAO-B Enzyme Binding Properties.....	101
5.16	Evaluation of M122 Ligand and MAO-B Enzyme Binding Properties.....	103
6	Conclusion	106
	References	109
	Curriculum Vitae	119

List of Tables

Table 1.1	MAO inhibitors	11-12
Table 2.1	<i>MAOA</i> gene mRNA products	17
Table 2.2	<i>MAOB</i> gene mRNA products	21
Table 3.1	Common natural coumarin derivatives	29
Table 3.2	Examples of coumarin sub-types	30
Table 4.1	2-D Structures of 125 coumarin derivatives	46-58
Table 5.1	Ki and free binding energy values of 125 ligands for MAO enzymes	72-74

List of Figures

Figure 1.1 Monoamine Oxidase A secondary structure.....	4
Figure 1.2 Monoamine Oxidase B secondary structure	4
Figure 1.3 Hydrophobicity graphic of MAO-A enzyme's amino acids	5
Figure 1.4 Hydrophobicity graphic of MAO-B enzyme's amino acids	5
Figure 1.5 3-D representation of FAD coenzyme and its interactions with MAO-B	6
Figure 1.6 Superimpose of MAO isoenzymes.	7
Figure 1.7 Hydrophobic binding sites.	8
Figure 1.8 MAO-A enzyme 3-D representation.	8
Figure 1.9 MAO-B enzyme 3-D representation	9
Figure 1.10 3-D representation of neurotransmitters related to MAO enzymes.....	10
Figure 1.11 Oxidation of amines by MAO-bound FAD	11
Figure 1.12 Molecular 3-D structures of inhibitors.	13
Figure 2.1 <i>MAOA</i> cytogenetic location on chromosome Xp11.3.....	15
Figure 2.2 <i>MAOA</i> gene's exons map.	16
Figure 2.3 Transcription factors and their binding sites in <i>MAOA</i> gene promoter.	16
Figure 2.4 <i>MAOA</i> estimated expression levels on different tissues and blood.....	17
Figure 2.5 <i>MAOB</i> gene location on P arm of X chromosome	19
Figure 2.6 <i>MAOB</i> exons map	20
Figure 2.7 Transcription factors and their binding sites in <i>MAOB</i> gene promoter.	21
Figure 2.8 <i>MAOB</i> estimated expression levels on different tissues and blood.....	22
Figure 3.1 Coumarin 3-D structure with Vanilla flowers	24

Figure 3.2 Rings in coumarin (C ₉ H ₆ O ₂).....	25
Figure 3.3 Perkin coumarin synthesis reaction.	27
Figure 3.4 Penchmann coumarin synthesis	28
Figure 3.5 Palladium-catalyzed oxidative cyclocarbonylation reaction of 2-vinylphenols.....	28
Figure 3.6 Scaffold for natural coumarin derivatives.....	29
Figure 3.7 3-D structure of 3,4-Benzo-7-(6-bromoallyloxy)-8- methylcoumarin.....	31
Figure 3.8 3-D representation of resveratrol-coumarin hybrid compounds.	32
Figure 3.9 7-Oxycoumarin derivative	33
Figure 3.10 3-D structure of an anti-inflammatory coumarin derivative.....	34
Figure 4.1 Coumarin scaffold	37
Figure 4.2 Atoms' positions in isoalloxazine ring of FAD	39
Figure 4.3 Grid box options to adjust grid parameter (left), AutoDock4.2 grid box performing (right).	40
Figure 4.4 AutoDock 4.2 molecular graphics.....	61
Figure 5.1 K _i values of the best 25 ligands for MAO-A enzyme	65
Figure 5.2 K _i values of the best 26-50 ligands for MAO-A enzyme.	65
Figure 5.3 pK _i values of the best 25 ligands for MAO-A enzyme	66
Figure 5.4 Comparison of K _i values of 25 ligands had the best results for MAO-A enzyme	67
Figure 5.5 Representation of selectivity index (SI) of first the best 25 ligands for MAOA.	68
Figure 5.6 The best 25 ligands' K _i values for MAO-B enzyme.	69
Figure 5.7 The best 26-50 ligands' K _i values for MAO-B enzyme	69
Figure 5.8 pK _i values of the best 25 ligands for MAO-B enzyme	70
Figure 5.9 2-D representation of the placing of M029 in MAO-A binding site	75
Figure 5.10 3-D representation of M029 with MAO-A.....	76
Figure 5.11 2-D representation of M029 ligand's position in MAO-B enzyme	78
Figure 5.12 3-D representation of M029' position in MAO-B enzyme.....	79
Figure 5.13 2-D representation of compound M109 and amino acids placing in binding site of MAO-A enzyme	80

Figure 5.14	3-D representation of M109 ligand and MAO-A enzyme.	81
Figure 5.15	2-D representation of compound M109 and amino acids placing in binding site of MAO-B enzyme.....	82
Figure 5.16	3-D representation of M109 ligand and amino acids placing active site of MAO-B enzyme.....	83
Figure 5.17	2-D representation of M115 ligand and MAO-A enzyme's amino acids position in the active site.....	84
Figure 5.18	3-D representation of compound M115 and MAO-A enzyme.	85
Figure 5.19	M115 ligand and MAO-B enzyme binding properties 2-D representation.	86
Figure 5.20	3-D representation of M115 ligand and MAO-B enzyme binding properties.....	87
Figure 5.21	2-D representation of ligand M118 and MAO-A enzyme active site.....	88
Figure 5.22	3-D representation of M118 and MAO-A enzyme.	89
Figure 5.23	2-D representation of M118 ligand and MAO-B's amino acids in the active site	90
Figure 5.24	3-D representation of compound M118 and MAO-B active site	91
Figure 5.25	3-D representations of valence electrons of M118 with MAO-B active site	92
Figure 5.26	2-D representation of M123 ligand and MAO-A enzyme	93
Figure 5.27	3-D representation of M123 ligand and MAO-A enzyme's active site.....	94
Figure 5.28	2-D representation of M123 ligand and MAO-B enzyme's related amino acids.....	95
Figure 5.29	3-D representation of M123 ligand and MAO-B enzyme positions.	96
Figure 5.30	2D representation of M106 ligand and MAO-B binding site ...	97
Figure 5.31	3-D representation of compound M106 and MAO-B enzyme's binding site amino acids.....	98
Figure 5.32	2-D representation of M061 ligand and MAO-B enzyme	99
Figure 5.33	3-D representation of M061 ligand and MAO-B enzyme	100
Figure 5.34	2-D representation of compound M101 and MAO-B enzyme.	101

Figure 5.35 M101 ligand and MAO-B binding position 3-D representation	102
Figure 5.36 M122 ligand and MAO-B enzyme binding properties 2-D representation	103
Figure 5.37 3-D representation of compound M122 and MAO-B enzyme.	104

List of Abbreviations

MAO	Monoamine Oxidase
MAOA	Monoamine Oxidase A
MAOB	Monoamine Oxidase B
ADMET	Absorption, Distribution, Metabolism, Excretion, Toxicity
PD	Parkinson 's Disease
AD	Alzheimer's Disease
FAD	Flavin Adenine Dinucleotide
VNTR	Variable Number Tandem Repeat
3-D	Three Dimensional
2-D	Two Dimensional
5-HT	Serotonin
MPTP	1-methyl-4-phenyl,1,2,3,6-tetrahydropyridin
NA	Norepinephrine
ADHD	Attention-Deficit/Hyperactivity Disorder
PARK2	Parkin RBR E3 Ubiquitin Protein Ligase
ERR	Estrogen-Related Receptors
TDI	Tolerable Daily Intake
LD50	Lethal Dose, 50%
PDB	Protein Data Bank

Chapter 1

Monoamine Oxidase Enzymes

1.1 Introduction

A healthy nervous system is the most valuable property that a person has got. Some disorders characterized with malfunction and damages in the nervous system are depression, Parkinson's disease (PD) and Alzheimer's disease [1, 2, 3, 4, 5]. These disorders had been studied extensively, numerous medicines had been improved. Selective and reversible inhibitors of Monoamine Oxidase (MAO) isoenzymes are promising methods in treatment of these disorders.

Since high amount of expenditures are made to synthesize compounds with drug potential and to search their ADMET properties, prediction of binding properties of inhibitors to protein and pre-selection through candidates have an important place in decreasing the expenditures and load of work.

Previous studies providing information about the most available scaffold models can be used for MAO enzymes. Recent studies [6, 7, 8, 9, 10] provides scaffolds of coumarin. In this study 125 different coumarin derivatives were tested with MAO-A and MAO-B enzymes and compared for their inhibitor properties.

In the first chapter, general properties of MAO isoenzymes, reaction mechanism of MAO enzyme and some MAO inhibitors' chemical structures and their effects on MAO enzymes were presented.

In the second chapter, genetic structures and expression properties of MAO isoenzymes were summarized.

In the third chapter, an overview of coumarin's properties, synthesis reactions and known properties of effects on MAO isoenzymes of coumarin derivatives and inhibition effects were given.

In the fourth chapter, material and method used in the design of coumarin derivatives, and calculation methods were presented.

In the fifth chapter, binding properties obtained from the result of docking studies, comparison of energy values and K_i values, and representation of interactions of the best ligands with MAO-A and MAO-B enzymes were outlined.

1.2 Related Disorders

Monoamine Oxidase is one of known targets for many neurological disorders [4]. Abnormal activation or level of MAO enzymes in humans leads to depression, hyperactivity, schizophrenia, irregular sexual maturation and other diseases [5].

Parkinson's disease (PD) is an age-related neurodegenerative disease where loss of

striatal-projecting dopaminergic neurons in the substantia nigra leads to the characteristic symptoms [2]. There are several mechanism causing PD.

Alzheimer is also age-related but caused by misfolding of beta amyloid proteins forming senile plaques in the brain [3], however as PD, Alzheimer may be result of multifactor. Consequently in Alzheimer disease brain structure and functions are affected negatively.

Another related disease to MAO enzymes is Schizophrenia is direct cause to psychiatric disorder. Although it cannot be said that polymorphism to schizophrenia, some polymorphism studies showed that there can be a correlation between *MAOA* and *MAOB* genes polymorphism (uVNTR and rs1137070 on *MAOA* and rs1799836 on *MAOB* genes) and schizophrenia. But more comprehensive studies on this topic are needed [11].

Depression is a neurological disorder might depend on environmental stress factors and hormonal modulator for instance reducing level of serotonin (5-HT) in neural system cause lower brain function. Since MAO-A enzyme catalyzes the serotonin, high MAO-A activity or increased number of MAO-A enzyme might involve in depression disorder [12].

1.3 General Structure of Monoamine Oxidase Enzymes

MAO (Monoamine oxidase) is a flavoenzyme which exists in all mammalian tissues, placed at the outer membrane of mitochondria as an integral protein. MAO isoenzymes have two isoforms: MAO-A and MAO-B [1].

MAO-A consists of 527 amino acids, MAO-B consists of 520 amino acids [13]. Considering their secondary structures, they are very similar in domain structure. Figure 1.1 and Figure 1.2 show the secondary structures. As seen in the figures, particularly the first 50 residues are very similar, and they have helix structures between 120-225 residues and β -strand structures between 60-110 residues and 265-400 residues intensively.

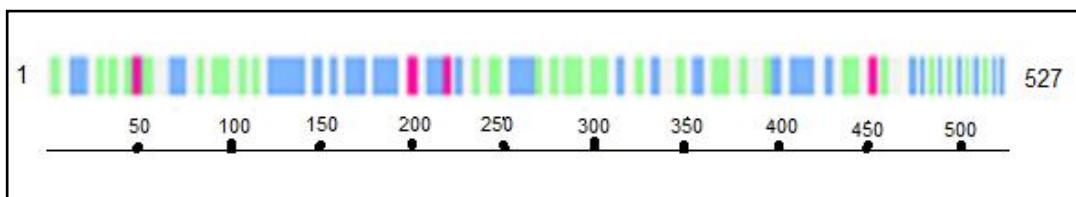


Figure 1.1: Monoamine Oxidase A secondary structure [14]. Blue lines point to helix, green lines to strand, pink lines to turn. Structure is taken from Uniprot website. Scale is generated via Paint.

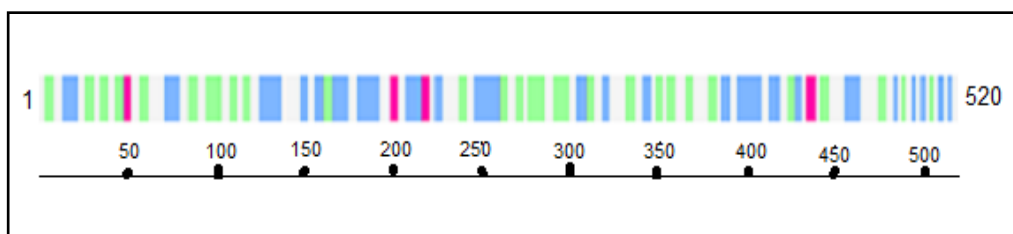


Figure 1.2: Monoamine Oxidase B secondary structure [15]. Blue lines point to helix, green lines to strand, pink lines to turn. Structure is taken from Uniprot website

The hydrophobicity is a property related to the solubility of an amino acid in water. Hydrophobic amino acids are localized in the interior of protein, and hydrophilic amino acids interact with the aqueous environment [16]. Figure 1.3 and Figure 1.4 show more hydrophobic regions of MAO isoenzymes.

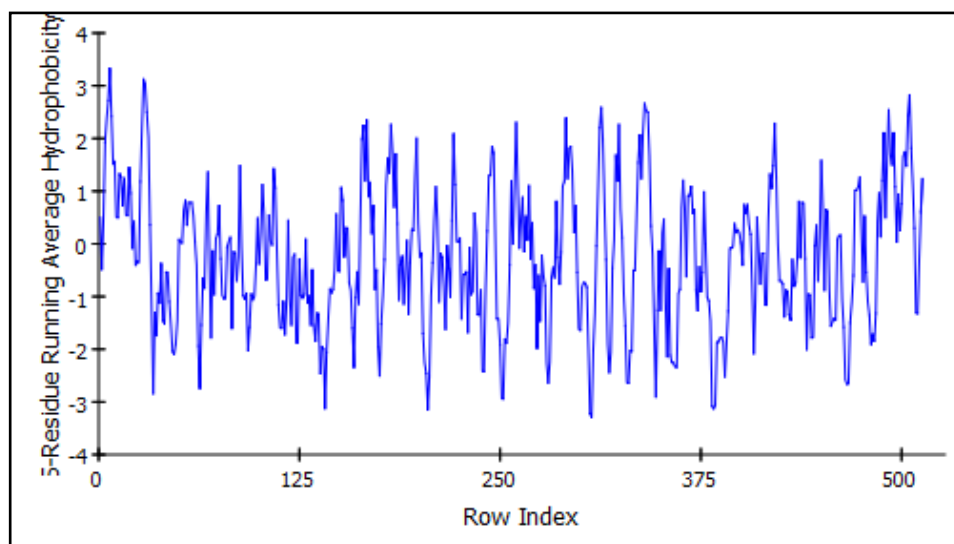


Figure 1.3: Hydrophobicity graphic of MAO-A enzyme's amino acids. Figure was drawn via Discovery Studio 3.5 Accelrys.

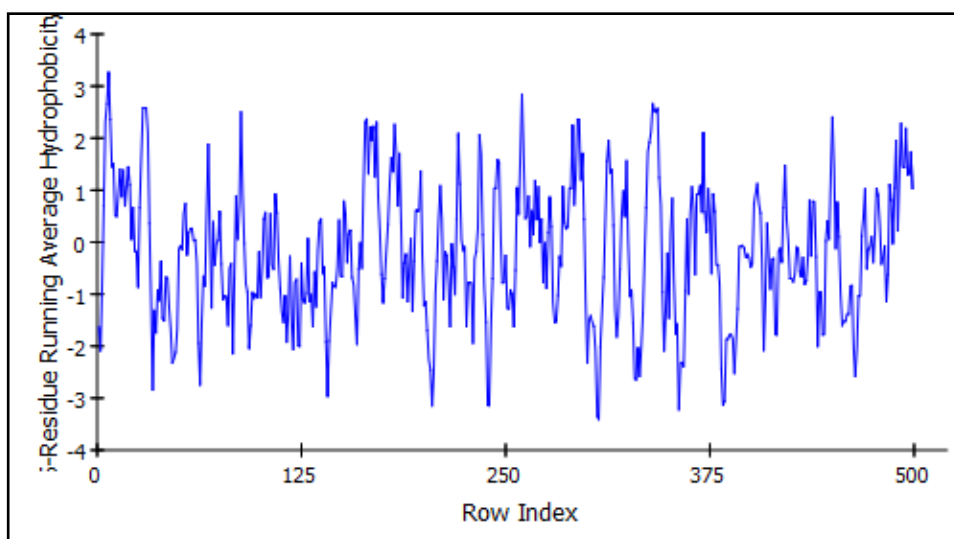


Figure 1.4: Hydrophobicity graphic of MAO-B enzyme's amino acids. Figure was drawn via Discovery Studio 3.5 Accelrys.

arrives to substrate-binding cavity. The volume of the MAO-A active site is $\sim 400 \text{ \AA}^3$ while the MAO-B active has $\sim 700 \text{ \AA}^3$ volume [18, 19].

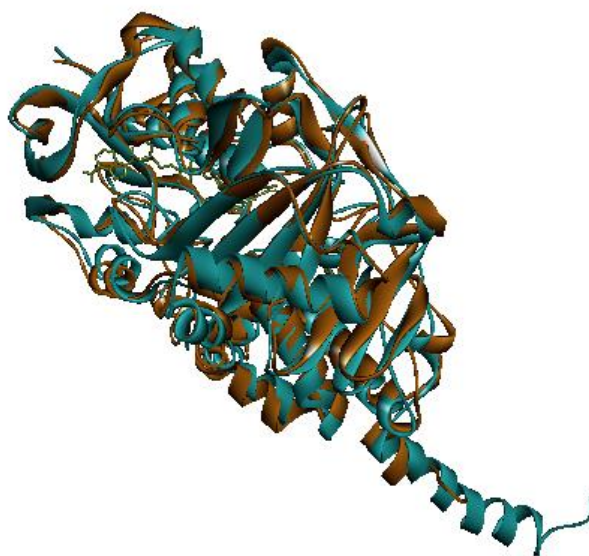


Figure 1.6: Superimpose of MAO isoenzymes. Blue structure represents MAO-A and orange structure represents MAO-B enzyme. Superimpose generated via Accelrys.

As seen in Figure 1.7, both isoenzymes have hydrophobic binding sites. While the MAO-A active site is a single cavity, the MAO-B active site consists of an entrance cavity (300 \AA^3) which leads, from the surface of the enzyme, to the substrate cavity ($\sim 400 \text{ \AA}^3$) [18, 3]. Since MAO-A does not have an entrance cavity; substrate reaches directly to one cavity. Specifically their active regions show similar amino acid sequences [13]. The most important difference is in the cavity shaping loop of MAO-A between the residues 210-216. In MAO-B they are located between the residues 201-207 which shows that $C\alpha$ movement up to 6 \AA . Therefore MAO-A has wider aromatic cage than that of MAO-B taking into bulkier aromatic groups [20].

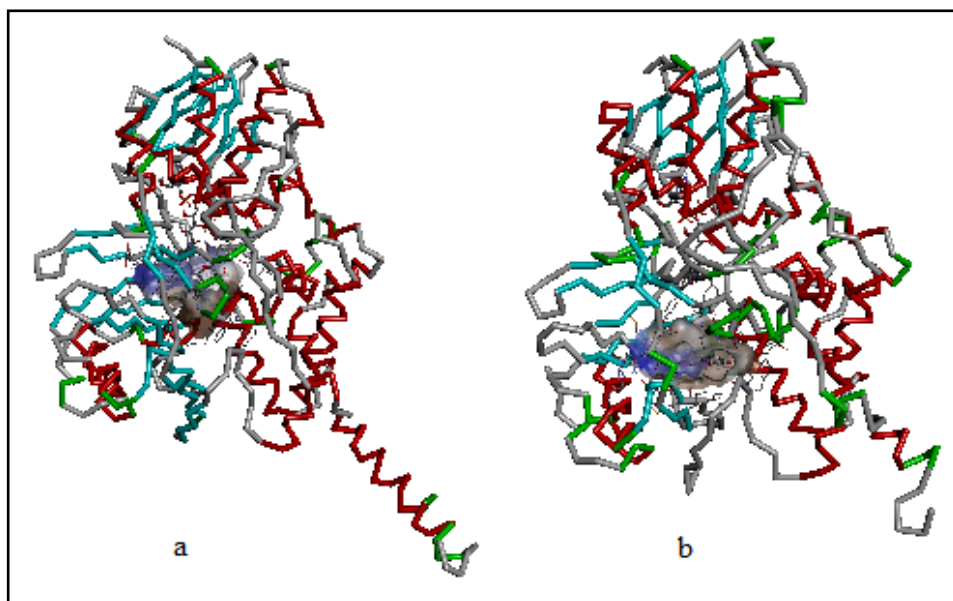


Figure 1.7: Hydrophobic binding sites. a) MAO-A , b) MAO-B enzymes. Blue surface represents lower and brown surface represents higher hydrophobicity.

Figure 1.8 shows 3-D shape of MAO-A enzyme and Figure 1.9 shows MAO-B enzyme.

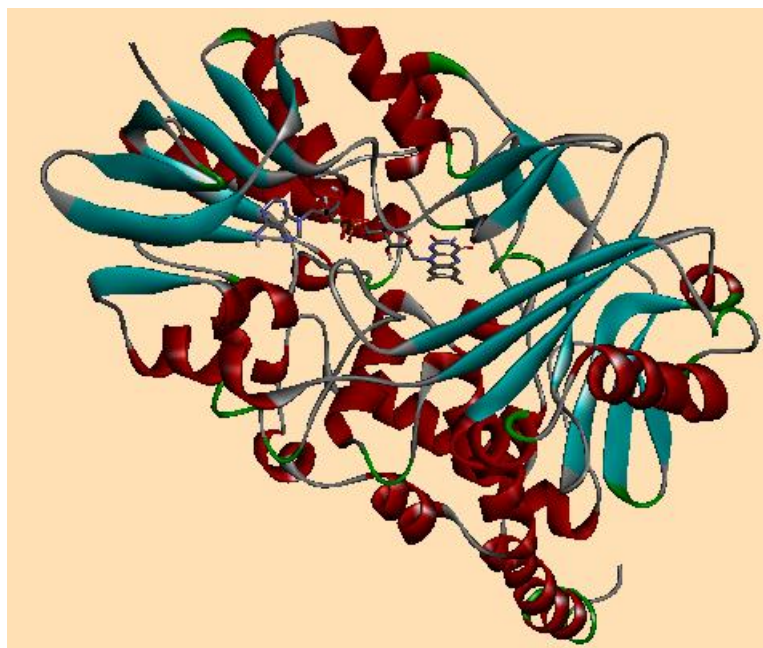


Figure 1.8: MAO-A enzyme 3-D representation.

Substrate cavity involves Ile180, Asn181, Phe208 and Ile335 residues in MAO-A and Leu171, Cys172, Ile199, Tyr325 in MAO-B. FAD coenzyme is surrounded by Tyr407, Tyr444 in MAO-A and Tyr398, Tyr435 in MAO-B [13, 21, 22, 23, 24].



Figure 1.9: MAO-B enzyme 3-D representation

The essential amino acids for ligand in MAO-A are 161st and 375th amino acids, as for MAO-B they are 152nd and 366th amino acids [13, 21, 22, 23, 24].

1.5 Effects of MAO Isoenzymes on Neurotransmitters

The neurotransmitters oxidized by MAO enzymes are dopamine, epinephrine, norepinephrine (NA), 1-methyl-4-phenyl,1,2,3,6-tetrahydropyridin (MPTP) and serotonin (5-HT). All these monoamines are responsible for changing myocardial function. Since heart tissues are affected by free radicals in the neural and hormonal system, the decrease of monoamines increases MAO-derived H₂O₂ production in heart tissue [25].

In the nervous system norepinephrine and serotonin oxidation is catalyzed with MAO-A enzyme, phenyl ethylamine and benzyl amine oxidation catalyzed with MAO-B. Dopamine, tyramine and tryptamine are non-selective substrates for MAO-A and MAO-B [26]. MAO-A is primarily responsible for the oxidation of tyramine (Figure 1.10). Therefore MAO-A's peripheral inhibition has been associated with the risk for an acute hypertensive syndrome known as the “cheese reaction” [27, 28].

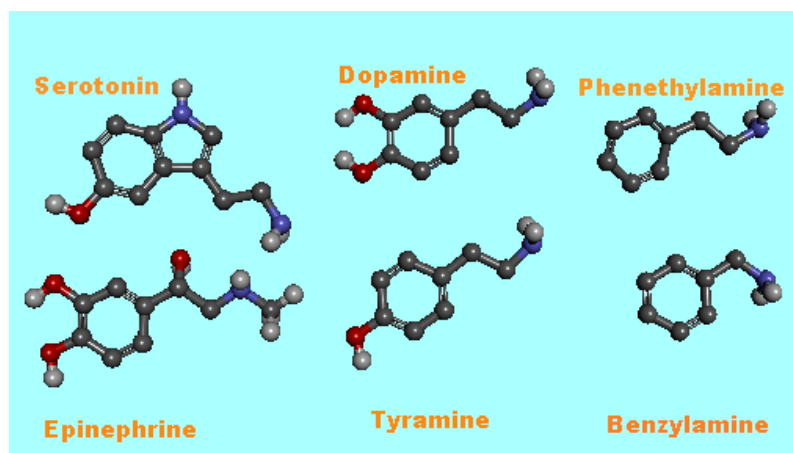


Figure 1.10: 3-D representation of neurotransmitters related to MAO enzymes

1.6 Amine Catalysis Reactions of MAO Isoenzymes

FAD (flavin adenine dinucleotide) is a redox cofactor in the reactions catalyzed by MAO (Figure 1.11) [29]. Monoamines are changed into related aldehydes with this reaction. The starting point is the breaking of C α -H bond. FAD reduced to FADH₂ and meanwhile amine is transformed to imine. In MAO reaction at the after step; when hydrogen peroxide is generated, FADH₂ is oxidized. Meanwhile imine hydrolyses to aldehyde and ammonia form. [30, 31, 32, 33, 11]

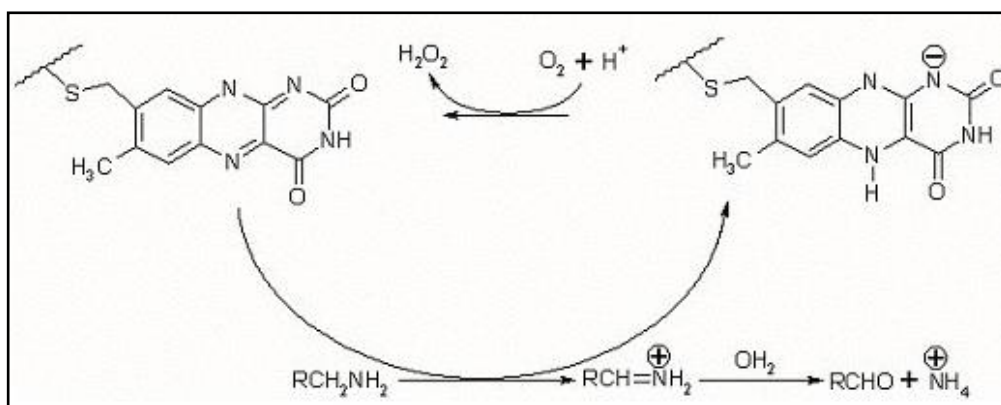


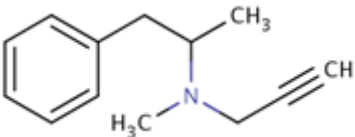
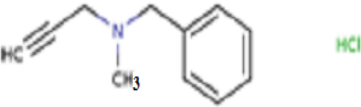
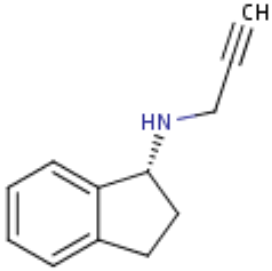
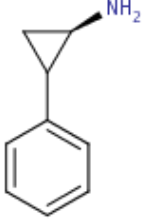
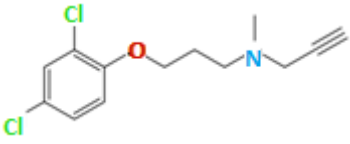
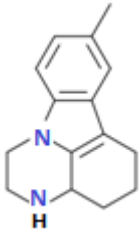
Figure 1.11: Oxidation of amines by MAO-bound FAD [29]

1.7 Monoamine Oxidase Inhibitors

MAO inhibitors are divided into two types as reversible or irreversible inhibitors. The first produced MAO inhibitors inhibit based on mechanism and they bind to proteins covalently [13]. These irreversible inhibitors have serious side effects like hallucination, schizophrenia and hypertension. Table 1.1 shows general MAO inhibitors' 2-D structures and their known properties against MAOs.

Table 1.1: MAO inhibitors

Structure of MAO Inhibitors	Medical Properties	Binding Properties
<p>Moclobemide</p>	Anti-depression	Reversible Selective MAO-A Inhibitor

 <p>Selegiline</p>	Anti-Parkinson	Irreversible Selective Inhibitor	MAO-B
 <p>Pargyline</p>	Anti-depression	Irreversible Selective Inhibitor	MAO-B
 <p>Rasagiline</p>	Anti-depression	Irreversible Selective Inhibitor	MAO-B
 <p>Tranylcypromine</p>	Anti-depression	Irreversible Nonselective Inhibitor	MAO-A
 <p>Clorgyline</p>	Anti-depression	Irreversible Selective Inhibitor	MAO-A
 <p>Pirlindole</p>	Anti-depression	Reversible Selective Inhibitor	MAO-A

Continuation of Table 1.1

Irreversible inhibitors have different mechanism than that of reversible inhibitors. Unknown selectivity of MAOIs causes lots of side effects as like hallucination, hypertension and hepatotoxicity [13].

As a new irreversible and selective MAO-B inhibitor Rasagiline, as a selective and reversible MAO-A inhibitor Harmine (Figure 1.12 (b)), as a reversible and selective MAO-B inhibitor Safinamide (Figure 1.12 (a)) [34, 35] are used.

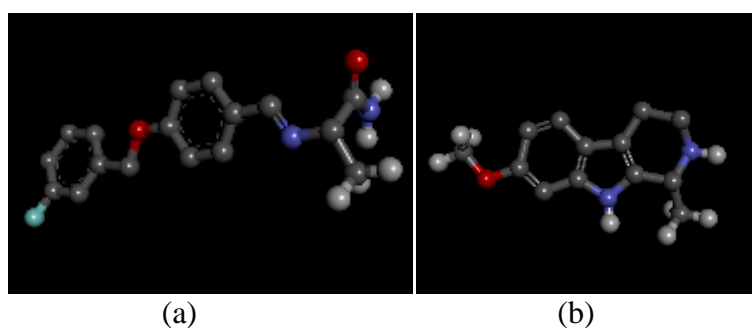


Figure 1.12: Molecular 3-D structures of inhibitors. (a) Safinamide, (b) Harmine. Turquoise ball represents Fluorine, red ball is Oxygen, navy blue ball is Nitrogen, grey ball is Carbon, white ball is Hydrogen atom.

Chapter 2

Properties of Human Monoamine Oxidase Genes

2.1 Introduction

MAO genes, that have common ancestral gene [3], lay side by side on the X chromosome. Males are affected directly because of *MAO* genes' inheritance condition, if they have mother carrying a *MAO* gene mutation.

Recent studies on *MAO* genes deficient mice show that both isoenzymes involve in a large spectrum of mental disorders, some of them are autism, anxiety, impulse-control disorders and ADHD [36].

Recent data shows that *MAOA* gene is related to 107 disorders and to *MAOB* gene is related to 59 disorders [37, 38]. When the excess of disorders is pointed out, it can be said that also *MAOA* and *MAOB* genes and protein function must be studied comprehensively.

Inheritance pattern of this gene creates an advantage for polymorphism studies on *MAO* genes and in observations of it during the generations.

2.2 MAOA Gene

MAOA gene is a member of a *MAOs* gene family being responsible for production Monoamine oxidase A enzyme which catalyzed monoamines. A mutation in this gene causes Brunner Syndrome that is characterized by non-dysmorphic mild mental retardation including disturbed regulation of impulsive aggression. Male patients are affected by borderline mental retardation and exhibit abnormal behavior, but female carriers have normal intelligence and behavior [39]. This gene has multiple transcript variants according to splicing process [40].

2.2.1 Positional Properties of *MAOA* Gene

MAO genes are placed in the p arm of X chromosome (Figure 2.1), so males inherit only a single maternal copy.

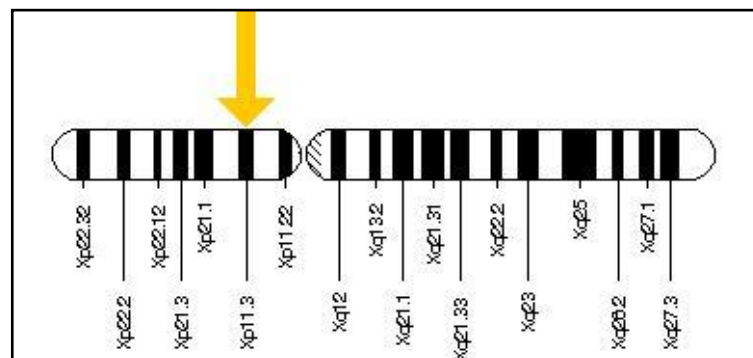


Figure 2.1: *MAOA* cytogenetic location on chromosome Xp11.3 [41]. Figure was taken from Genetics Human References website.

MAOA gene is located on the short arm of the X chromosome [42] at position p11.3.

MAOA gene had 8 exons and 1088 bp mRNA (Figure 2.2) [43] is between

43,654,906 to base pair 43,746,823 of X chromosome [42].

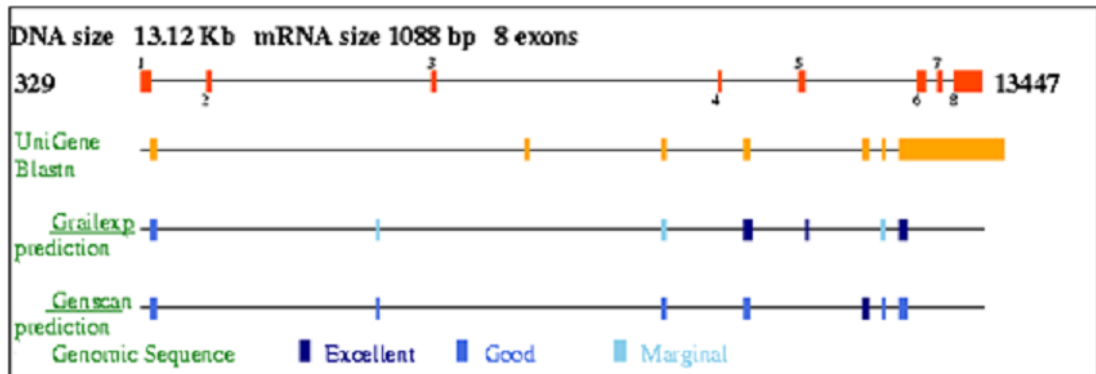


Figure 2.2: *MAOA* gene's exons map [43]. Figure was taken from Genatlas website.

2.2.2 Expression of *MAOA* Gene

MAOA gene is expressed with over 200 transcription factors [44]. Eight of them are shown in Figure 2.3 corresponding to their binding sites in this gene promoter.



Figure 2.3: Transcription factors and binding sites in *MAOA* gene promoter [44]. Figure was taken from Sabiosciences website.

This gene has 4 transcripts (Table 2.1) [40]. MAOA-001 is expressed at different levels on different tissues. Expression levels are shown in Figure 2.4.

Table 2.1: MAOA gene mRNA products [40]

	Length of nucleotide sequence (bp)	Length of protein	
MAOA-001	4015	527	Protein coding
MAOA-201	2383	394	Protein coding
MAOA-002	935	-	Processed transcript
MAOA-003	557	-	Processed transcript

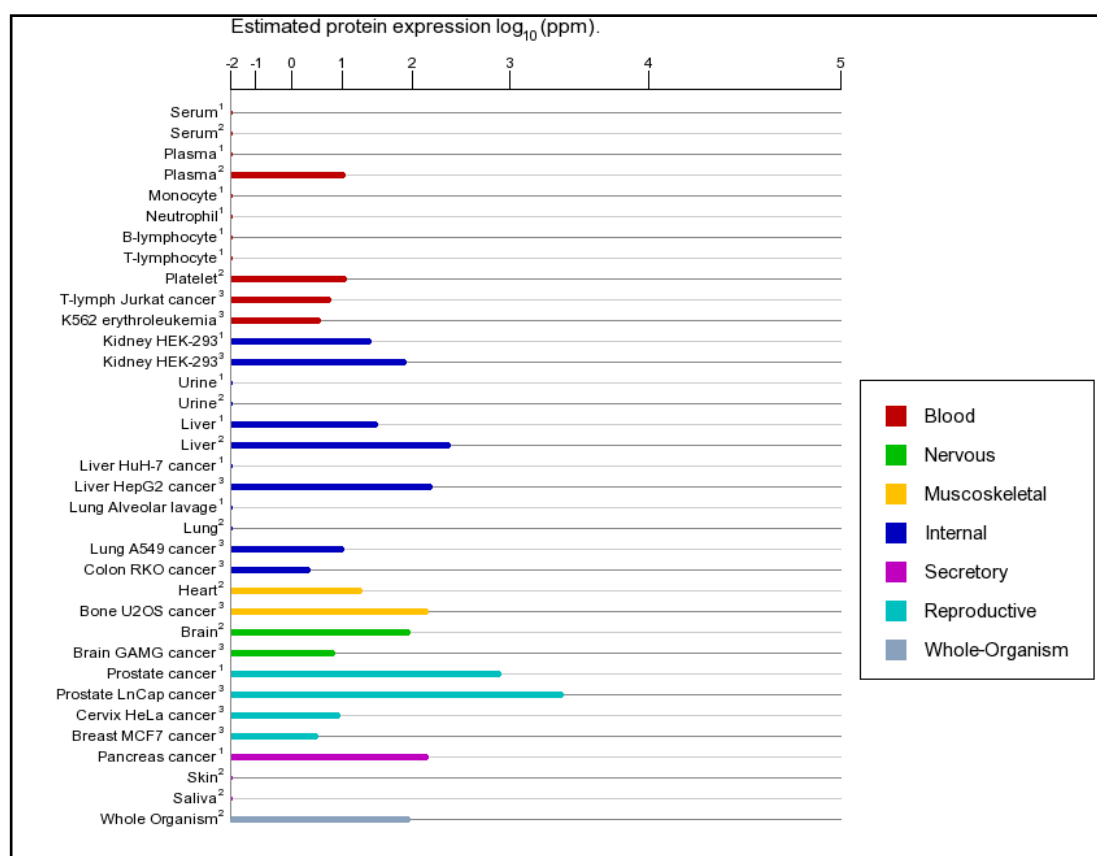


Figure 2.4: MAOA estimated expression levels on different tissues and blood [45]. Figure was taken from GeneCards website.

2.2.3 Disorders Related to *MAOA* Gene

MAOs play roles in several psychiatric conditions, including chronic stress, major depressive disorder and alcohol dependence [46]. 10 disorders from 107 disorders related to *MAOA* according to MalaCards [47] are; social phobia, substance abuse, paranoid schizophrenia, serotonin syndrome, borderline personality disorder, novelty seeking personality, hepatic encephalopathy, anxiety disorder, post-traumatic stress disorder, specific phobia.

Novel roles of *MAOA*, *MAOB* and serotonin are regulating of intermediate progenitor cells proliferation in the developing brain [48].

The over expression of protein in female causes panic disorders. The protein under expression causes lower platelet *MAOA* activity in children by ADHD (Attention-deficit/hyperactivity disorder), inattentive, and hyperactive changes than control children [49].

The *MAOA* gene was called as “warrior gene” after a study was done with Rhesus macaque monkeys [50]. When Rhesus monkeys had five and six repeat in the *MAOA* gene’s VNTR upstream, they had 1.3 fold overall activity than 7-repeat or more repeats [50]. On the other hand, different from human *MAOA* gene, if there are lower repeats in this gene, MAO-A enzyme is expressed at higher levels [50]. In fact that *MAOA* gene itself is not responsible for aggression. Therefore it is not a particular gene for psychiatric disorders had a direct relation with violence propensity [51].

Corresponding to a study was done by Sabol et al. (1997) there is a *MAOA* subtype

was related to transcriptional regulation had a 30 bp repeat polymorphism (MAO-A30bp-rpt) [52].

Looking into MAO-A30bp-rpt allele frequencies, it can be seen vary between ethnic groups worldwide [53].

Most of epidemiological studies on variants of MAO-A30bp-rpt revealed a correlation between MAO-A30bp-rpt and some disorders as like anxiety, depression, and addiction (for example alcoholism). Some studies related to the 3-repeat allele of MAO-A30bp-rpt, alleged without being based on clear data that lower MAO-A activity and higher dopamine levels are related with risk-taking [53, 54]. Hence, Gibbons supposed it as a “warrior gene” in 2004 [55].

2.3 MAOB Gene

2.3.1 Positional Properties of MAOB Gene

MAOB gene is placed in p11.3 of X chromosome, between 43,625,858-43,741,693 nucleotides of reverse strand (Figure 2.5) [56].

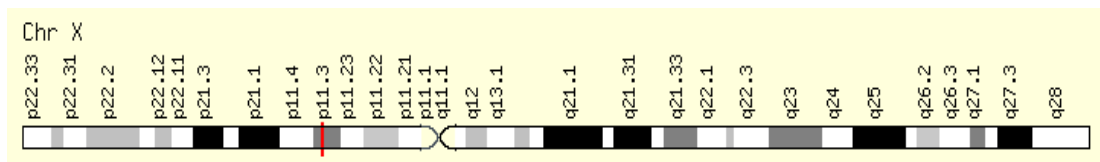


Figure 2.5: *MAOB* gene location on P arm of X chromosome (bands according to Ensembl, locations according to GeneLoc) [56]

DNA size: 115.81 Kb

mRNA size: 2537 bp

15 exons (Figure 2.6)

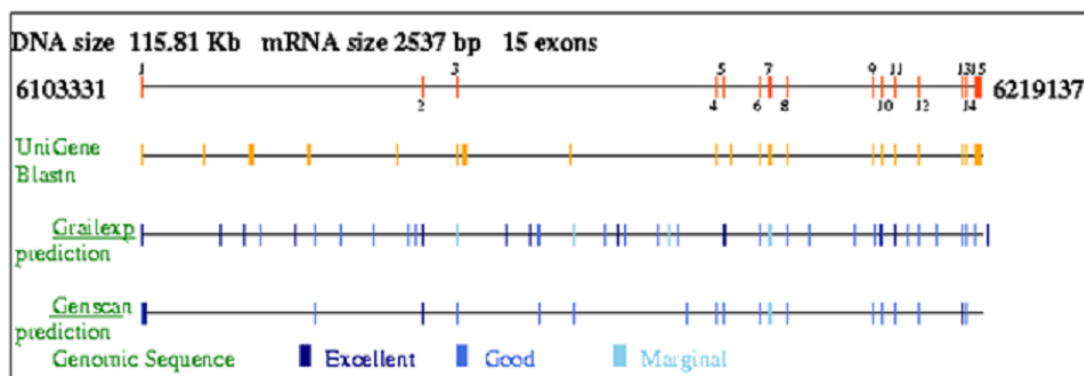


Figure 2.6: *MAOB* exons map [57]. Figure was taken from Genatlas website.

Human *MAOB* gene consist of 15 exons, exon 12 codes FAD-binding site of *MAO* gene as the most conserved region and this region shows 93.9 % similarity in *MAOA* and *MAOB* genes. When high similarity is considered, it can be said that these two genes might have a common ancestral gene that had been duplicated afterwards. The high structural and functional similarity of these two MAO enzymes based on their genetic relationship [58].

The promoter region of *MAOB* gene to base -1,369 from ATG (starting point of mRNA translation) was also sequenced to identify variants with potential functional effects on gene transcription [59]. Recent studies demonstrated that Transforming growth factor β -inducible early gene (*TIEG*)₂ shows dual functions as a repressor at CACCC element and as an activator at the distal Sp1 sites of *MAOB* promoter. *TIEG*₂ has an effect on *MAOB* expression and mRNA level [60, 61]

2.3.2 Expression of *MAOB* Gene

Figure 2.7 displays the most relevant transcription factor binding sites in this gene promoter [62].

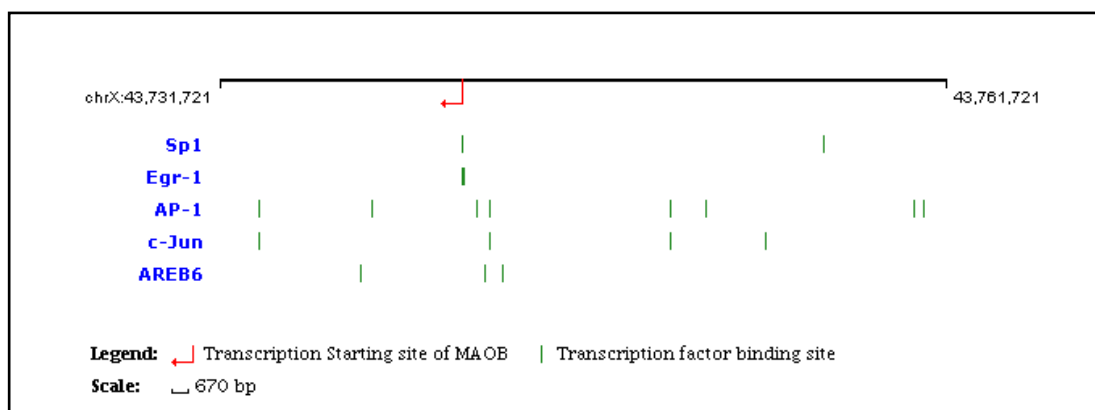


Figure 2.7: Transcription factors and binding sites in *MAOB* gene promoter [62]
Figure was taken from Sabiosciences website.

This gene has 5 transcripts (Table 2.2) [63]:

Table 2.2: *MAOB* gene mRNA products

	Nucleotide sequence length (bp)	Protein length (a.a)	
MAOB-001	2566	520	Protein coding
MAOB-201	1862	504	Protein coding
MAOB-202	1660	411	Protein coding
MAOB-002	857	-	Processed transcript
MAOB-004	325	-	Processed transcript

MAOB expression levels differ tissue by tissue. *PARK2* suppresses the transcription of *MAOA* and *MAOB* to control oxidative stress induced by dopamine oxidation [64]. In the adrenal gland, cranial nerve, uterus and platelet it is expressed highly for human. Expression levels in other tissues and blood is shown on Figure 2.8.

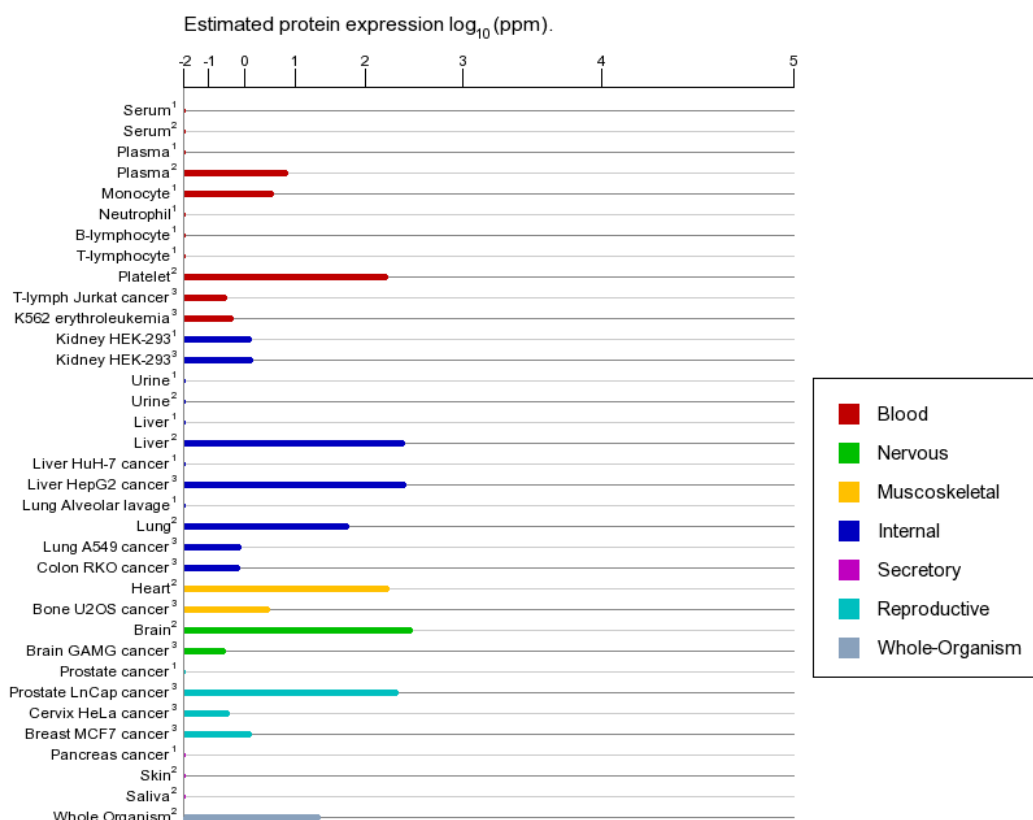


Figure 2.8: *MAOB* estimated expression levels on different tissues and blood [56]. Figure was taken from GeneCards website

Three types (α , β , γ .) Estrogen-related receptors (ERR) increased the transcription of *MAOs A* and *B*, the effects were abolished by parkin, but not by its PD-linked mutants [64].

Mutagenesis studies show that on the 156th amino acid C/S change [65], 345th C/S change [65], 389th C/A change [66, 65], 397th C/S change [65] cause complete loss of activity of protein product of *MAOB* gene. On 158th amino acid T/A change causes

dramatic loss of activity [66], on 382nd H/R change causes significant loss of activity [66].

2.3.3 MAOB Gene Related Disorders

In line with hypothesis of lower platelet MAO activity in different types of psychopathology, children with different subtypes of ADHD (Attention-deficit/hyperactivity disorder) had significantly lower platelet MAO-B activity than control children [49].

The increase of MAO-B protein may be accepted as a signal for Parkinson disease and also MAO-B platelet protein level may serve as a biomarker for age-related dementia, especially AD [67]. Although it has been reported that over *MAOB* mRNA and enzymatic activity in platelet related to Alzheimer's and Parkinson's diseases, it is not clear what is the cause of enhanced *MAOB* mRNA level causing these diseases in the brain [68, 59].

Chapter 3

Coumarin Derivatives

3.1 The Potential Behind of Vanilla Smell

If it could be gone into deeps of luscious vanilla's secretion around the seed, it would be encountered with molecule at Figure 3.1. The gallant of the odoriferous is one of the main characters of our thesis at the same time. Actually, Guibourt had been encountered with this molecule by using his chemist abilities in 1820. The name derives from "cumaru", an Amazonian dialect name for the Tonka bean [69] which had been first isolated plant.



Figure 3.1: Coumarin 3-D structure with Vanilla flowers, drawn by Accelrys

Coumarins comprise of a large family compounds. Some of which have natural and synthetic origin may have several pharmacologic activities. MAO inhibition modifies coumarins too. Coumarin can be obtained from plants and used in medicinal chemistry [70]. The usage of coumarin in the medical reach areas dates back many years. The reason why they are used based on the fact that they have lots of derivatives. Approximately; 1300 coumarin derivatives are obtained from plants, bacteria and fungi [71].

3.2 Chemical and Structural Properties of Coumarin

Coumarin with other name 2-H-Chromen-2-one is a white lactone consisting of a benzene ring and α -pyrone ring (Figure 3.2). The coumarin nucleus (benzo-2-pyrone) is derived from cinnamic acid (phenyl acrylic skeleton) via bio-synthesis. The hydroxyl group at 7th position of coumarin nucleus has an important place in biosynthesis. Since coumarin family has variable structures, their structural variations can change their biological activity [72].

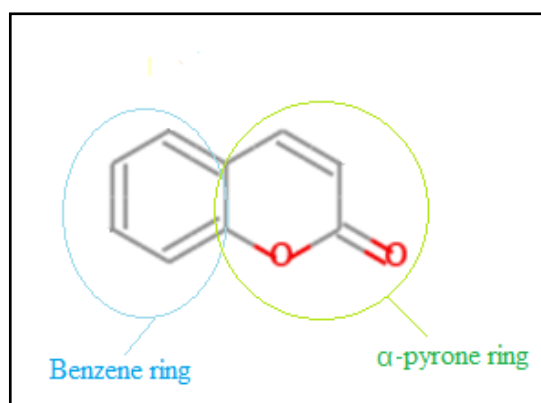


Figure 3.2: Rings in coumarin ($C_9H_6O_2$)

Molecular weight: 146

Crystal structure: Orthorhombic

Solubility: Very soluble in alcohol and ether, not soluble in water

Organoleptic Properties: Vanilla smell

Melting Point: 69 °C, Boiling Point: 290 °C [72]

The special nice smell just like newly-mown hay of coumarin is one of the main reasons for the industrial synthesis [73]. On the other hand, coumarins possess a number of biological activities like anticoagulant, antimicrobial, anti-inflammatory, analgesic, antioxidant, anticancer, antiviral, antimalarial [74], anti-osteoporosis, antiseptic, anti-HIV, anti-hypertension, anti-arrhythmia, antifungal [75], antinociceptive [76]. Coumarin itself and 7-hydroxycoumarin have been reported to inhibit the proliferation of a number of human malignant cell lines in vitro and have demonstrated activity against several types of animal tumors [77]. Although coumarin is a secondary phytochemical with hepatotoxic and carcinogenic properties, according to clinical data related to hepatotoxicity effect of coumarin, this compound is rather useful for using as a medicine [78].

3.3 Toxic Effects of Coumarin

It should be noted that coumarin is moderately toxic with a LD50 of 275 mg/kg [73]. Using the human data, a tolerable daily intake (TDI) of 0.1 mg/kg body weight was derived, confirming that of European Food Safety Authority. Nutritional exposure may be considerably, and is mainly due to use of cassia cinnamon, which is a popular spice [78].

3.4 Founding of Coumarins in Natural Products and Artificial Synthesis

Being fragrant chemical compound, it can be found in natural products, such as in vanilla grass (*Anthoxanthum odoratum*), sweet woodruff (*Galium odoratum*), sweet clover (*Melilotus L.*), sweet grass (*Hierochloe odorata*) [69], tonka been tree (*Dipteryx odorata*), cassia cinnamon (*Cinnamomum aromaticum*), fraxinus bark (*Cortex fraxini*) [79].

On the other hand, the most accessible route to coumarin is the one originally presented by Sir William Perkin. Coumarin can be obtained with following reaction as shown Figure 3.3,

- 1) Phenol is converted to salicylaldehyde with Reimer-Tiemann reaction.
- 2) Then salicylaldehyde is exposed to Perkin reaction with acetic acid and sodium acetate to occur an unsaturated acid.
- 3) In result of intramolecular esterification of the last product coumarin is formed [73].

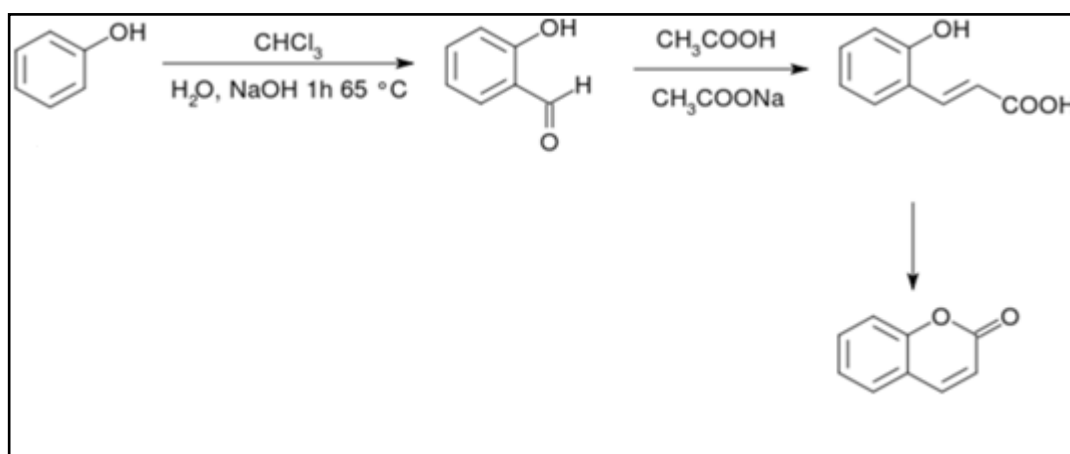


Figure 3.3: Perkin coumarin synthesis reaction [73]

Another coumarin synthesis pathway (Figure 3.4) is Pechmann Coumarin Synthesis [80]:

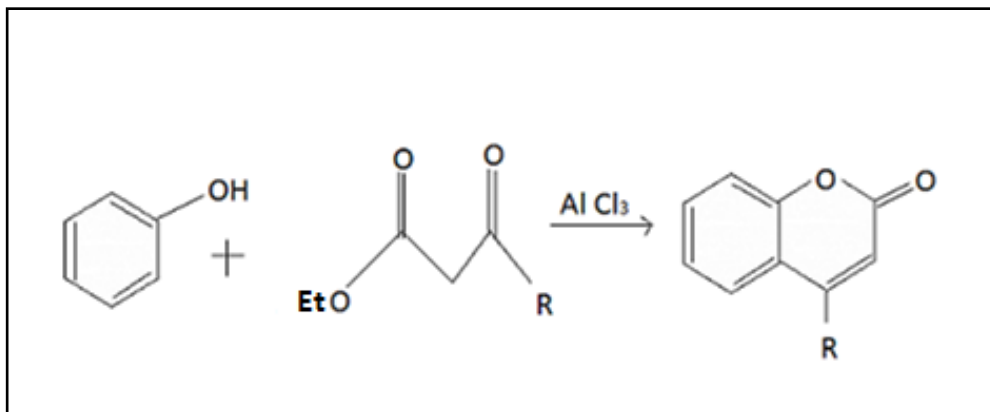


Figure 3.4: Pechmann coumarin synthesis [80]

For a direct synthesis of various coumarins, the following palladium-catalyzed oxidative cyclocarbonylation reaction is useful (Figure 3.5).

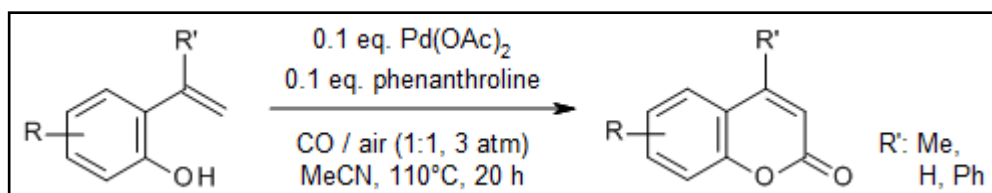


Figure 3.5: Palladium-catalyzed oxidative cyclocarbonylation reaction of 2-vinylphenols [81]

This reaction begins with 2-vinylphenols for the synthesis of various coumarins directly in good yields in the presence of low pressures of CO, and air or 1,4-benzoquinone as the oxidant. The reaction conditions are attractive in terms of environmental considerations and operational simplicity [81].

3.5 Classification of Coumarin Derivatives

Coumarin family has numerous kinds of structures, since their basic structures and lots of types substitutions allows this kindness. The most common coumarin derivatives in nature are Umbelliferone (7-hydroxycoumarin), Esculetin (6,7-Dihydroxycoumarin) and Scopoletin (7-hydroxy-6-methoxycoumarin) [72]. Table 3.1 shows most often common coumarin derivatives in nature with specific names. Figure 3.6 shows coumarin scaffold's 4th, 6th and 7th positions which can have side groups shown with Table 3.1.

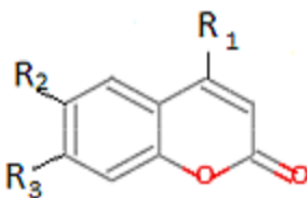


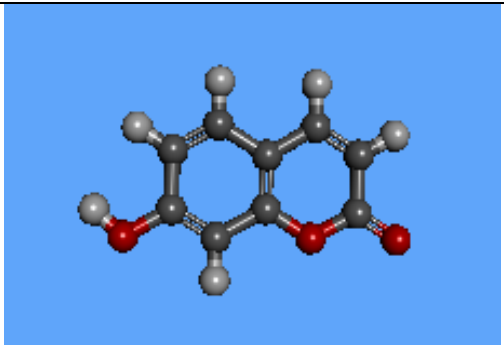
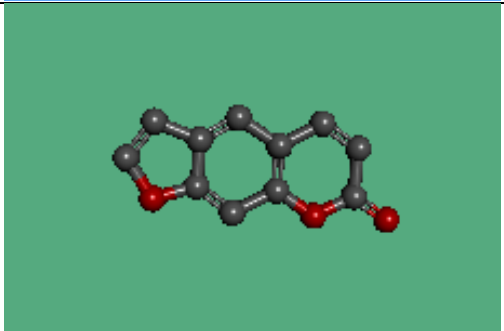
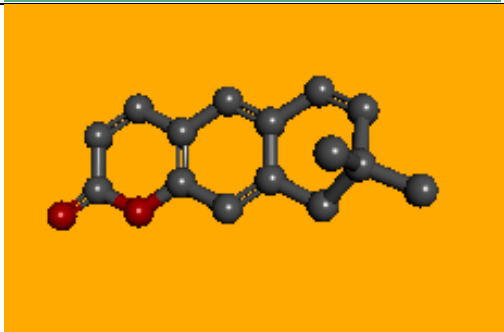

Figure 3.6: Scaffold for natural coumarin derivatives

Table 3.1: Common natural coumarin derivatives [72]

Type of derivative	R ₁	R ₂	R ₃
Coumarin	H	H	H
Herniarin	H	H	OCH ₃
Esculetin	H	OH	OH
Umbelliferone	H	H	OH
Scopoletin	H	OCH ₃	OH
Methyl-umbelliferone	CH ₃	H	OH

Also four main coumarin subtypes as can be seen in Table 3.2 are the simple coumarins, furanocoumarins, pyranocoumarins and the pyrone-substituted coumarins [82]. Their 3-D structures are drawn by Discovery Studio Accelrys program.

Table 3.2: Examples of coumarin sub-types. Grey ball represents Carbon, red ball represents Oxygen, white ball represents Hydrogen.

Classification	Properties	Example
Simple coumarin	Alkoxyated or hydroxylated, groups on benzene	
Furanocoumarin	5-membered furan ring	
Pyranocoumarin	6-membered pyran ring	
Pyrone-substituted coumarin	Substitution on pyrone ring in 3 rd and 4 th positions	

3.6 Effects of Coumarin Derivatives on MAO Enzymes

The interpretation of the chemical binding structure of models allows derivative some chemical features, which can be considered important in the hMAO-B selectivity. For instance, the furan ring or the =CRX fragment (R: any group linked through carbon; X: electronegative atom and =: double bonds) in the ligand structure decreases the selectivity [27].

Compounds that have acetyl/bromoallyloxy groups in the 7th position of coumarin have good inhibitory activity against MAO-A and MAO-B (Figure 3.7). Bulky groups such as cyclohexyl or phenyl in the 3,4-positions of the 7-acetyl coumarin derivatives increase inhibitory activities of them with both MAO-A and MAO-B but decrease the selectivity. On the other hand replacement of the acetyl substituent at the 7-position with the bromoallyloxy group shows very high MAO-B inhibitory activity (IC_{50} of about 1.2 nM and 1.5 nM) and MAO-B selectivity (nearly 100-fold and 1600-fold) with respect to MAO-A isoform [7].

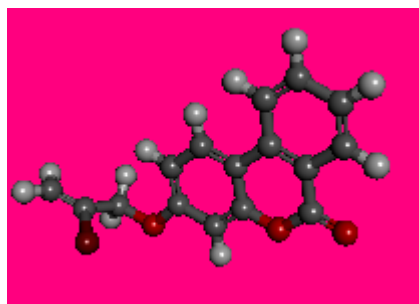


Figure 3.7: 3-D structure of 3,4-Benzo-7-(6-bromoallyloxy)-8-methylcoumarin

Lipophilicity is an important property for MAO-B inhibition potency of 7-substituent coumarins, correlation of pIC_{50} values with $\log P$ values demonstrates it [83].

It is unclear why the inhibitory potency against MAO-B is affected by the length of the side chain [84]. Coumarin analogs interact with non-covalent bonds to human MAO-B complexes [85].

When an aranyl group is in the 3rd position in coumarin nucleus, substituent which is in the 7th position does not increase the potency against MAO-B inhibition. Actually the important thing in terms of QSAR approach is the moiety which is in the pyrone ring for a 7-substituted coumarin derivative by the time antiparkinson activity of coumarin is considered. [10].

The resveratrol-coumarin hybrid compounds ((a), (b), (c) in Figure 3.8), shows high selectivity for the MAO-B isoenzyme and inhibitory activity in the nano to picomolar range [8].

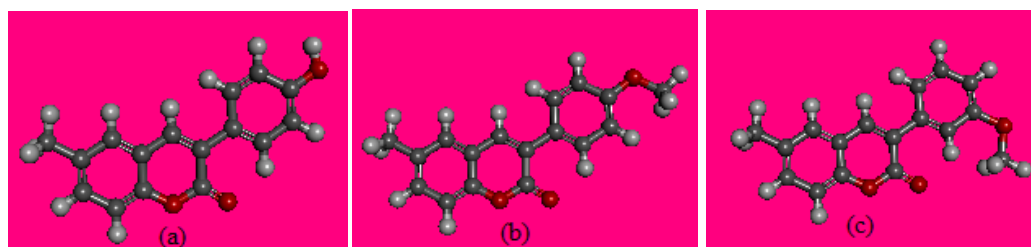


Figure 3.8: 3-D representation of resveratrol-coumarin hybrid compounds.

In addition, Santana et al. also found that coumarins with electronegative groups substituted at the position 3 of γ -pyrone nucleus decrease the hMAO-B selectivity [27, 9].

According to recent study of Abdelhafez (2013) the main atoms and groups of the 7-Oxycoumarin derivatives (Figure 3.9) interacts with hydrogen bonds to MAO-A

active site. In the result of this study, correlation in coumarin derivatives and % inhibition ratio of MAO-A was found at pM levels and of MAO-B at μM levels with AutoDock binding affinities. 7-Oxycoumarin derivatives (4-methyl and/or 3,4-dimethylumbelliferone with acyclic acetohydrazide moiety) in vitro shows % inhibition against MAO-A of 5.01 pM and in vivo ED 50 % of 0,009143 μM . This compound was tightly bound into MAO-A through four hydrogen bonds via its 2-C=O of pyrone and C=O of pyrrolidine or pyrazolidine. The interacted amino acids of MAO-A receptor are NH of Asn181, OH of Tyr444 and with a lower extent NH of Gln215 and C=O of Ala111 [6].

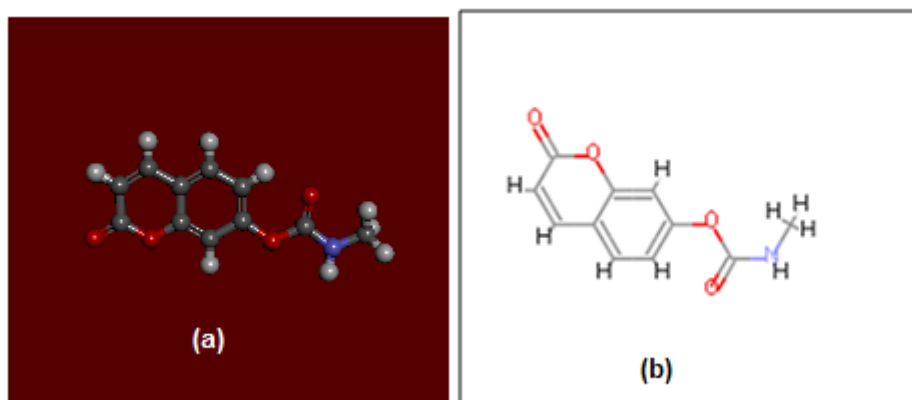


Figure 3.9: 7-Oxycoumarin derivative a) 3-D image (4-methyl and/or 3,4-dimethylumbelliferone with acyclic acetohydrazide moiety) b) Its 2-D image (drawn with Accelrys)

3.7 Other Medical Effects of Coumarin Derivatives

3.7.1 Antioxidant Activity

The free radical scavenging activities of coumarin derivatives are related to the number and position of the hydroxyl group on the benzenoid ring of the coumarin. In

hydroxylated coumarin, the substituent at C-2, C-4, C-7 positions is reported to play a key role in enhancing the activity [86, 87]. To show antioxidant activity, a coumarin derivative has to possess at least one hydroxyl group [88].

3.7.2 Anti-inflammatory Effects of Coumarins

The compound (3-chloro-7-methyl-9H-pyrano [2,3-e] benzo-1,4-oxazine-2,9-dione) in the Figure 3.10 shows maximum anti-inflammatory effect on time dependant study and this may due to the presence of chlorine at 3rd positions, methyl at 7th positions on the aromatic ring of the coumarin respectively [74].



Figure 3.10: 3-D structure of an anti-inflammatory coumarin derivative

3.7.3 Roles of Coumarin in Treatment of High Protein Edema

Coumarin and numerous other benzopyrones have been tested in high protein edema, and all have been shown to successfully reduce the swelling [69]. Coumarin (particularly Esculetin) is ideal natural reducer of edema in legs. If coumarins are used with compression stocking, they give positive results in reducing swelling in legs. Therefore in case venous are insufficient, coumarin cure is recommended [89].

3.7.4 Anti-tumor Activity

Specifically it is expected to increase biological activity in case fluorine and sulfonamide groups are inserted at the coumarin nucleus, because they have known antibacterial and antitumor activity when fluorine and heterocyclic groups are together in coumarin derivative [90].

3.7.5 Coumarin in Leukemia

8-nitro-7-hydrocoumarin displays cytotoxic properties, inducing cell death by apoptosis. Overall esculetin exhibits the strongest antiproliferative effect on the carcinoma cell lines tested. Esculetin (6,7-Dihydroxycoumarin) and 7-hydroxycoumarin inhibits tyrosine phosphorylation in EGF-stimulated tumour cells in a time – and dose- dependent manner [82].

3.7.6 Chromone and Coumestan Derivatives

Chromone and coumestan scaffolds are structurally similar to coumarin. In this concept when the properties of chromone and coumestan derivatives were considered C6-substituted chromones are more potent MAO-B inhibitors than the C7-substituted chromones, because there is a potential hydrogen bond among these with Tyr398 which is anticipated to occur with the C6-substituted chromones, but not the C7-substituted chromones [18]. As for coumestan derivatives, in these derivatives, methoxy and allyloxy coumestan derivatives are more active than methylenedioxy and ethylenedioxy coumestan derivatives. Methoxy derivatives showed better activity than allyloxy derivatives [91].

Chapter 4

Material and Methods

4.1 Introduction

The first step was to obtain available coordinate files of ligands and protein molecules. The second step was to perform grid calculations for every ligand molecule. At the third step, protein and ligand was docked.

During this study various computational molecular modeling tools were used. The drawing was done with Discovery Studio Accelrys software. Docking was performed with AutoDock 4.2. The MAO-A and MAO-B proteins had been taken from PDB (Protein Data Bank). The results of docking were read from *.dlg files. The best 50 results of MAO-A, the best 50 results of MAO-B, the best 25 results for correlation of K_i values between MAO-A and MAO-B according to selectiveness properties being corresponding differences of affinities, were shown. At the light of these results, the best five results for each one were illustrated to cast light on the interactions between the ligand and the binding site of MAO protein cavity.

4.2 Preparation of Ligands

Our aim is to perform 125 different ligand structures using 5 different side groups on coumarin scaffold. Previous studies [76, 92, 10, 8] shows that 3rd, 4th and 7th positions on coumarin are specifically important for MAO inhibition potency. Hence in this study 3rd, 5th and 7th positions were selected to add side groups to observe changes in the activity (Figure 4.1).

The selected five side groups are;

Methoxy (-OCH₃), Fluorine (-F), Bromine (-Br), Amide (-C(O)NH₂) and Phenyl (-C₆H₅).

Especially Fluorine and bulky groups affect the potency, additionally hydroxy group in 7th position increase the affinity to MAO-B enzyme. Previous studies demonstrate the Bromine, amide and phenyl have the most potent inhibitory activity against MAO-B enzyme [7].

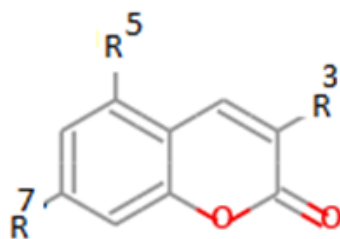


Figure 4.1: Coumarin Scaffold

The drawing was performed first on the paper. These 2D pictures were drawn in 3D using Discovery Studio 3.5. After performing 3D structure of the ligand on a new

window, 2D image was taken applying “Show 2D Structure” by changing “Display Style” at the end of adjusting 2D images were saved as *.png format and 3D files were saved as *.mol2 and *.pdb formats.

These 125 *.pdb files firstly were tried to minimize with pdb2pqr web tool but files could not be transformed pqr format. Hence another web based minimizer were tried, but also YASARA’s transformed files were not reliable for pdb format, at the last, “clean geometry” tool of Discovery Studio was used to optimize these 125 ligands’ 3D shapes. At the end of the optimization, these files were saved as both pdb and mol2 formats. Because *.mol2 files could not be opened in AutoDock4.2 on Windows7, *.pdb files were used to obtain *.pdbqt files for each ligands. At the stage of drawing, all ligands were drawn together all hydrogen atoms in Discovery Studio. The redundant hydrogen atom on the phenyl ring being side group that had been added by program was removed meticulously by rotating the molecule. Pdbqt files are necessary file formats for AutoDock 4.2. Because the polar hydrogens and partial charges are added to molecule and AutoDock 4 atom types are in the pdbqt file.

4.3 Preparation of Proteins

Pdbqt files of MAO-A and MAO-B were obtained directly from *.pdb files that had been prepared at previous study [13]. MAO isoenzymes’ cocrystalized structures had been reached from PDB (Protein Data Bank); human MAO-A (2Z5X) with harmine (resolution 2.2 Å) and human MAO-B (2Z5V) with safinamide (resolution 1,6 Å). These pdb files had been opened with Discovery Studio 3.5 and first, ligand (harmine

for MAO-A and safinamide for MAO-B) had been cleaned. Lost residues had been completed, then atoms which are in the active site had been minimized. Waters which are around the protein had been removed. pH value had been adjusted 7.2. At the last step *.pdb files had been converted to *.pdbqt files using AutoDock 4.2

4.4 Docking Study of Coumarin Derivatives with MAO-A and MAO-B

The prepared *.pdbqt files for coumarin derivatives and MAO-A and MAO-B were used to perform *.gpf files for each docking.

Grid option was used to perform *.gpf (Grid Parameter File) files. For Grid Calculation, pdbqt file which belong to MAO-A was selected as “Macromolecule”. Ligand’s pdbqt file was opened as “Set Map Types”. In the grid box, “spacing longs” was taken as 0.375, grid box size was kept 70x70x70. X, Y, Z values in the “center grid box” is the N5 atom of the FAD (Figure 4.2).

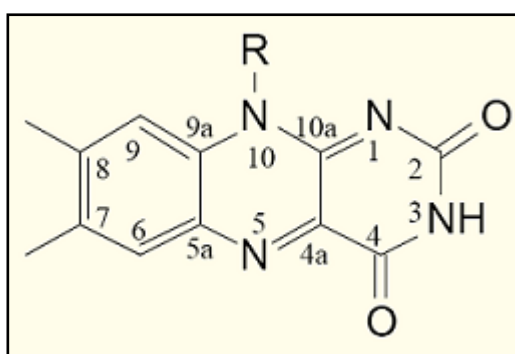


Figure 4.2: Atoms' positions in isoalloxazine ring of FAD [93].

Therefore firstly MAO-A *.pdb file was viewed in the VMD. Molecule was imaged as ball and stick format, after confirming the FAD and its N5 atom in the MAO-A,

atom names were shown by using VMD tools and it was clear the N5 atom's name is FAD 600:NY1. Then MAO-A pdb file was opened with WordPad and in the Heteroatoms NY1 of FAD was found. Its coordinates are: 33.897 35.157 -13.250

Also MAO-B pdb file was opened, NY1's coordinates for MAO-B are: 55.724 151.605 21.259. Before closing this grid box window "close saving current" was clicked in the "File" option (Figure 4.3).

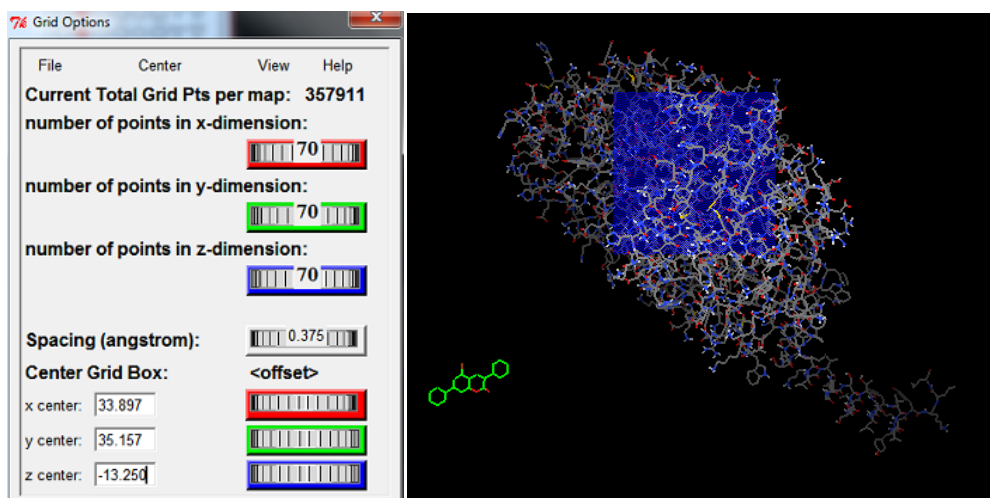


Figure 4.3: Grid box options to adjust grid parameter. AutoDock4.2 grid box (left), while performing (right).

In the output it was saved with each ligand's name as *.gpf file. After 125 ligand's grid calculations were done with MAO-A, also it was done with MAO-B but at this time center grid box values were changed according to MAO-B NY1 of FAD's X, Y, Z coordinates.

Map files' names which will be performed are written in the *.gpf file. Numbers of map files are equal to four more of number of atom types of ligand. *.glg file and map files are performed by autogrid4 writing on the terminal window;

```
.../autogrid4 -p M001.gpf -l M001.glg
```

A sample gpf file is below.

```
npts 70 70 70          # num.grid points in xyz
gridfld maoA.maps.fld  # grid_data_file
spacing 0.375          # spacing(A)
receptor_types A C HD N NA OA P SA # receptor atom types
ligand_types A C HD OA N    # ligand atom types
receptor maoA.pdbqt      # macromolecule
gridcenter 33.897 35.157 -13.25 # xyz-coordinates or auto
smooth 0.5              # store minimum energy w/in rad(A)
map maoA.A.map          # atom-specific affinity map
map maoA.C.map          # atom-specific affinity map
map maoA.HD.map         # atom-specific affinity map
map maoA.OA.map         # atom-specific affinity map
map maoA.N.map          # atom-specific affinity map
elecmap maoA.e.map      # electrostatic potential map
dsolvmap maoA.d.map     # desolvation potential map
dielectric -0.1465      # <0, AD4 distance-dep.diel;>0, constant
```

After two minutes, necessary map files and *.glg file are arisen. During these operations, apparent directories were formed for each ligands. At the beginning in each directory only one ligand's pdbqt, one protein pdbqt and related *.gpf file must exist. Otherwise, if it was more than one *.gpf files in the same directory, it would be

fault in performing new map files as from second ligand. Although all *.glg files are obtained, docking results are different when they were compared with apparent directories.

After performing *.gpf files, *.dpf files which are main docking parameter files were prepared by using AutoDock 4.2 docking algorithm. For this purpose, number of runs is taken as 10, number of generation = 27.000, number of evolutions = 5.000.000 since torsion numbers of ligands are smaller than 10.

Each *.dpf file that is belong to separate ligand was saved in the directory that is belong to one ligand and contain its *.gpf file additionally its ligand *.pdbqt and macromolecule *.pdbqt files.

A sample *.dpf file is below.

```
AutoDock_parameter_version 4.2    # used by AutoDock to validate parameter set
outlev 1                          # diagnostic output level
intelec                           # calculate internal electrostatics
seed pid time                      # seeds for random generator
ligand_types A C HD O A N        # atoms types in ligand
fld maoB.maps.fld                 # grid_data_file
map maoB.A.map                    # atom-specific affinity map
map maoB.C.map                    # atom-specific affinity map
map maoB.HD.map                   # atom-specific affinity map
map maoB.OA.map                   # atom-specific affinity map
```

```

map maoB.N.map          # atom-specific affinity map
elecmap maoB.e.map      # electrostatics map
desolvmap maoB.d.map    # desolvation map
move m118.pdbqt         # small molecule
about -2.449 2.6955 0.1781 # small molecule center
tran0 random            # initial coordinates/A or random
quaternion0 random      # initial orientation
dihe0 random            # initial dihedrals (relative) or random
torsdof 3               # torsional degrees of freedom
rmstol 2.0              # cluster_tolerance/A
extnrg 1000.0           # external grid energy
e0max 0.0 10000         # max initial energy; max number of retries
ga_pop_size 150         # number of individuals in population
ga_num_evals 5000000    # maximum number of energy evaluations
ga_num_generations 27000 # maximum number of generations
ga_elitism 1            # number of top individuals to survive to next generation
ga_mutation_rate 0.02   # rate of gene mutation
ga_crossover_rate 0.8   # rate of crossover
ga_window_size 10       #
ga_cauchy_alpha 0.0     # Alpha parameter of Cauchy distribution
ga_cauchy_beta 1.0     # Beta parameter Cauchy distribution
set_ga                  # set the above parameters for GA or LGA
sw_max_its 300          # iterations of Solis & Wets local search
sw_max_succ 4           # consecutive successes before changing rho
sw_max_fail 4           # consecutive failures before changing rho

```

```
sw_rho 1.0           # size of local search space to sample
sw_lb_rho 0.01       # lower bound on rho
ls_search_freq 0.06  # probability of performing local search on individual
set_psw1            # set the above pseudo-Solis & Wets parameters
unbound_model bound # state of unbound ligand
ga_run 10           # do this many hybrid GA-LS runs
analysis            # perform a ranked cluster analysis
```

Lamarckian genetic algorithm was used to perform maximum number of energy evaluation and maximum number of generations for each docking parameter files in order to calculate energy values for each position of ligand in the protein.

After obtaining *.glg files and map files, in the same directories *.dlg (docking log file) files are performing utilizing map files and *.dpf file.

In the terminal window of Ubuntu, after entering the related directory that contain a *.dpf file, *.dlg file was created by writing following command:

```
.../autodock4 -p M001.dpf -l M001.dlg
```

In this command M001 is any ligand and M001.dpf is its prepared dpf file.

In the individual computer and on the Ubuntu, this process takes ten-fifteen minutes for one docking. In this study 250 dockings were arisen. Then results were read from *.dlg files by looking to the lowest energy value.

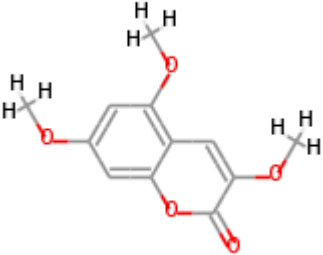
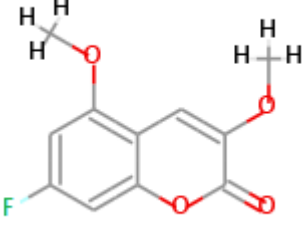
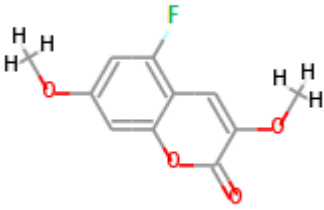
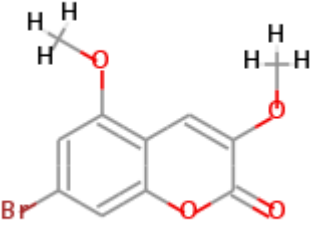
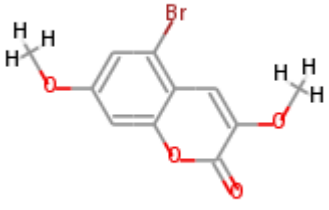
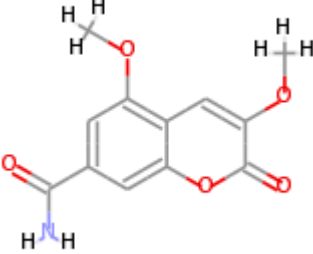
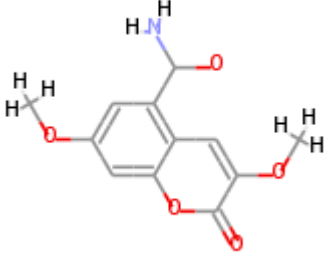
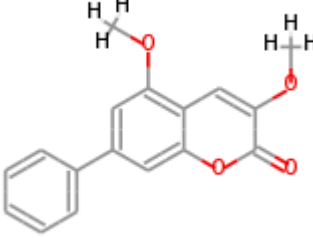
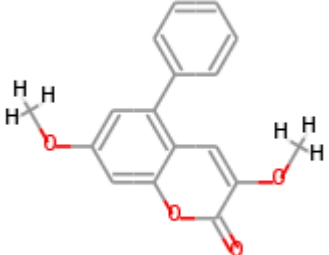
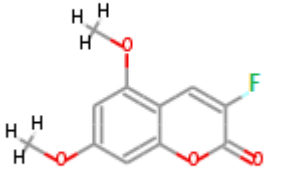
At the beginning of selection available grid size, in order to decide true grid measures, randomly selected five ligands had been docked with both MAO-A and MAO-B enzymes with a view to decide available grid box sizes. Hence during the grid calculation of these five ligands the grid box size being taken 60 X 60 X 60. When the docking results were compared, the results were seen that they had got better results which had been performed with 70 X 70 X 70 grid box. Other 120 coumarin derivatives were docked by taking account of this situation.

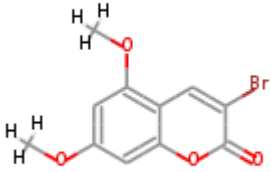
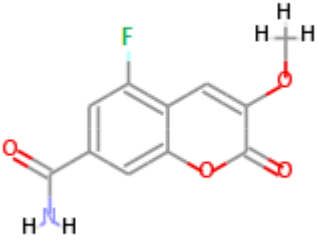
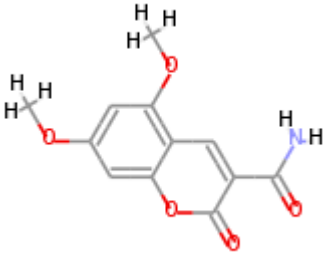
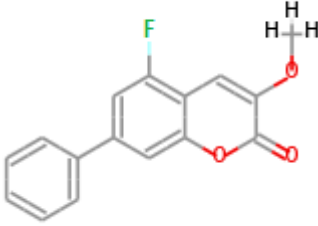
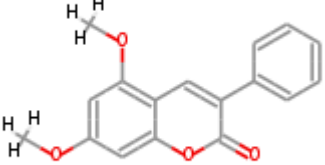
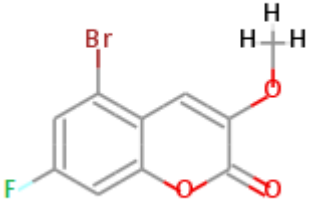
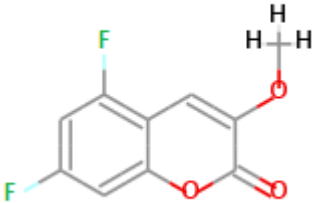
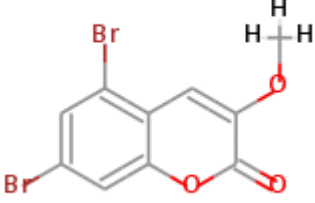
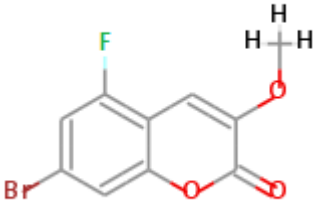
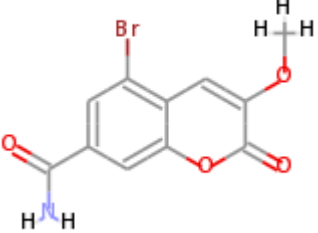
In order to examine binding properties of coumarin derivatives with MAO-A and MAO-B enzymes, the coordinates found in the *.dlg file belonging to the lowest energy values obtained from AutoDock 4.2 docking process were added to end of related MAO enzyme *.pdbqt file. Then this file was opened with Discovery Studio 3.5 Accelrys program and all interactions were observed via tools of this program.

Particularly occurred pi-pi, pi-sigma, pi-caution interactions and polar interactions were appeared, and van der Waals forces could be observed corresponding their grandeurs. Additionally distance of pi-pi interactions and polar interactions were predicted via Accelrys program.

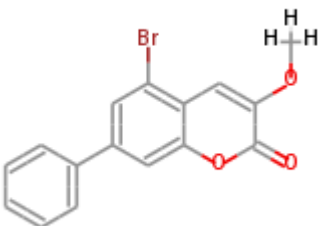
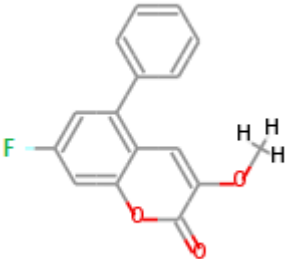
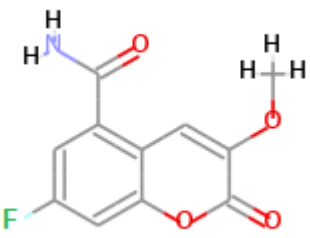
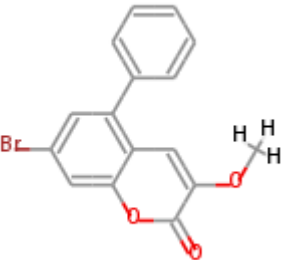
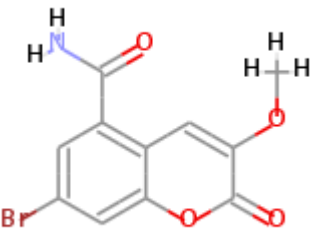
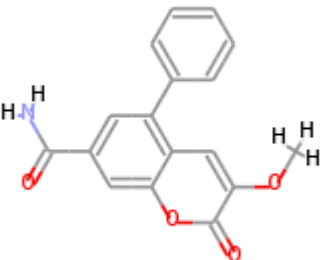
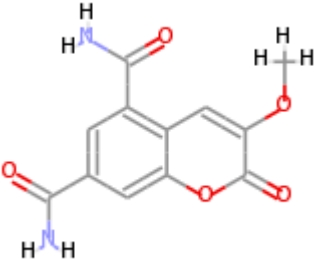
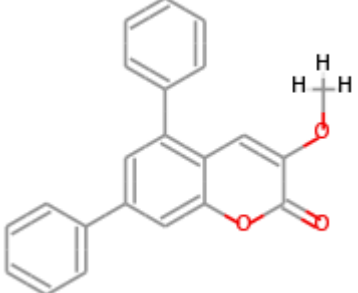
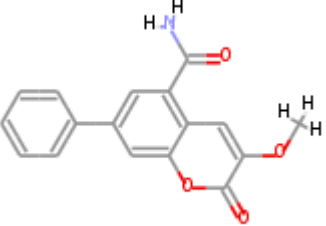
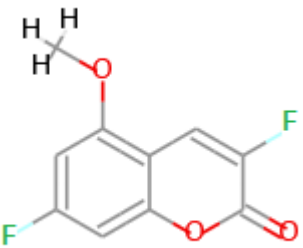
Table 4.1 shows 125 coumarin derivatives' 2-D structures drawn by Discovery Studio Accelrys program depending on three dimensional structures occurred on this software.

Table 4.1: 2-D Structures of 125 Coumarin Derivatives

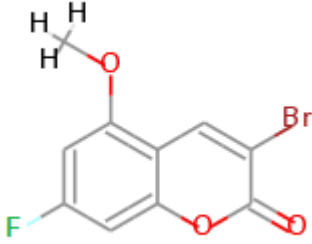
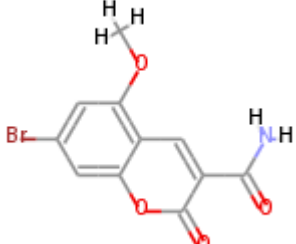
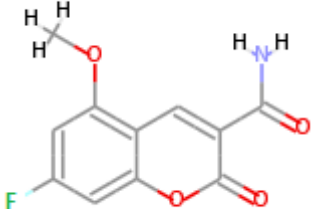
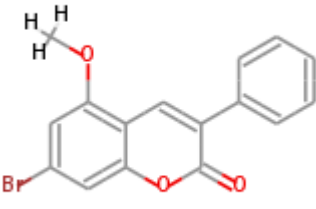
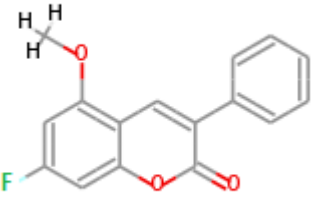
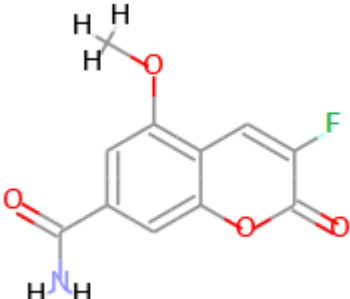
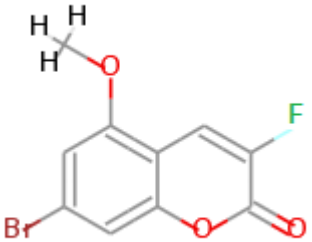
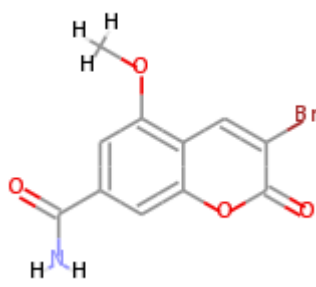
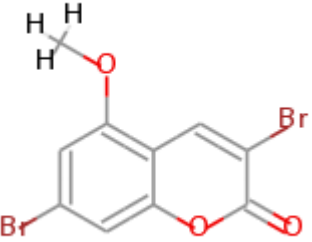
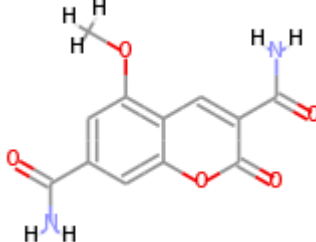
 <p>M001</p>	 <p>M006</p>
 <p>M002</p>	 <p>M007</p>
 <p>M003</p>	 <p>M008</p>
 <p>M004</p>	 <p>M009</p>
 <p>M005</p>	 <p>M010</p>

 <p>M011</p>	 <p>M016</p>
 <p>M012</p>	 <p>M017</p>
 <p>M013</p>	 <p>M018</p>
 <p>M014</p>	 <p>M019</p>
 <p>M015</p>	 <p>M020</p>

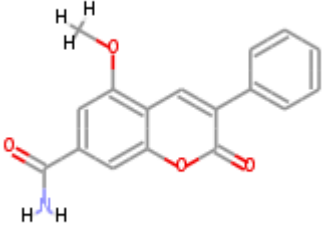
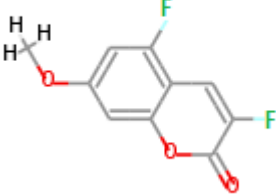
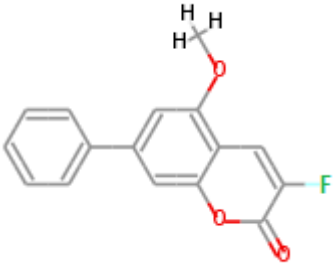
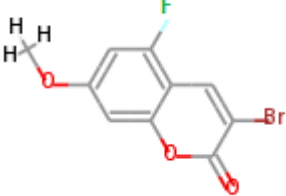
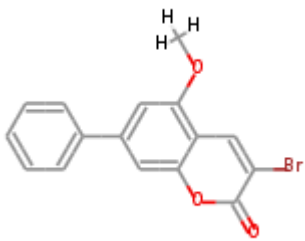
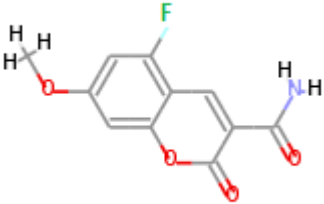
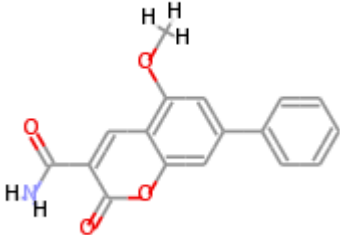
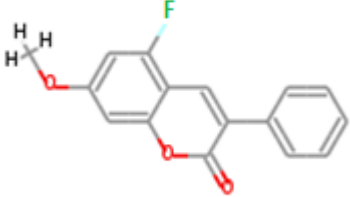
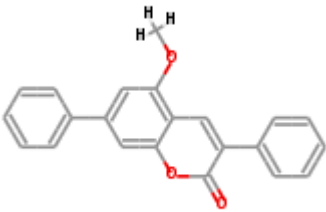
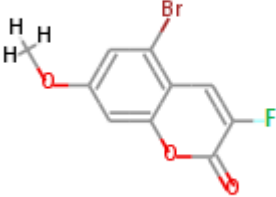
Continuation of Table 4.1

 <p>M021</p>	 <p>M026</p>
 <p>M022</p>	 <p>M027</p>
 <p>M023</p>	 <p>M028</p>
 <p>M024</p>	 <p>M029</p>
 <p>M025</p>	 <p>M030</p>

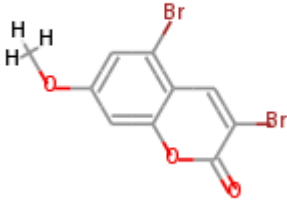
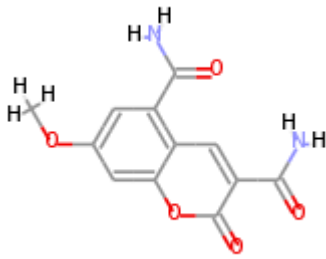
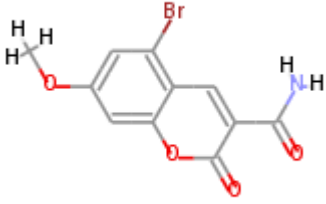
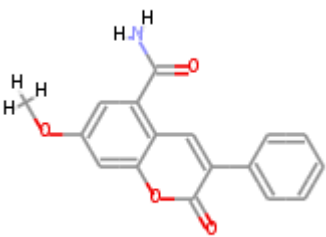
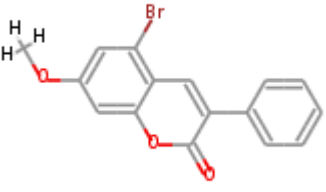
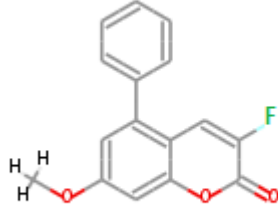
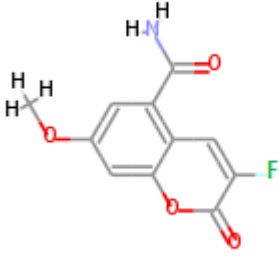
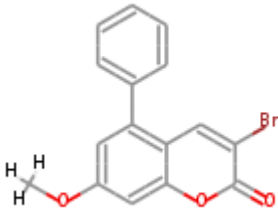
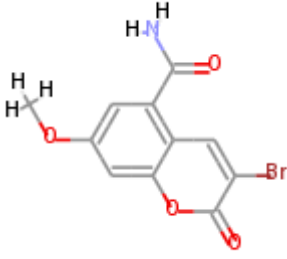
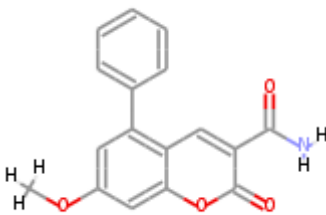
Continuation of Table 4.1

 <p>M031</p>	 <p>M036</p>
 <p>M032</p>	 <p>M037</p>
 <p>M033</p>	 <p>M038</p>
 <p>M034</p>	 <p>M039</p>
 <p>M035</p>	 <p>M040</p>

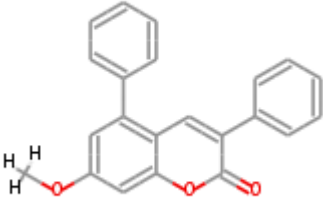
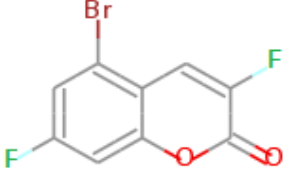
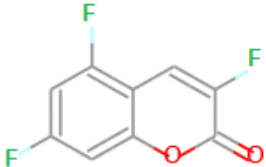
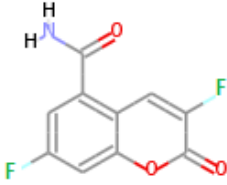
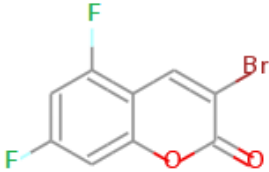
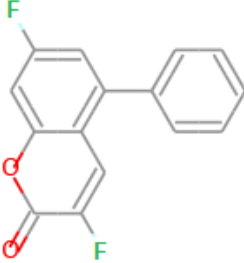
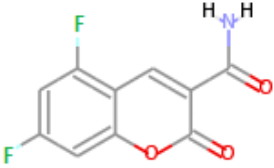
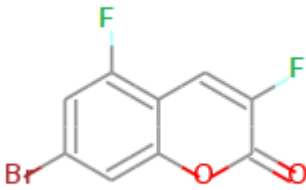
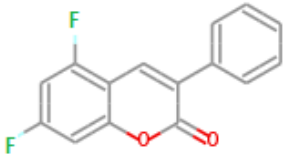
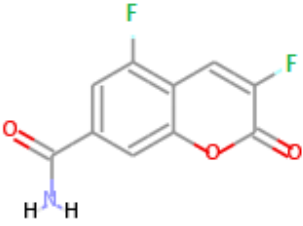
Continuation of Table 4.1

 <p>M041</p>	 <p>M046</p>
 <p>M042</p>	 <p>M047</p>
 <p>M043</p>	 <p>M048</p>
 <p>M044</p>	 <p>M049</p>
 <p>M045</p>	 <p>M050</p>

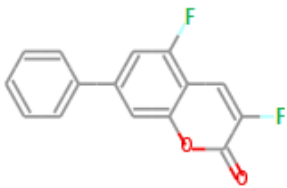
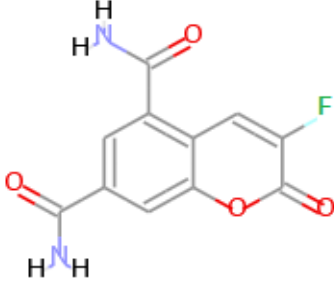
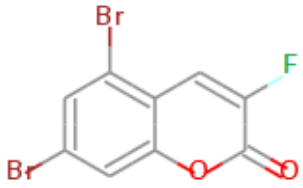
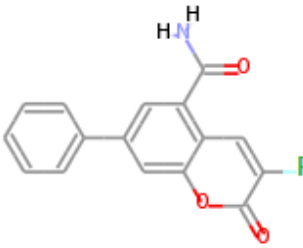
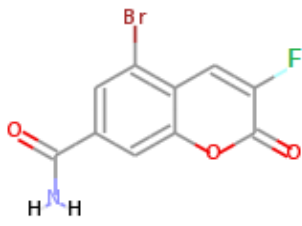
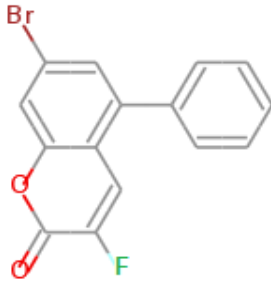
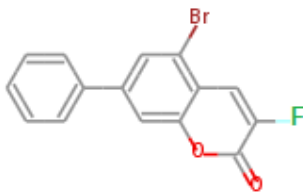
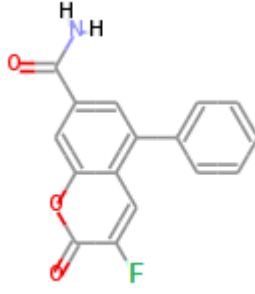
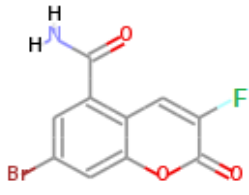
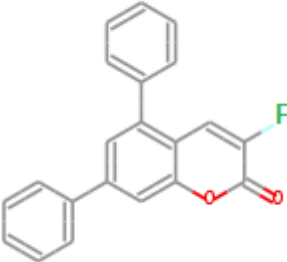
Continuation of Table 4.1

 <p>M051</p>	 <p>M056</p>
 <p>M052</p>	 <p>M057</p>
 <p>M053</p>	 <p>M058</p>
 <p>M054</p>	 <p>M059</p>
 <p>M055</p>	 <p>M060</p>

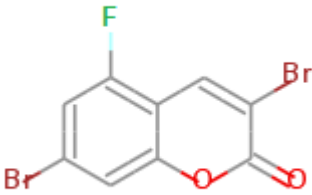
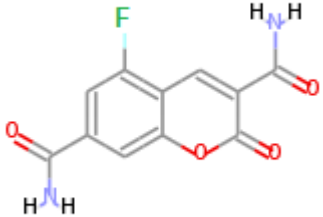
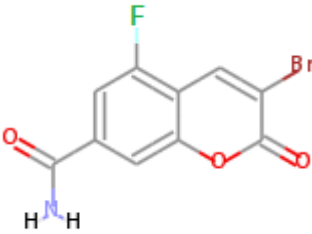
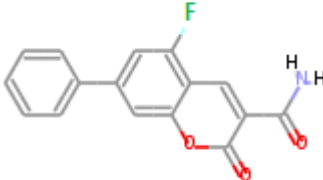
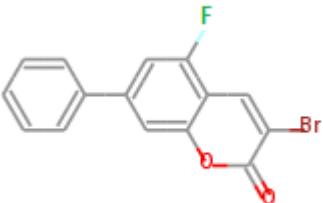
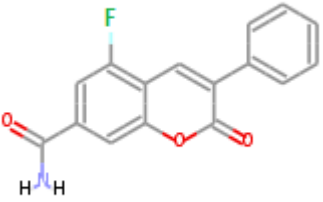
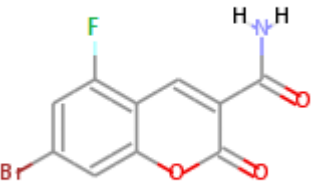
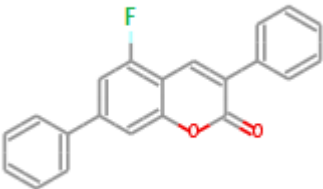
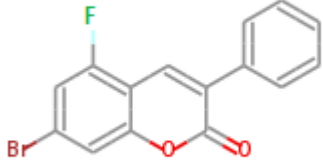
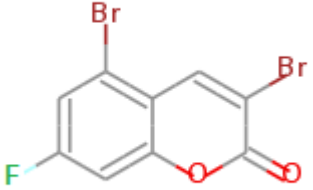
Continuation of Table 4.1

 <p>M061</p>	 <p>M066</p>
 <p>M062</p>	 <p>M067</p>
 <p>M063</p>	 <p>M068</p>
 <p>M064</p>	 <p>M069</p>
 <p>M065</p>	 <p>M070</p>

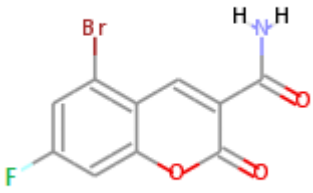
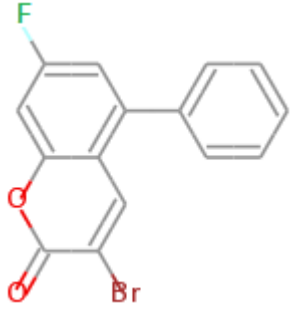
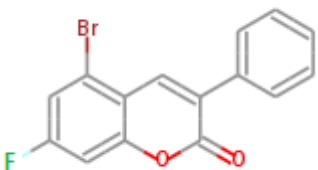
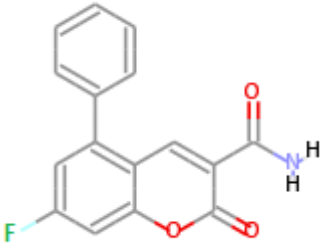
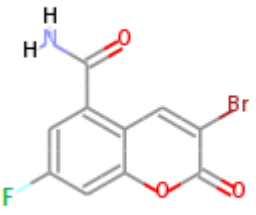
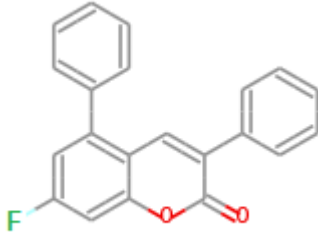
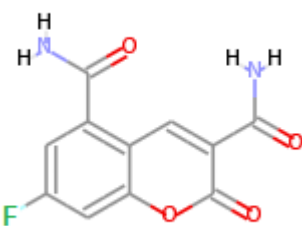
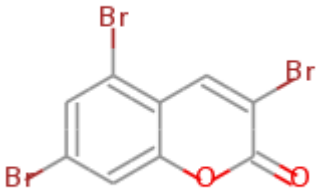
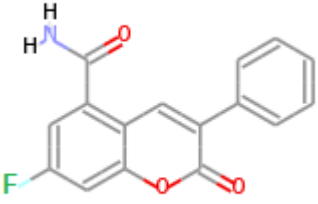
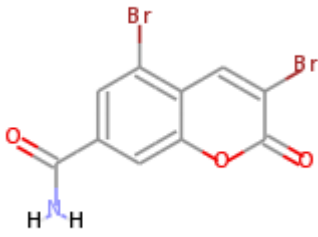
Continuation of Table 4.1

 <p>M071</p>	 <p>M076</p>
 <p>M072</p>	 <p>M077</p>
 <p>M073</p>	 <p>M078</p>
 <p>M074</p>	 <p>M079</p>
 <p>M075</p>	 <p>M080</p>

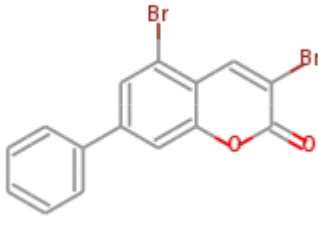
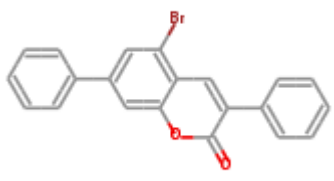
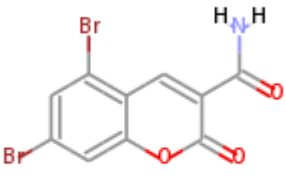
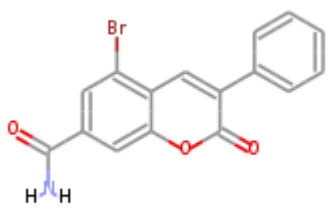
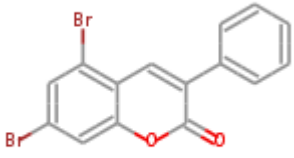
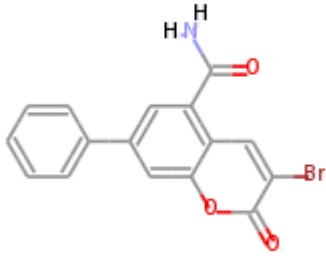
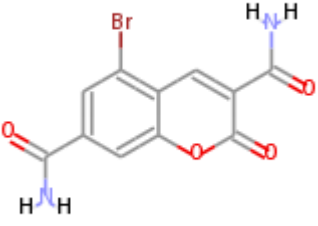
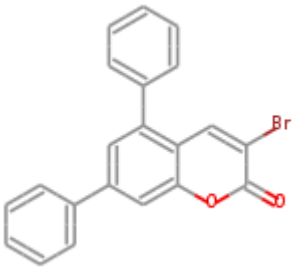
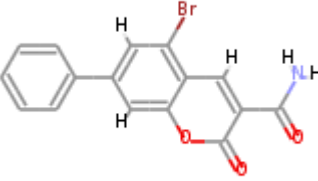
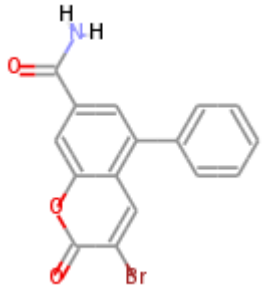
Continuation of Table 4.1

 <p>M081</p>	 <p>M086</p>
 <p>M082</p>	 <p>M087</p>
 <p>M083</p>	 <p>M088</p>
 <p>M084</p>	 <p>M089</p>
 <p>M085</p>	 <p>M090</p>

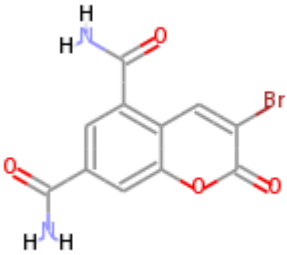
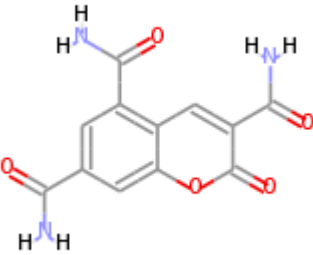
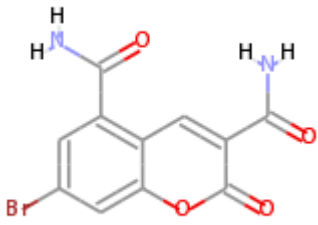
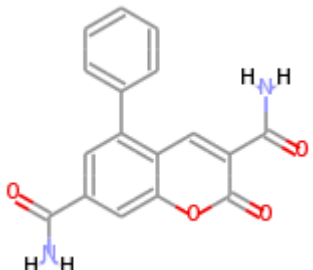
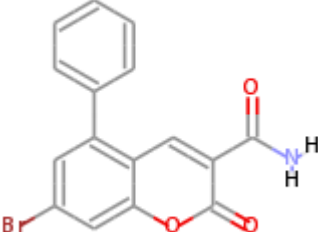
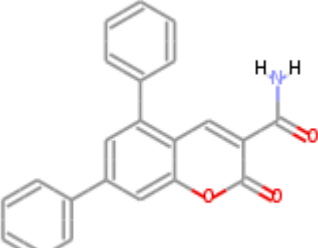
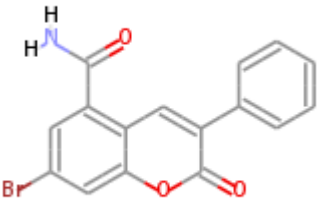
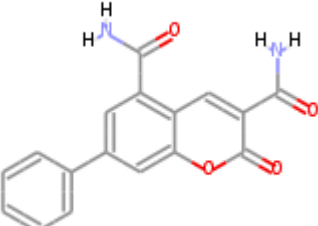
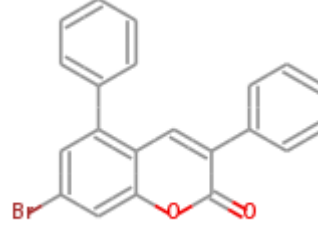
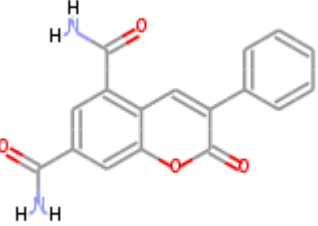
Continuation of Table 4.1

 <p>M091</p>	 <p>M096</p>
 <p>M092</p>	 <p>M097</p>
 <p>M093</p>	 <p>M098</p>
 <p>M094</p>	 <p>M099</p>
 <p>M095</p>	 <p>M100</p>

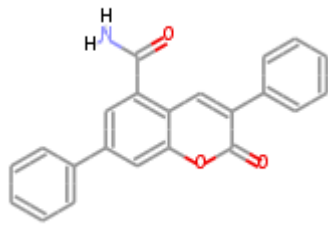
Continuation of Table 4.1

 <p>M101</p>	 <p>M106</p>
 <p>M102</p>	 <p>M107</p>
 <p>M103</p>	 <p>M108</p>
 <p>M104</p>	 <p>M109</p>
 <p>M105</p>	 <p>M110</p>

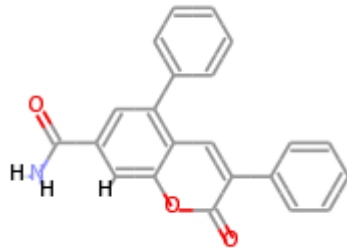
Continuation of Table 4.1

 <p>M111</p>	 <p>M116</p>
 <p>M112</p>	 <p>M117</p>
 <p>M113</p>	 <p>M118</p>
 <p>M114</p>	 <p>M119</p>
 <p>M115</p>	 <p>M120</p>

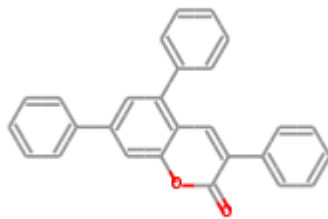
Continuation of Table 4.1



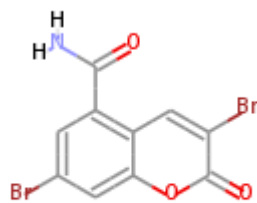
M121



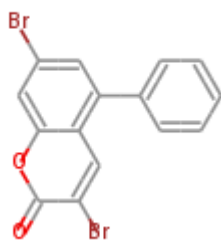
M122



M123



M124



M125

Continuation of Table 4.1

4.5 Molecular Modeling

Molecular Modeling is the improved models simulated the behavior of the molecules by the aid of theoretical methods and computational applications. Molecular Modeling is used in the area of computational biology, drug design and computational chemistry to study the behavior of small molecules and complex biological systems and materials. Computers have an important place in performing Molecular Modeling of any comprehensible measured system. This technique describes the molecules at atomic level; meanwhile it deals with electrons as the smallest unit [94].

4.6 Molecular Mechanics

Molecular Mechanics is based on Newtonian mechanics to explain molecule's physical condition. The interactions between neighboring atoms are explained with chemical bonds (like covalent, ionic, hydrogen bonds) or non-bonded interactions like van der Waals forces. The Lenard-Jones potential is similar to van der Waals forces. The electrostatic interactions are found by Coulomb's law. Atoms are placed specific internal coordinates, atomic velocities are determined in dynamical simulations, related to temperature of the system. Potential function related to the system internal energy is sum of potential and kinetic energies. The minimization of potential energy is to become the most natural condition of the system's behavior [94]. Performing of molecular potential energy is shown in Equation-3.1

$$E = E_{bonds} + E_{angle} + E_{dihedral} + E_{electrostatic} + E_{van\ der\ Waals} \quad (3.1)$$

A potential function (Equation-3.1) computes the molecular potential energy that is the sum of bond lengths, bond angles, torsion angles and electrostatic interactions and van der Waals forces. A set of parameters contains bond angles, bond lengths, force constants, partial charge values, van der Waals forces construct the force field [94].

A force field is developed by quantum calculations and experimental data. As related to energy minimization, lowest energy states are more stable in biological processes. Molecular dynamics computes the behavior of a system as a function of time by using Newton's laws of motion, which is $F_{\text{net}} = ma$ [94].

The force on an atom is defined as the negative gradient of the potential energy function. While energy minimization finds the most stable condition for a molecule or a complex system by comparing the states of similar systems, molecular dynamics gives information about a molecule's behavior by taking into consideration the temperature effects [94].

4.7 The Environment in the Molecular Modeling

The environment may be selected as vacuum or solvent such as water. If it is a biological molecule, pH value must be adjusted as near real condition. The vacuum environment is preferred for gas-phase simulations, while presence of solvent molecules is available for explicit solvent simulations, if the effect of solvent is estimated using an empirical mathematical expression, it will be implicit solvation simulations [95].

4.8 Application Areas

Molecular Modeling methods are commonly used to explain structure, membrane properties and thermodynamics of biological or polymeric systems [94].

4.9 AutoDock 4.2

AutoDock 4.2 is a very versatile molecular docking program used computational methods in order to find free energy of binding and lowest K_i values using its own scoring function based on AMBER force field for proteins and ligand interactions additionally RNA and DNA molecules (Figure 4.4) [96].

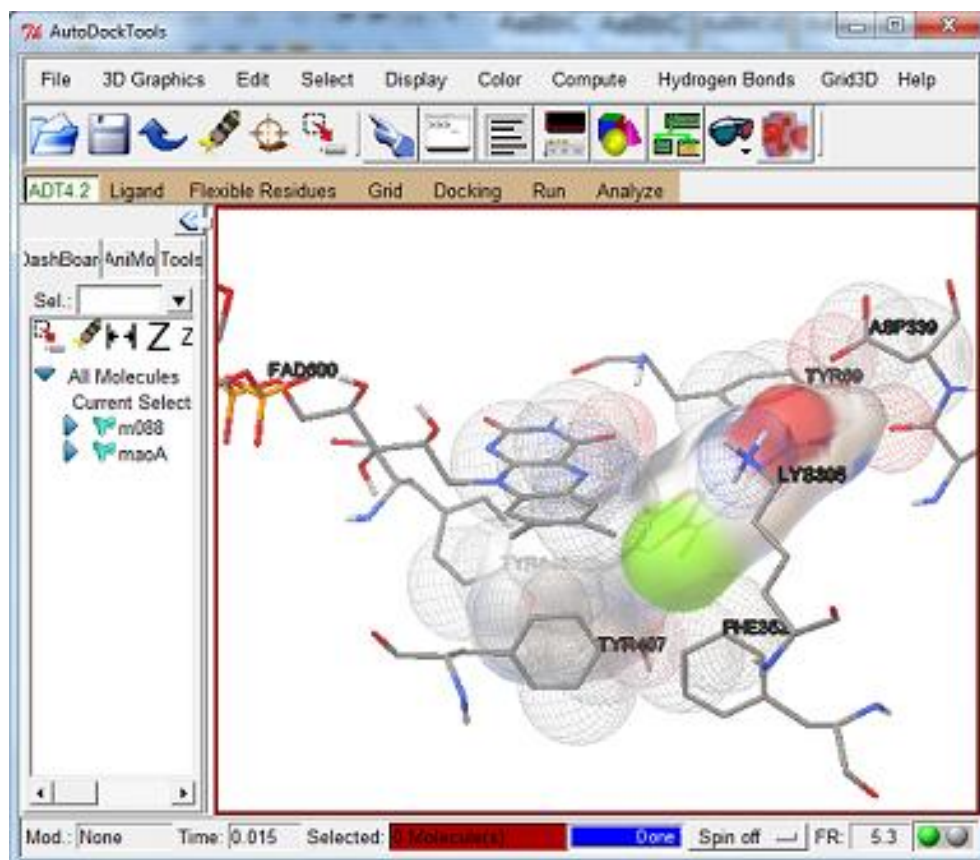


Figure 4.4: AutoDock 4.2 molecular graphics

4.10 Equations

The molecular mechanics-based terms are multiplied by coefficients that are determined by linear regression analysis of complexes with known 3D structures and known binding free energies. According to AutoDock 4.2, these free weights (W_{vdW} , W_{H-bond} , W_{elec} , W_{desolv} , W_{tor}) can be set in the parameter file [97].

All energies which is performed to molecular free energy of binding is used in order to calculate AutoDock ΔG [97] are shown in Equation-3.2.

Molecular Mechanics Terms

- van der Waals

$$\Delta G_{vdW} = W_{vdW} \sum_{i,j} (A_{ij} / r_{ij}^{12} - B_{ij} / r_{ij}^6)$$

- Hydrogen Bonding

$$\Delta G_{H-bond} = W_{H-bond} \sum_{i,j} E(t) * (C_{ij} / r_{ij}^{12} - D_{ij} / r_{ij}^{10} + E_{hbond})$$

- Electrostatics

$$\Delta G_{elec} = W_{elec} \sum_{i,j} (q_i * q_j) / (\epsilon(r_{ij}) * r_{ij})$$

- Desolvation (AutoDock 3)

$$\Delta G_{desolv} = W_{desolv} \sum_{i(C),j} (S_i * V_j * \exp(-r_{ij}^2 / (2 * \sigma^2)))$$

- Torsional

$$\Delta G_{tor} = W_{G_{tor}} N_{tor} \tag{3.2}$$

In the above equations ΔG_{vdW} is Lenard-Jones 6/12 potential for dispersion/repulsion interactions. A and B are Amber force field's parameters. In the second equation r_{ij} is distance between the atoms i and j. E(t) is directional weight that depends on the angle (t) between the probe and the target atom. In the third equation depends on

coulomb potential. Electrostatic interaction between charged particles q_i and q_j are partial charges of the atoms, ϵ is the permittivity. In the fourth equation desolvation potential based on the volume (V_j) of the atoms surrounding a given atom. S_i and σ are weighting factors for volumes and distance. In the fifth equation ΔG_{tor} is torsional entropy on binding. N_{tor} is number of rotatable bonds [13, 98].

Chapter 5

Results and Discussion

5.1 Introduction

In this chapter, 125 coumarin derivatives are assessed according to their binding affinities and binding energies for MAO-A and MAO-B enzymes.

At the first step, *.dlg files which had been produced by AutoDock4 were read to obtain lowest energy levels for each docking. In ten runs the best docking results were taken to constitute a table formed of binding energies and K_i values. Graphics were generated from docking results of ligands that had the best first 50 results.

Figure 5.1 and Figure 5.2 shows K_i values belonging to the best 50 ligands for MAO-A enzyme, Figure 5.6 and Figure 5.7 shows K_i values for MAO-B, Figure 5.3 shows pK_i values of the best 25 results for MAO-A, Figure 5.8 shows pK_i values for MAO-B and Figure 5.4 shows a comparison of K_i values for MAO-A and MAO-B enzymes.

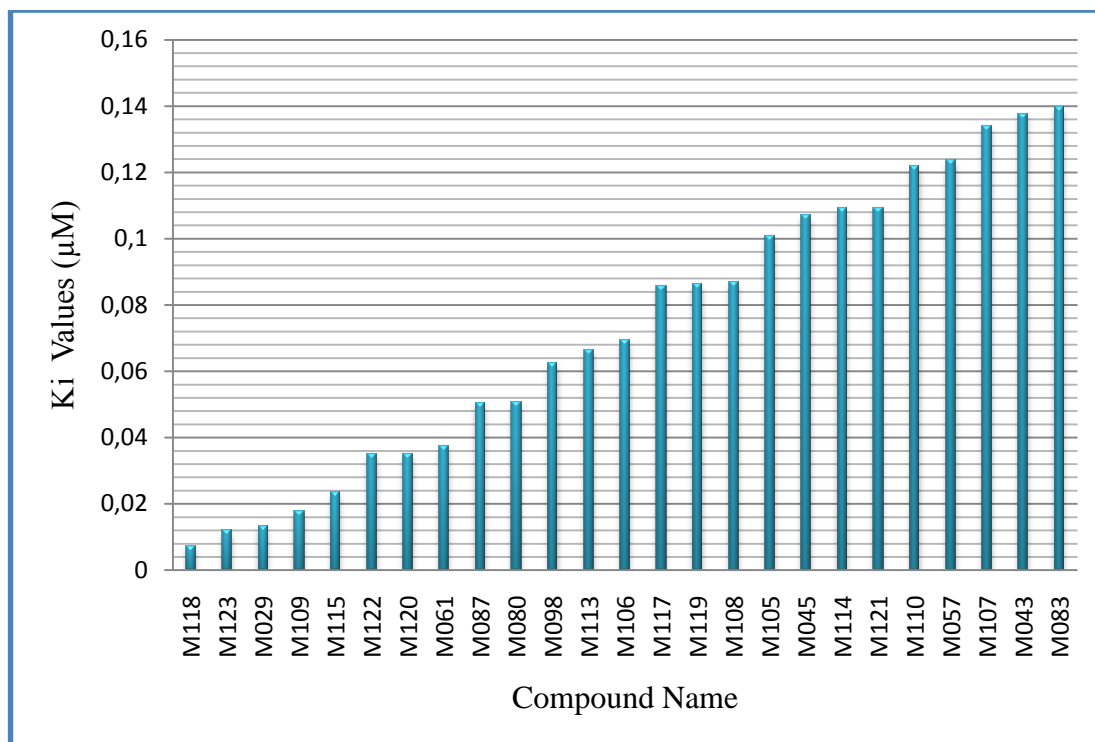


Figure 5.1: Ki values of the best 25 ligands for MAO-A enzyme

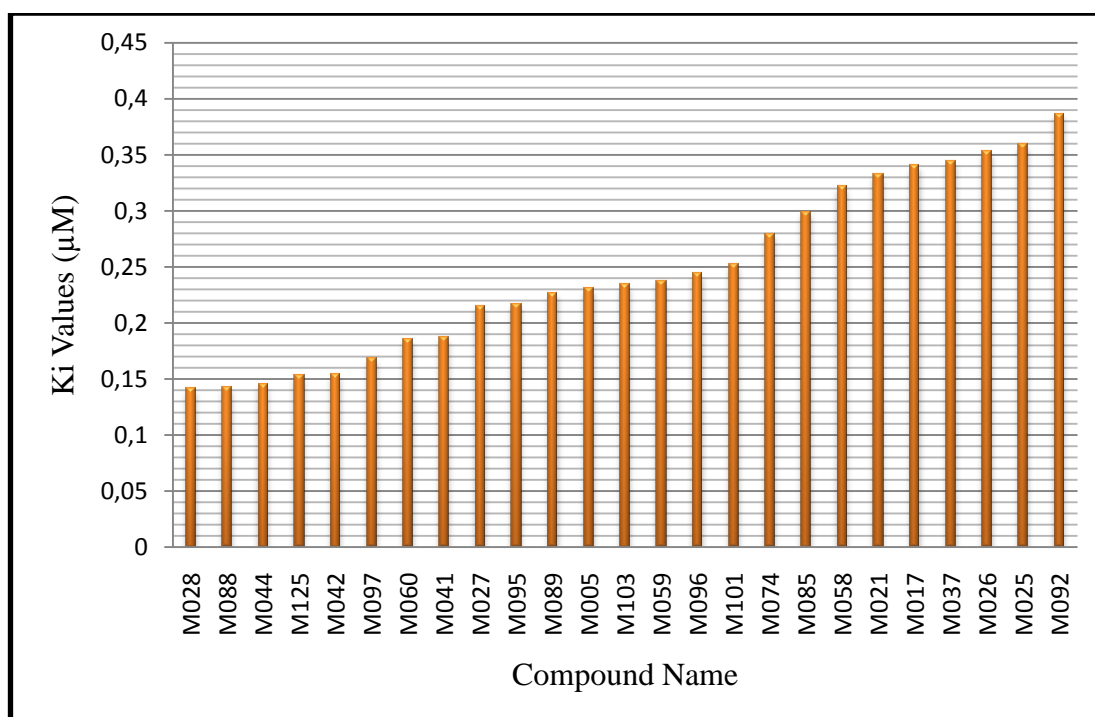


Figure 5.2: Ki values of the best 26-50 ligands for MAO-A enzyme

When it was assessed the molecular structures of ligands placed in Figure 5.1 and Figure 5.2, as a QSAR approaches it can be said that phenyl and amide groups at 3rd, 5th or 7th positions are important generally in binding to MAO-A enzyme. Figure 5.1 and Figure 5.2 takes K_i values as micromolar. The best ligand is compound M118 had 0.00725 μM inhibition constant for MAO-A enzyme. Range between first 50 ligands 0.00725 μM – 0.38645 μM . According to these results, since these 50 ligands have more effective K_i values in comparison Moclobemide, they can be seen as promising inhibitor candidates in terms of this study.

Observing Figure 5.3, it can be said that although there are similar $pK_{i(\text{MAO-A})}$ between M122 and M083, ligands between M118-M115, which are first five ligands corresponding to $pK_{i(\text{MAO-A})}$, have steeper curve. It shows that first five ligands in this graphic might be available inhibitor candidates for MAO-A enzyme.

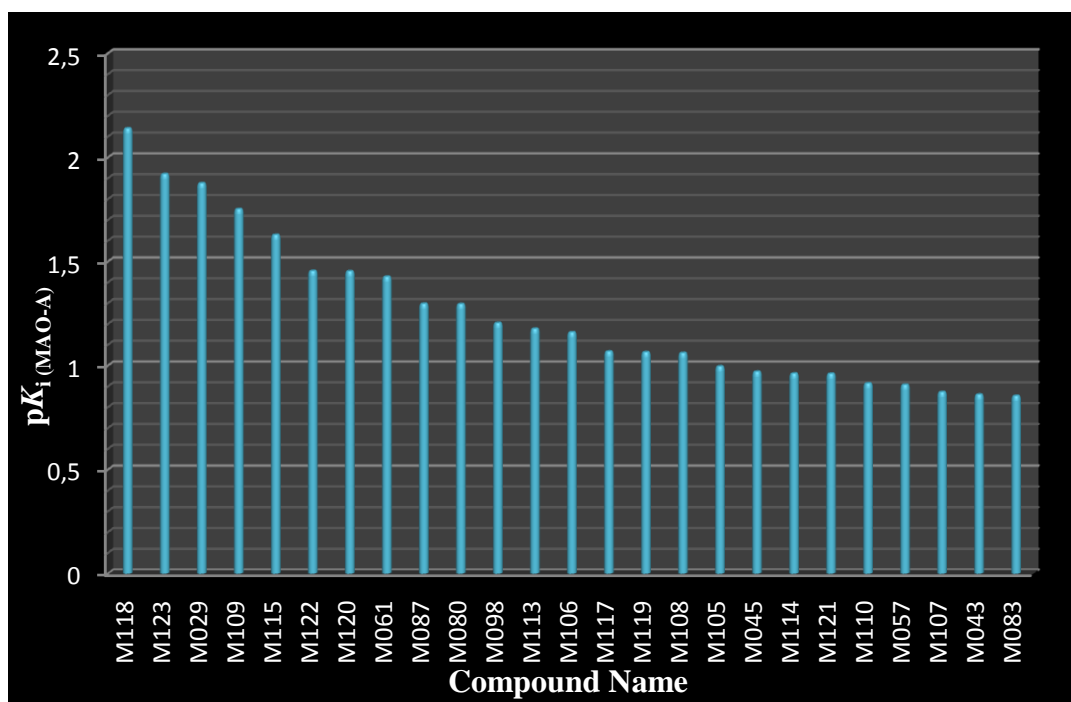


Figure 5.3: pK_i values of the best 25 ligands for MAO-A enzyme

According to Figure 5.4, compound M121 has important difference in terms of inhibition constant, but it is not the most selective ligand corresponding to K_i values of docking results as shown Table-5.1. Although M121, M114 and M083 are the compounds drawn attention in terms of selectivity, they are not the best third selective ligands.

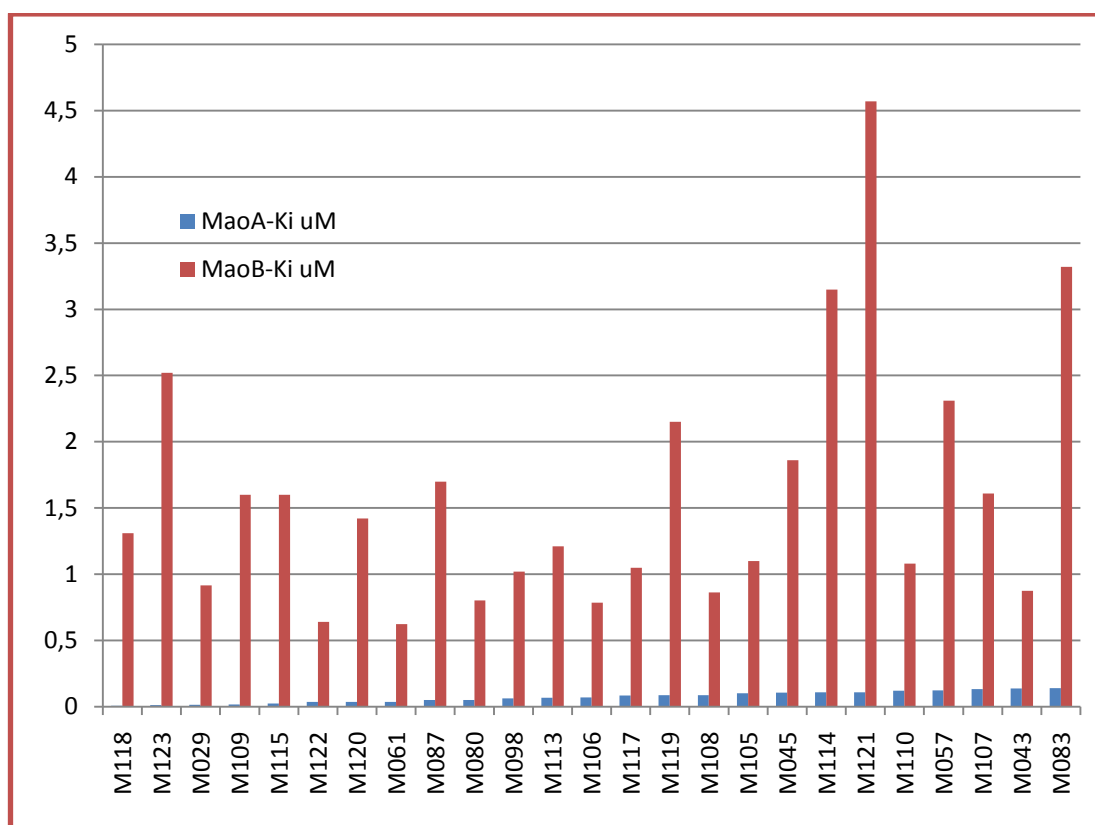


Figure 5.4: Comparison of K_i values of 25 ligands having the best results for MAO-A enzyme

The best five selective ligands are; M123 as 209 fold, M118 as 180 fold, M109 as 90 fold, M029 as 68 fold, M115 as 67 fold selective for MAO-A enzyme (Figure 5.5).

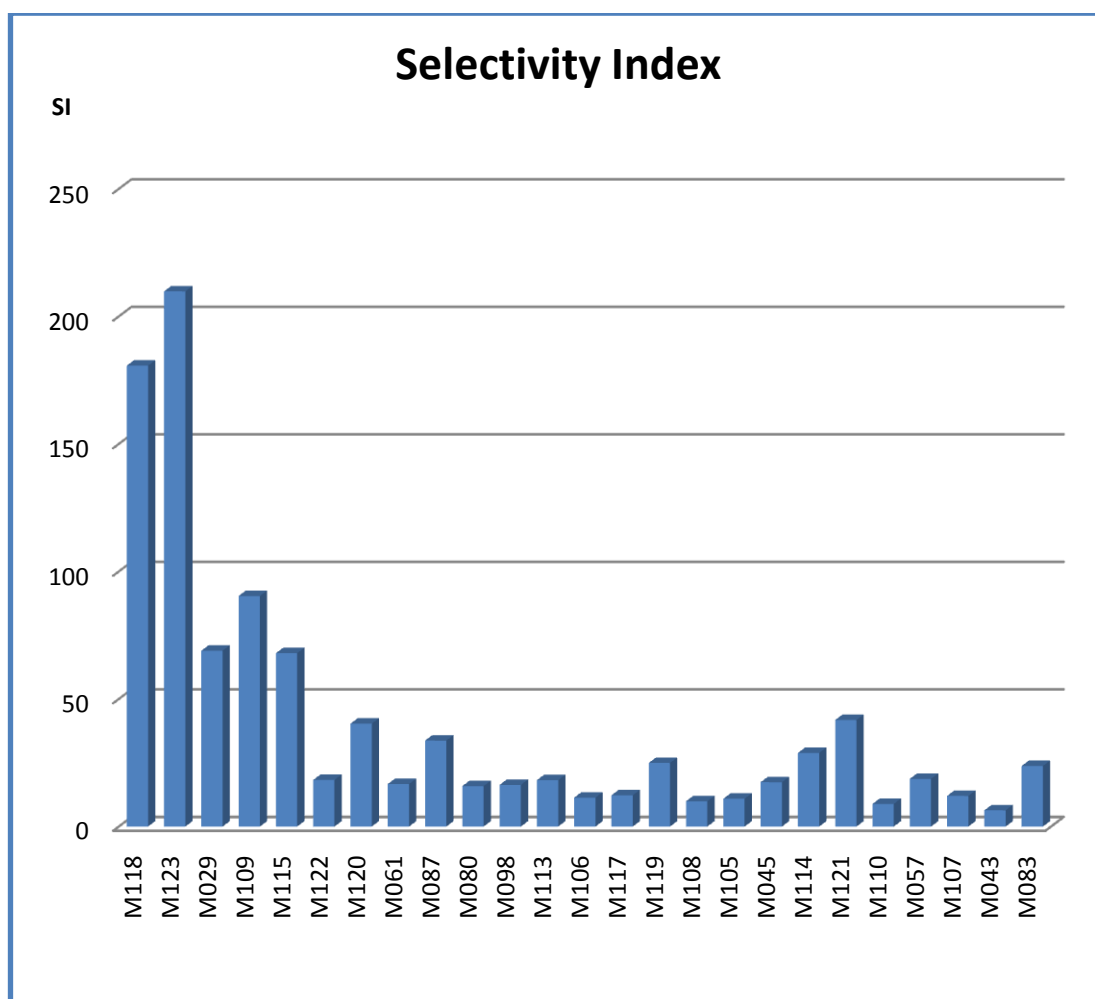


Figure 5.5: Representation of selectivity index (SI) of first the best 25 ligands for MAOA. $SI = K_i(MAO-B/MAO-A)$.

Corresponding to Figure 5.6 and Figure 5.7, first ten ligands have K_i values at nanomolar levels until $1 \mu M$ but all of them have higher inhibition constants than MAO-A.

On the other hand, ligands shown in Figure 5.6 had more effective values in comparison with Selegiline. Therefore these ligands are non-selective but more potent inhibitor candidates for MAO-B inhibition.

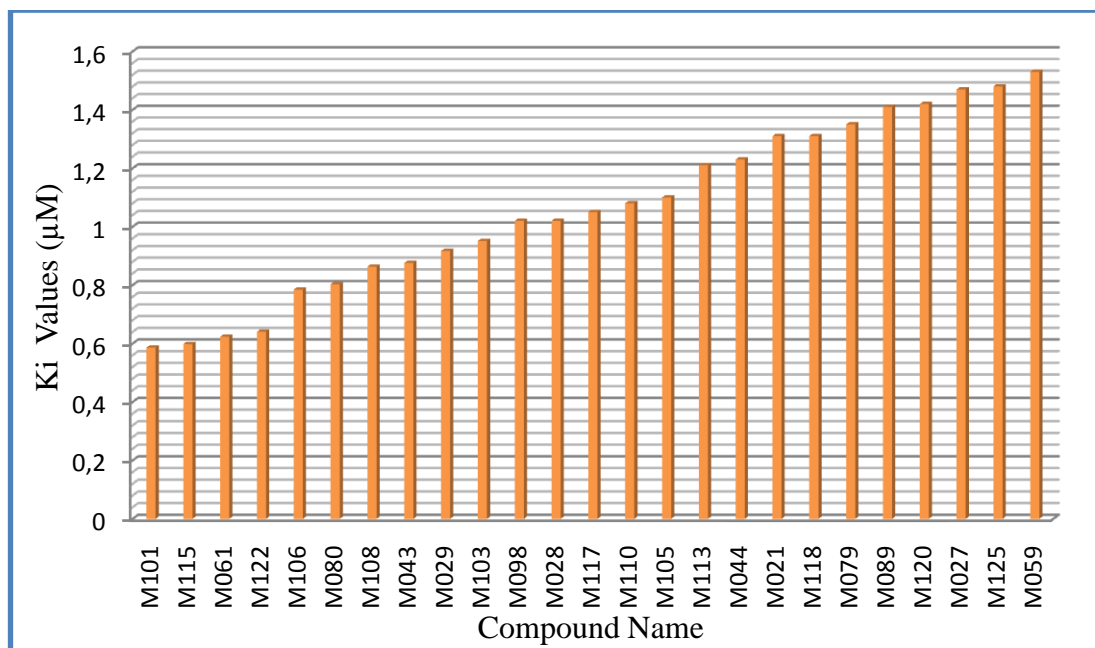


Figure 5.6: The best 25 ligands' Ki values for MAO-B enzyme

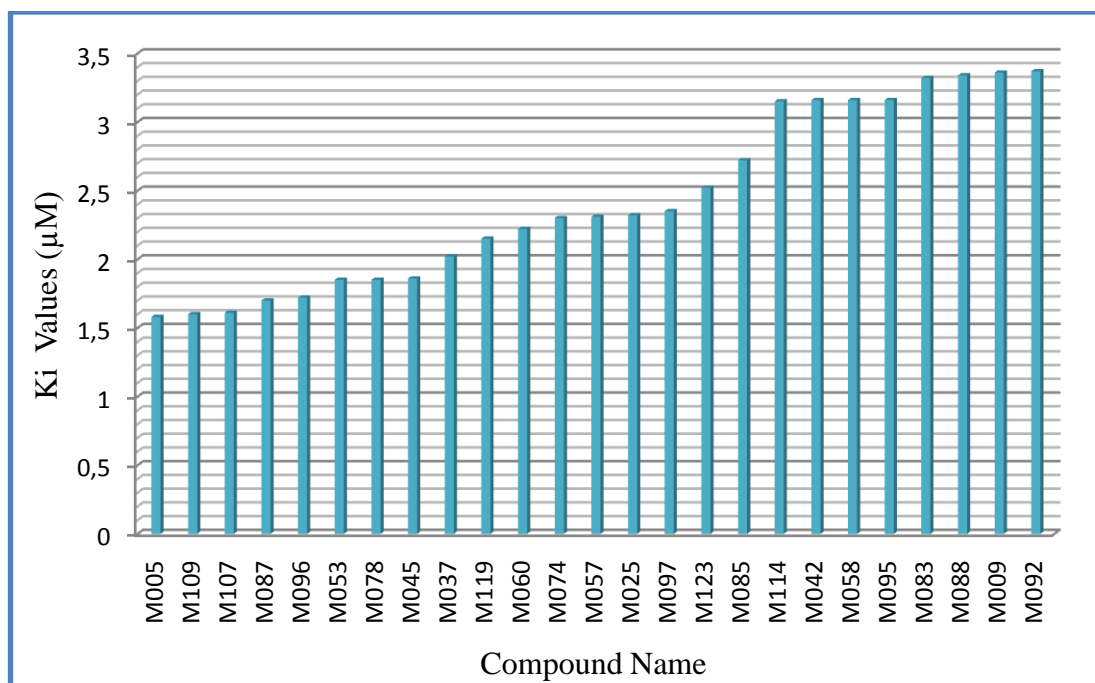


Figure 5.7: The best 26-50 ligands' Ki values for MAO-B enzyme

$pK_{i(\text{MAO-B})}$ shown in Figure 5.8 begin with 0.23 belonging to M101 ligand being the best for MAO-B in 125 ligands, down suddenly after compound M122. This situation shows us the importance of which position placed phenyl and Bromine in the coumarin nucleus during MAO-B inhibition.

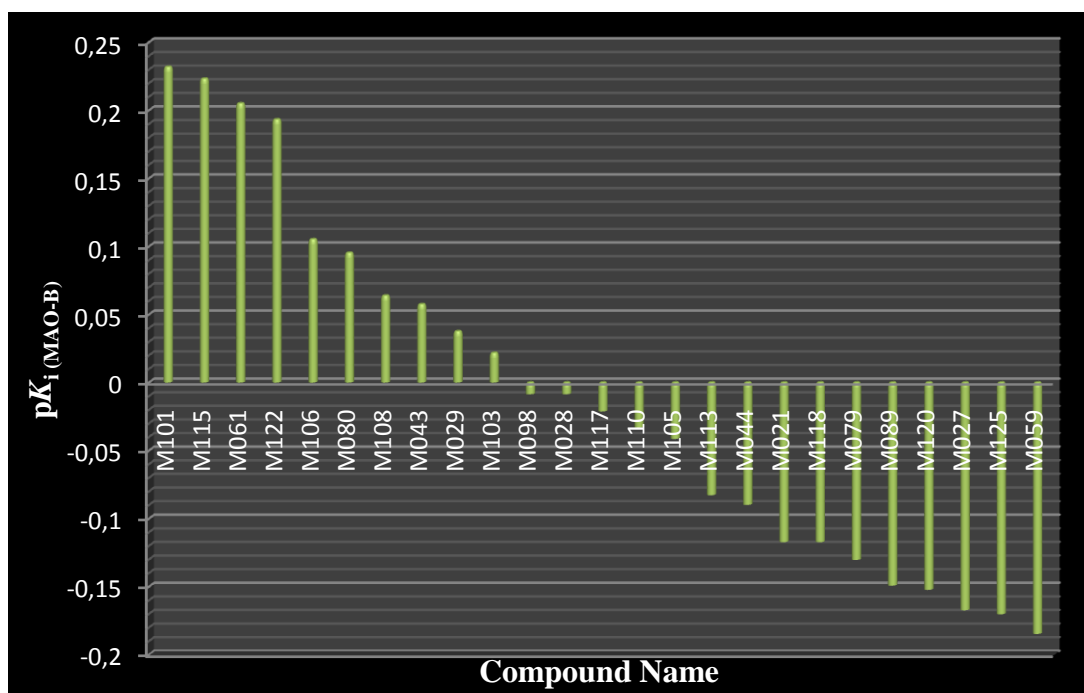


Figure 5.8: pK_i values of the best 25 ligands for MAO-B enzyme

In summary, in addition to one ligand having 209 fold smaller K_i value for MAO-A enzyme than MAO-B, these ligands have low K_i values both for MAO-A and MAO-B. Particularly against MAO-A, they have better binding specificity in comparison with Moclobemide and Selegiline inhibitors' inhibition constants. Therefore it will be useful to improve these derivatives in order to find a more selective inhibitor. However, also results of this study in the following pages are illustrating about properties of atoms which are needed to be existed and needed to be increased.

Most ligands designed in this study bind to MAO-A enzyme better than MAO-B or

they bind to both enzymes at similar levels.

While selecting five the best ligands, we looked into the smallest K_i value and binding energy according to *.dlg files arisen by AutoDock4.2 calculation. When looking for binding properties of these the best ligands, it was seen that M098 and M106 ligands had been drawn incorrectly. However, these two ligands showed better results for MAO-B and they achieved to enter into first five. Hence these two ligands were drawn and docked again. But these false drawn ligands show that if an extra hydrogen existed at the 1st position of phenyl ring which is in the 7th position of coumarin, this coumarin derivative would be more active to MAO-B enzyme.

5.2 Docking Results

Table 5.1 shows all inhibition constant (K_i) and free binding energy (ΔG) values obtained from *.dlg files belonging to 250 docking performed by AutoDock4 Amber force field. The range of K_i values were between 0.00725-48.15 μM for MAO-A enzyme and 0.5861-77.99 μM for MAO-B enzyme. The range of free binding energy values were between -11.10 kcal/mol and -5.89 kcal/mol for MAO-A and between -8.50 kcal/mol and -5.60 kcal/mol for MAO-B enzyme. The ligand having the worst result was compound M062. M062 had 48.15 μM inhibition constant for MAO-A and 77.99 μM for MAO-B enzyme. On the other hand, it can be seen that values are near to each others roughly.

Table-5.1: Ki and free binding energy values of 125 ligands for MAO enzymes

Ligand Name	MAO-A ΔG Kcal/mol	MAO-A Ki μM	MAO-B ΔG Kcal/mol	MAO-B Ki μM	Selectivity Index Ki(MAO-B /MAO-A)
M001	-7.04	6.93	-6.85	9.52	1.37
M002	-6.96	7.94	-6.46	18.26	2.30
M003	-7.66	2.43	-6.78	10.73	4.42
M004	-7.76	2.07	-6.89	8.87	4.29
M005	-9.05	0.23087	-7.91	1.58	6.84
M006	-6.4	20.49	-6.46	18.34	0.90
M007	-7.12	6.08	-6.34	22.7	3.73
M008	-7.18	5.42	-6.37	21.43	3.95
M009	-8.32	0.79658	-7.47	3.36	4.22
M010	-6.3	24.09	-6.08	35.01	1.45
M011	-6.98	7.59	-6.98	7.63	1.01
M012	-6.92	8.5	-7.05	6.83	0.80
M013	-8.57	0.52199	-7.36	4.04	7.74
M014	-6.27	25.15	-6.05	36.98	1.47
M015	-7.17	5.56	-6.62	13.97	2.51
M016	-7.34	4.18	-6.35	22.17	5.30
M017	-8.82	0.34045	-7.19	5.39	15.83
M018	-7.05	6.77	-6.12	32.9	4.86
M019	-7.81	1.88	-6.94	8.15	4.34
M020	-8.29	0.83693	-7.13	5.89	7.04
M021	-8.84	0.33229	-8.03	1.31	3.94
M022	-7.15	5.78	-6.14	31.51	5.45
M023	-7.81	1.9	-7.06	6.63	3.49
M024	-7.93	1.53	-6.61	14.22	9.29
M025	-8.79	0.35902	-7.69	2.32	6.46
M026	-8.80	0.35275	-7.23	5.05	14.32
M027	-9.09	0.21547	-7.96	1.47	6.82
M028	-9.35	0.14103	-8.17	1.02	7.23
M029	-10.74	0.0133	-8.24	0.91686	68.94
M030	-6.61	14.18	-6.42	19.53	1.38
M031	-6.96	7.89	-6.93	8.38	1.06
M032	-7.00	7.39	-7.21	5.17	0.70
M033	-8.32	0.80022	-7.02	7.2	9.00
M034	-7.12	6.03	-6.39	20.67	3.43
M035	-7.42	3.66	-6.83	9.83	2.69
M036	-7.57	2.82	-6.93	8.38	2.97
M037	-8.82	0.34408	-7.77	2.02	5.87
M038	-7.05	6.8	-6.54	15.99	2.35
M039	-7.59	2.72	-7.00	7.35	2.70

M040	-7.66	2.42	-7.11	6.12	2.53
M041	-9.18	0.18716	-7.42	3.65	19.50
M042	-9.29	0.15427	-7.50	3.16	20.48
M043	-9.36	0.1377	-8.26	0.87582	6.36
M044	-9.33	0.14493	-8.06	1.23	8.49
M045	-9.51	0.10695	-7.82	1.86	17.39
M046	-6.50	17.17	-5.77	58.93	3.43
M047	-6.92	8.52	-6.65	13.3	1.56
M048	-7.01	7.22	-6.77	10.85	1.50
M049	-8.63	0.46892	-7.12	6.01	12.82
M050	-6.94	8.15	-6.29	24.5	3.01
M051	-7.63	2.57	-7.05	6.81	2.65
M052	-7.58	2.8	-6.95	8.02	2.86
M053	-8.67	0.44168	-7.82	1.85	4.19
M054	-6.97	7.79	-6.56	15.67	2.01
M055	-7.66	2.42	-7.22	5.08	2.10
M056	-7.74	2.14	-6.82	9.99	4.67
M057	-9.42	0.12361	-7.69	2.31	18.69
M058	-8.86	0.32198	-7.50	3.16	9.81
M059	-9.04	0.2374	-7.94	1.53	6.44
M060	-9.19	0.18483	-7.71	2.22	12.01
M061	-10.13	0.03739	-8.47	0.62352	16.68
M062	-5.89	48.15	-5.60	77.99	1.62
M063	-6.64	13.51	-6.55	15.91	1.18
M064	-6.67	12.83	-6.84	9.68	0.75
M065	-8.27	0.86227	-6.78	10.73	12.44
M066	-6.75	11.22	-6.14	31.72	2.83
M067	-7.00	7.41	-6.20	28.59	3.86
M068	-8.59	0.50123	-7.07	6.57	13.11
M069	-6.77	10.97	-6.11	33.15	3.02
M070	-6.89	8.84	-6.21	27.95	3.16
M071	-8.48	0.60513	-6.75	11.29	18.66
M072	-7.38	3.92	-6.62	13.99	3.57
M073	-7.50	3.16	-6.83	9.88	3.13
M074	-8.94	0.27944	-7.69	2.3	8.23
M075	-7.42	3.65	-6.73	11.64	3.19
M076	-7.63	2.55	-6.77	10.83	4.25
M077	-8.67	0.44136	-7.37	3.96	8.97
M078	-8.62	0.48251	-7.82	1.85	3.83
M079	-8.64	0.46699	-8.01	1.35	2.89
M080	-9.95	0.05059	-8.32	0.80283	15.87
M081	-7.39	3.84	-6.60	14.51	3.78
M082	-7.78	1.99	-6.79	10.6	5.33

Continuation of Table 5.1

M083	-9.35	0.13977	-7.47	3.32	23.75
M084	-7.50	3.18	-6.88	9.04	2.84
M085	-8.90	0.2994	-7.59	2.72	9.08
M086	-7.37	3.99	-6.95	8.11	2.03
M087	-9.96	0.05043	-7.87	1.7	33.71
M088	-9.34	0.1421	-7.47	3.34	23.50
M089	-9.07	0.22611	-7.98	1.41	6.24
M090	-7.52	3.05	-6.80	10.29	3.37
M091	-7.63	2.55	-6.66	13.24	5.19
M092	-8.75	0.38645	-7.47	3.37	8.72
M093	-7.33	4.23	-6.75	11.33	2.68
M094	-7.52	3.09	-6.65	13.28	4.30
M095	-9.09	0.21724	-7.50	3.16	14.55
M096	-9.02	0.24399	-7.87	1.72	7.05
M097	-9.24	0.16809	-7.68	2.35	13.98
M098	-10.13	0.03761	-8.18	0.57968	15.41
M099	-8.12	1.12	-7.41	3.7	3.30
M100	-8.23	0.9338	-7.39	3.85	4.12
M101	-9.00	0.25181	-8.50	0.58616	2.33
M102	-8.10	1.15	-7.30	4.42	3.84
M103	-9.04	0.23443	-8.22	0.95096	4.06
M104	-8.36	0.74916	-7.37	3.93	5.25
M105	-9.54	0.10088	-8.13	1.1	10.90
M106	-9.77	0.0337	-8.33	0.32413	9.62
M107	-9.38	0.13395	-7.90	1.61	12.02
M108	-9.63	0.08691	-8.27	0.86317	9.93
M109	-10.58	0.0177	-7.91	1.6	90.40
M110	-9.43	0.12169	-8.14	1.08	8.88
M111	-8.40	0.69184	-7.45	3.45	4.99
M112	-8.14	1.08	-7.33	4.22	3.91
M113	-9.79	0.06648	-8.07	1.21	18.20
M114	-9.50	0.10911	-7.51	3.15	28.87
M115	-10.41	0.02354	-8.49	1.6	67.97
M116	-8.40	0.69519	-7.41	3.73	5.37
M117	-9.64	0.08553	-8.16	1.05	12.28
M118	-11.10	0.00725	-8.03	1.31	180.69
M119	-9.64	0.08619	-7.73	2.15	24.94
M120	-10.17	0.0352	-7.98	1.42	40.34
M121	-9.50	0.10938	-7.29	4.57	41.78
M122	-10.17	0.03507	-8.45	0.64062	18.27
M123	-10.81	0.01201	-7.64	2.52	209.83
M124	-8.23	0.92426	-7.20	5.29	5.72
M125	-9.30	0.1535	-7.95	1.48	9.64

Continuation of Table 5.1

5.3 Evaluation of M029 Ligand and MAO-A Enzyme

According to docking results of M029 ligand (5,7-diphenyl-3-methoxycoumarin derivative) and MAO-A as shown in Figure 5.9 and Figure 5.10; it is increasing the binding affinity if the coumarin scaffold carries bulky groups on the 5th and 7th positions. Because these groups are participating easily van der Waals interactions especially with amino acids that have short side group as like glycine and alanine.

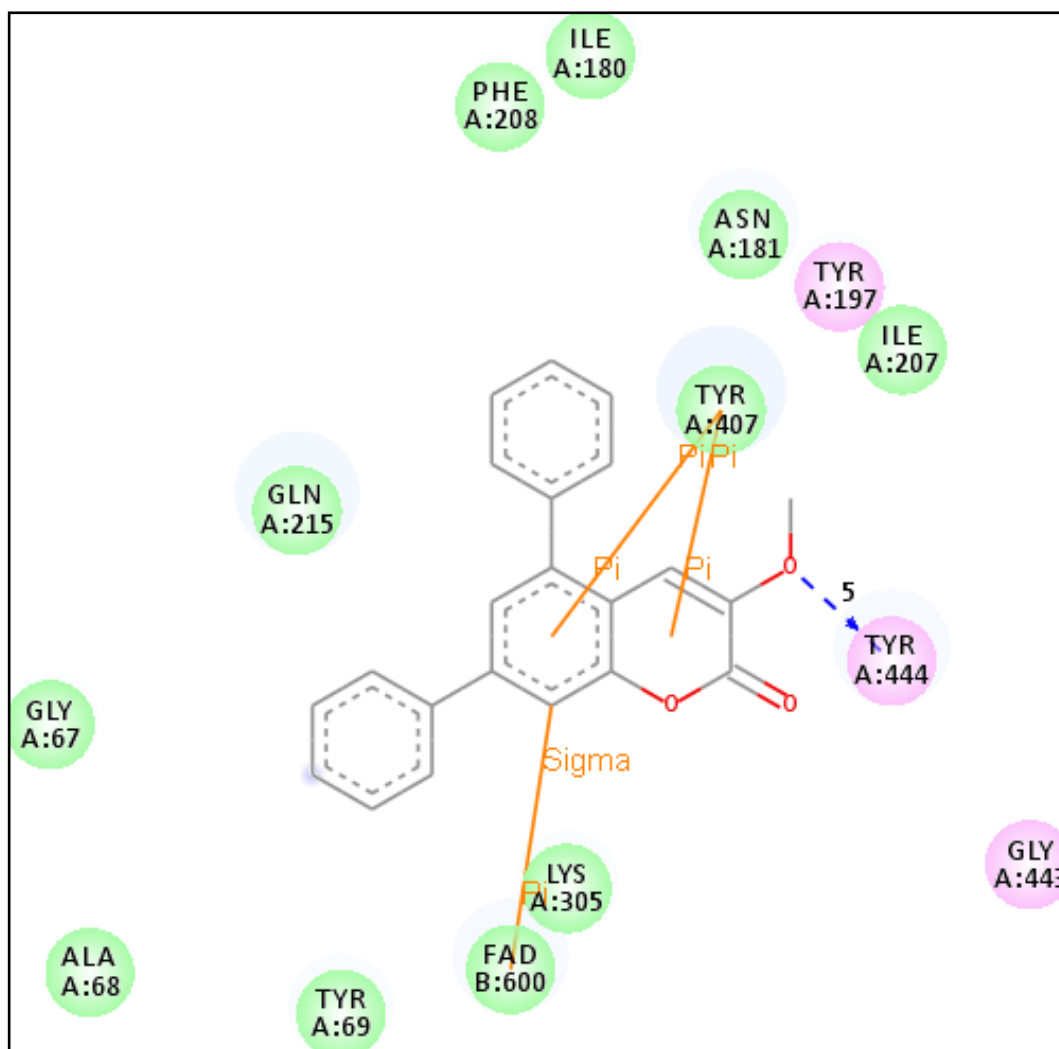


Figure 5.9: 2-D representation of the docked orientation of M029 in MAO-A binding site

Two pi-pi interactions took place between the phenyl ring and α -pyrone ring of the inhibitor and Tyr407 amino acid where was in the aromatic cage.

It was seen that van der Waals interactions between ligand's atoms and Gly67, Ala68, Tyr69, Lys305, Ile207, Phe208, Ile180 amino acids. Particularly Asn181 achieved strong van der Waals interactions and Gln215 performed very strong van der Waals forces. When it was examined to electrostatic interactions, plainly Tyr197 and Gly443 rendered electrostatic interactions with the ligand.

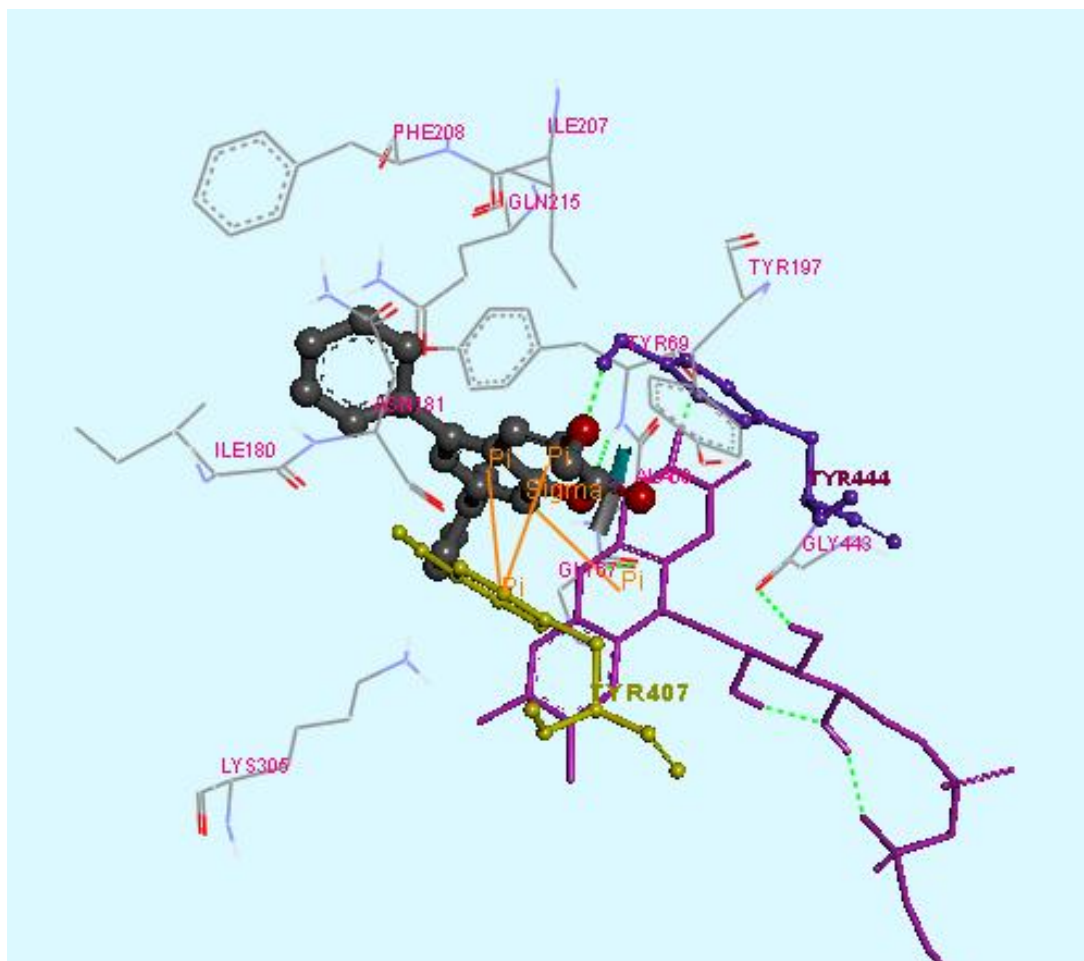


Figure 5.10: 3-D representation of M029 with MAO-A enzyme. Yellow amino acid is TYR407, dark purple molecule that is above the ligand is TYR444, dark pink large molecule is FAD, red balls represent Oxygen atoms, grey balls are Carbons

A polar interaction is seen between Tyr444 and methoxy that is in the third position of ligand, this hydrogen bond length is 5 Å. There are one each pi-pi interactions between benzene ring and α -pyrone ring of coumarin scaffold with Tyr407 amino acid. The pi-pi interactions performing Tyr407 and benzene ring has 4.1 Å distance, other pi-pi interactions has 3.5 Å distance. Apparently, as peculiar to ligand M029, it was occurred a pi-sigma interactions that have 3.7 Å distance between C4 atom of ligand and B:FAD600 atom. For M029 ligand (5,7-diphenyl-3-methoxycoumarin derivative) according to *.dlg file produced by AutoDock4.2, Ki value is 13.3 nM and free binding energy is -10.74 kcal/mol. When results table is taken into account, compound M029 is the best third ligand for MAO-A.

5.4 Evaluation of M029 Binding Properties for MAO-B Enzyme

Although ligand M029 hasn't good binding results for MAO-B, it made lots of interactions with around amino acids. Also the most important ones of them are four pi interactions. The pi interactions that are seeing at Figure 5.11 and Figure 5.12 performed between coumarin scaffold and the near polar amino acids intensively. A pi-pi interaction that has 5.58 Å distance was performed between α -pyrone ring of M029 and Tyr326 of MAO-B. Other pi-pi interaction has 4.79 Å range was formed between benzene ring of M029 ligand's coumarin nucleus and Tyr326 amino acid. Also α -pyrone ring of ligand has a pi-sigma interaction has 3.97 Å with Ser200. Another pi-sigma interaction that has 3.25 Å range was occurred between phenyl ring which is in the 5th position of coumarin scaffold and Thr201 amino acid. As seen in Figure 5.11, phenyl ring which is in the 5th position of coumarin has strong electrostatic interactions with Thr201. In addition to this, Tyr326, Pro102, Ile199,

Ser200 have slightly strong electrostatic interactions with the compound M029 (5,7-diphenyl-3-methoxycoumarin derivative).

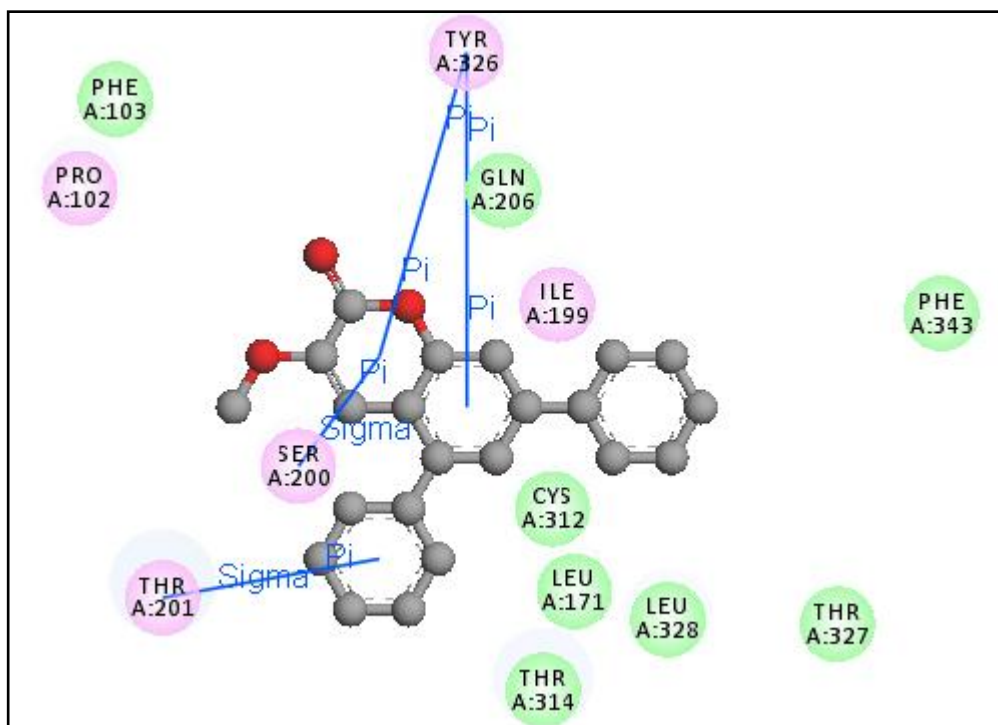


Figure 5.11: 2-D representation of M029 ligand's position in MAO-B enzyme. Red balls represent Oxygen atoms; grey balls represent Carbon atoms in the ligand

As can be seen easily at 3-D representation of Figure 5.12 since Thr314 is opposite to phenyl ring which is in the 5th position of coumarin, it was strong van der Waals interactions between them. On the other hand Leu328 and Gln206 amino acids have slightly strong van der Waals interactions with ligand's atoms. Other amino acids made van der Waals interactions are Phe103, Thr327 and Cys312.

Interestingly, in spite of plurality of the interactions, compound M029 the best fourth selective inhibitor in these 125 ligands according to obtained results from this study. Ki value 916.8 nM and free binding energy (ΔG) is -8.24 kcal/mol for MAO-B.

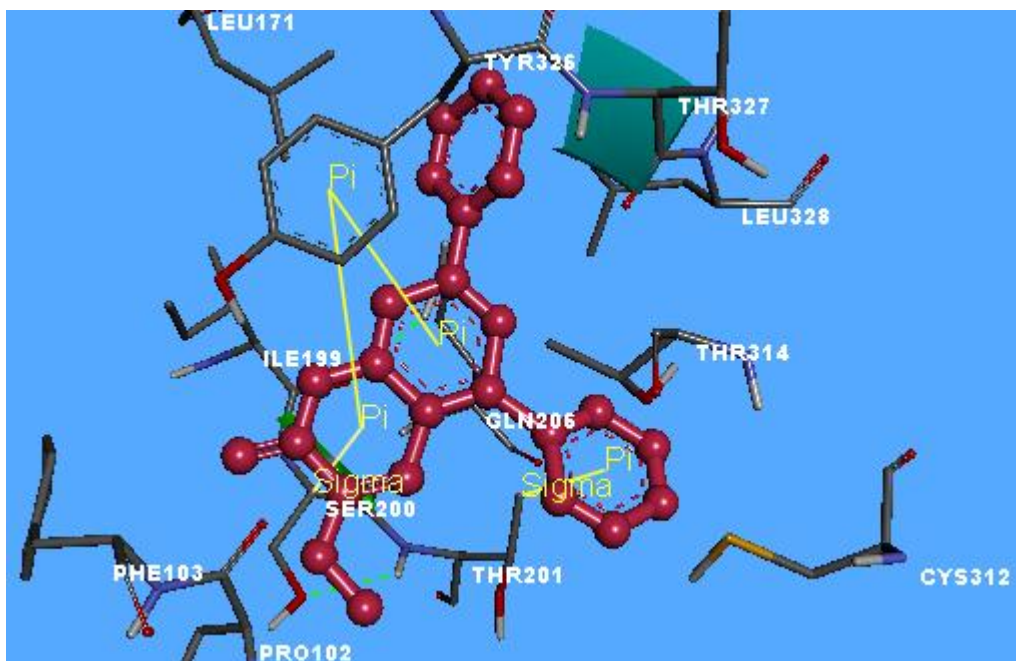


Figure 5.12: 3-D representation of M029' position in MAO-B enzyme. Ligand is represented with pink ball and stick format; grey ball represents Carbon atom.

According to calculated K_i results, compound M029 is more effective to MAO-A 69 fold than MAO-B.

In light of the foregoing it can be said that compound M029 is a hopeful inhibitor candidate for MAO-A in the treatment of depression.

5.5 Evaluation of M109 Ligand with MAO-A Enzyme

M109 (3-Bromo-5,7-diphenylcoumarin derivative) has lots of vary interactions with amino acids placing MAO-A enzyme binding cavity, particularly numerous van der Waals interactions. Ligand M109 has Br atom at the 3rd position. Hence it is important performing a polar interaction between Br atom and Tyr444 amino acid had 5.2 Å distance that is known a specific amino acid to active site.

As being at M029 ligand, also in here, some pi interactions were come across between Tyr407 and coumarin nucleus. A strong van der Waals force was occurred between this amino acid and coumarin nucleus. As can be seen in Figure 5.13, a pi-pi interaction was made between Tyr407 and α -pyrone nucleus that has 3.35 Å distance. Other pi-pi interaction had 3.98 Å distance was formed between also Tyr407 and benzene ring of coumarin derivative.

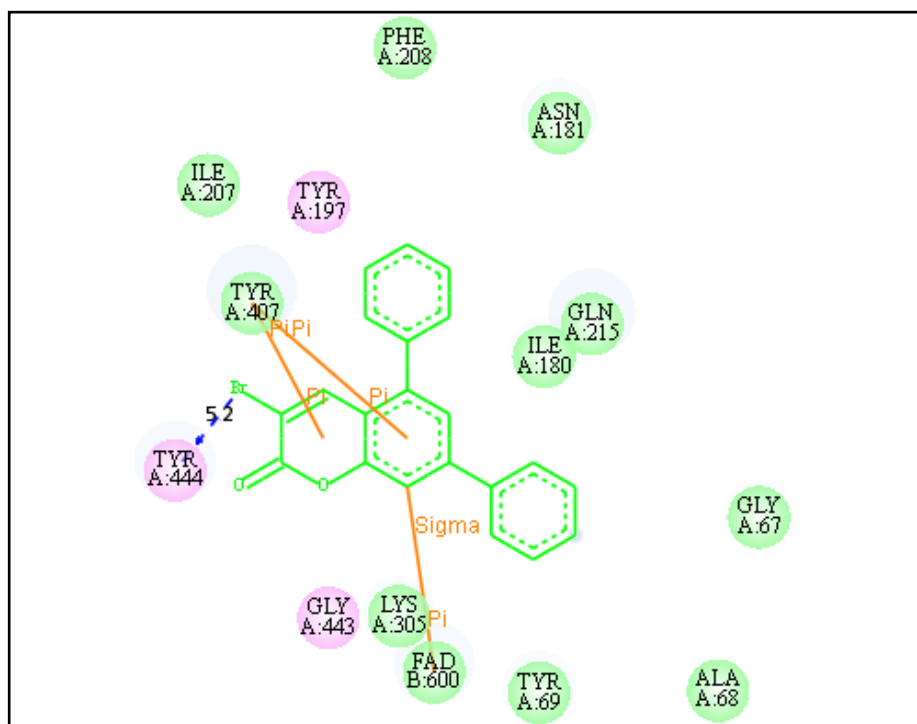


Figure 5.13: 2-D representation of compound M109 and amino acids placing in binding site of MAO-A enzyme

A pi-sigma interaction had 3.6 Å distance was performed between Carbon atom at the 8th position of ligand and FAD B:600 aromatic ring. This interaction is shown in clearly Figure 5.14.

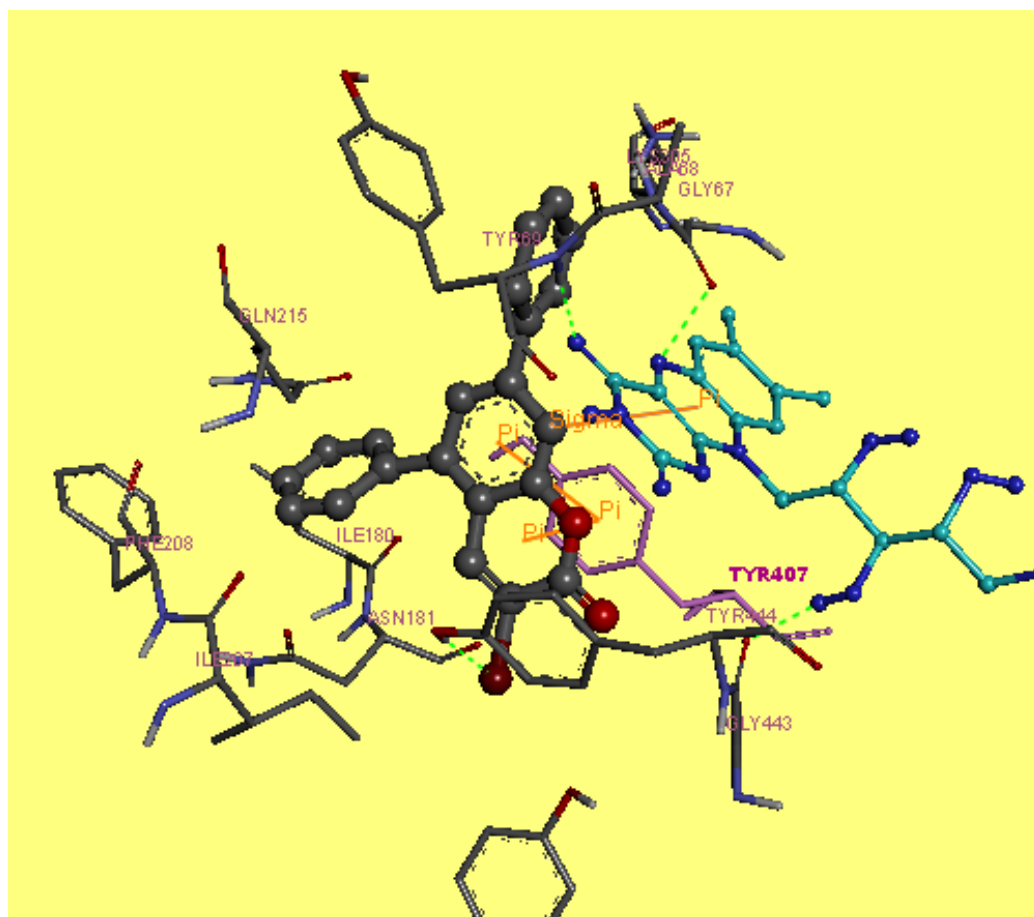


Figure 5.14: 3-D representation of M109 ligand and MAO-A enzyme. Blue molecule represents FAD molecule, navy blue balls are Nitrogen, purple molecule represents Tyr407, polar interactions are shown with green dashed lines.

Some electrostatic interactions were performed between Tyr197 and ligand' atoms. Phe208, Ile207, Gly67, Ile180, Tyr69, Ala68, Lys305 amino acids rendered van der Waals interactions with M109 ligand. Particularly Gln215 carried out strong van der Waals interactions with coumarin nucleus. Apparently Asn181 made slightly strong van der Waals interactions with M109 ligand (3-Bromo-5,7-diphenylcoumarin derivative). K_i value of M109 ligand with MAO-A is 17.70 nM, free binding energy value is -10.58 kcal/mol. Compound M109 is the best 4th ligand seeing MAO-A binding properties. It can be considered as a potential inhibitor candidate because of muchness of the interactions and shortness of pi-pi interaction distance.

5.6 Evaluation of M109 Ligand with MAO-B Enzyme

M109 has less aromatic interactions with MAO-B enzyme active site. The main group that has important role in terms of strong interactions was phenyl at 5th position of ligand. Figure 5.15 shows these interactions as 2-D shape by aid of Discovery Studio 3.5 Accelrys Software.

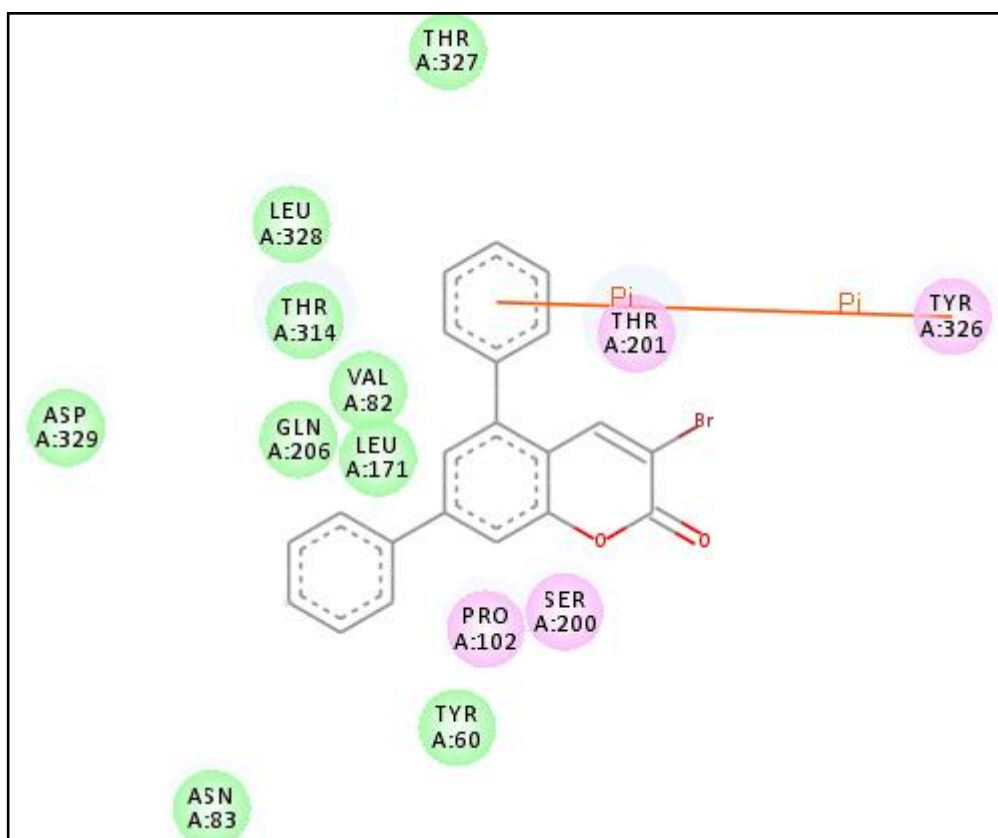


Figure 5.15: 2-D representation of compound M109 and amino acids placing in binding site of MAO-B enzyme

As can be seen in Figure 5.16 a pi-pi interaction was occurred between Tyr326 and phenyl ring which is in the 5th position of coumarin scaffold has distance of 3,99 Å. This amino acid installed slightly strong electrostatic interactions with this aromatic group of ligand.

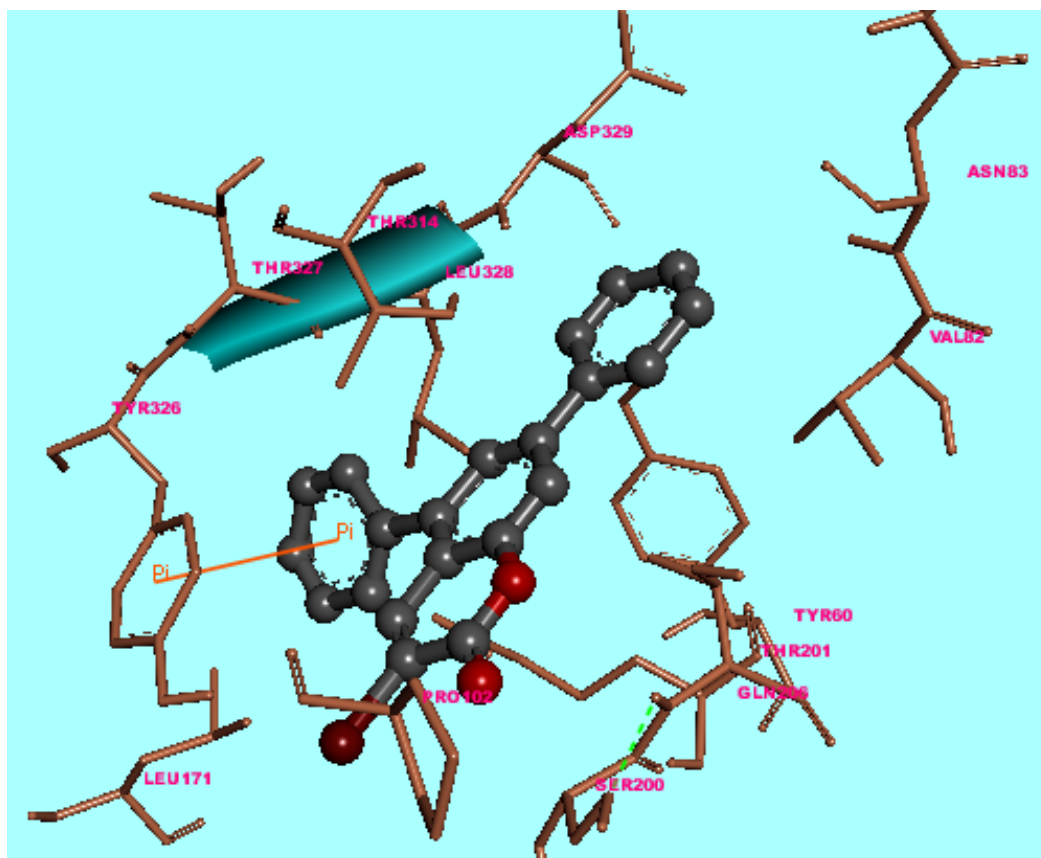


Figure 5.16: 3-D representation of M109 ligand and amino acids placing active site of MAO-B enzyme. Burgundy ball represents Bromine atom, red balls are Oxygen atoms, grey balls are Carbon atoms.

Apparently, strong electrostatic interactions were performed between the same phenyl ring and Tyr201 amino acid. It was observed strong van der Waals interactions between Thr314 and ligand's atoms. It was observed at average strong van der Waals forces between atoms of ligand and Leu328, Val82, Asp329 amino acids. As for Asn83, Tyr60, Leu171, Gln206, Thr327, it was seen that weaker van der Waals interactions had been performed with coumarin derivative's atoms.

Ki value for MAO-B is 1.60 μM , free binding energy is -7.90 kcal/mol. Compound M109 have 90 fold better inhibition to MAO-A enzyme than MAO-B.

5.7 Evaluation of Binding Properties between Compound M115 and MAO-A Enzyme

Compound M115 has a Bromine atom at the 7th position, and phenyl rings at 3rd and 5th position of coumarin scaffold. As can be seen Figure 5.17 and Figure 5.18, one each pi-pi interactions were formed between Tyr407 amino acid and α -pyrone ring and benzene ring of coumarin nucleus. The length of the pi-pi interaction which was performed between Tyr407 and α -pyrone ring is 4.4 Å. Other pi-pi interaction has 3.59 Å distance that was formed with benzene. A pi-sigma interaction that has 3.27 Å distance was observed between FAD B:600 and Carbon atom at the 6th position of ligand.

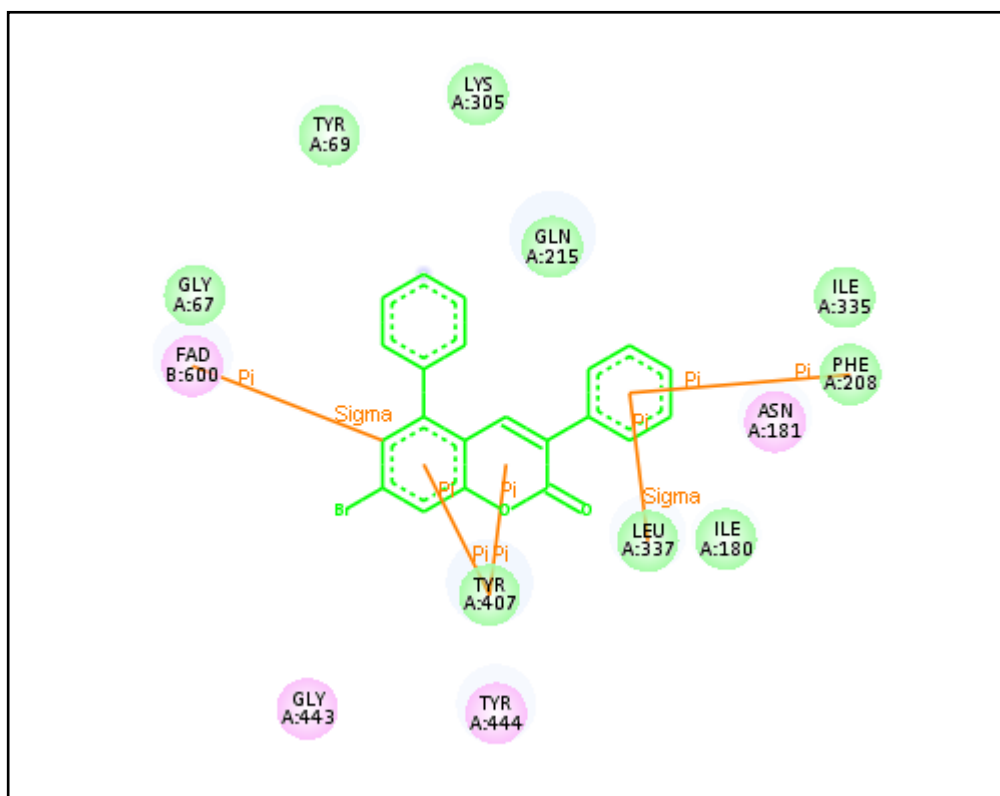


Figure 5.17: 2-D representation of M115 ligand and MAO-A enzyme's amino acids position in the active site

Another pi-sigma interaction was formed which has 3.75 Å distance between phenyl at 3rd position of ligand and Leu337 amino acid. Same phenyl ring made pi-pi interaction which has 4.98 Å distance with phenyl ring of Phe208 amino acid as shown Figure 5.18.



Figure 5.18: 3-D representation of compound M115 and MAO-A enzyme. Green ball and stick molecule represents M115 ligand, polar interactions are shown with green dashed lines.

Some electrostatic interactions were occurred with Gly67, Tyr444, Asn181 amino acids. Van der Waals interactions were occurred between ligand and Tyr69, Lys305, Gln215, Ile335 and Ile180 amino acids. Compound M115 (7-Bromo-3,5-diphenyl-coumarin derivative) has relatively good docking results, considering K_i value and free binding energy to MAO-A enzyme. Compound M115 has a different property when taken account docking results in terms of selectivity. Because compound M115 has the best 5th docking result in 125 results to MAO-A enzyme, also this compound has the best 2nd docking result for MAO-B and the best 5th compound in terms of

selectivity. K_i value of compound M115 is 23.54 nM, free binding energy is -10.41 kcal/mol for MAO-A enzyme.

5.8 Evaluation of M115 and MAO-B Binding Properties

Compound M115 (3-Bromo-5,7-diphenylcoumarin derivative) had a few interactions with MAO-B enzyme but it has amenable results with both of two enzymes. Two phenyl rings which is in the 5th and 7th positions of coumarin nucleus have valuable responsibility while interact with MAO-B enzyme's amino acids as seen in Figure 5.19. Also these phenyl rings are important in the settlement to binding cavity.

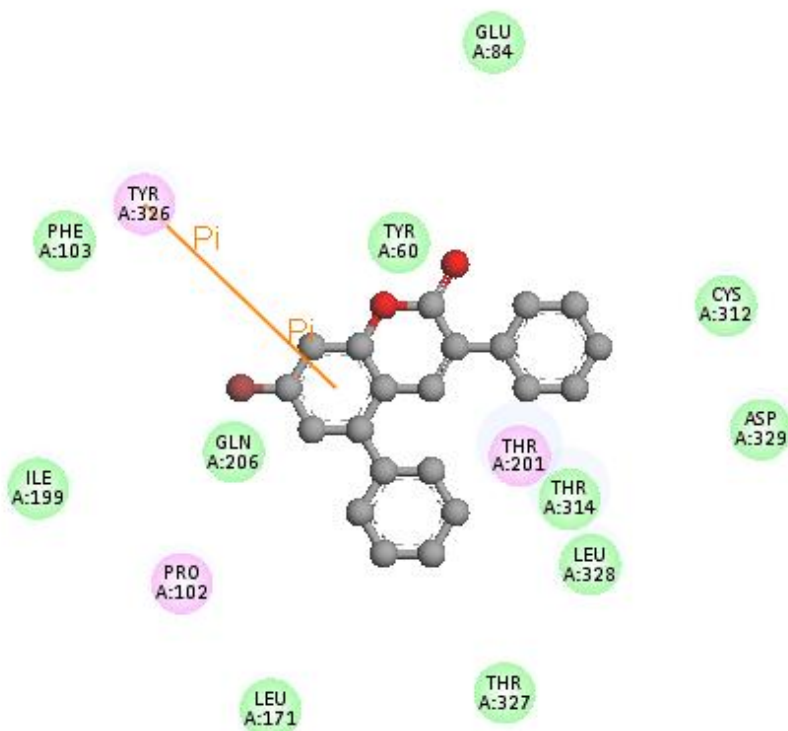


Figure 5.19: M115 ligand and MAO-B enzyme binding properties 2-D representation. Red balls represent Oxygen atoms, grey balls are Carbon atoms and burgundy ball is Bromine atom

Strong van der Waals forces were occurred between Thr314 and these phenyl rings of coumarin derivative. As shown in Figure 5.20, a pi-pi interaction that had 5.28 Å distance was formed between Tyr326 and benzene ring of coumarin nucleus.

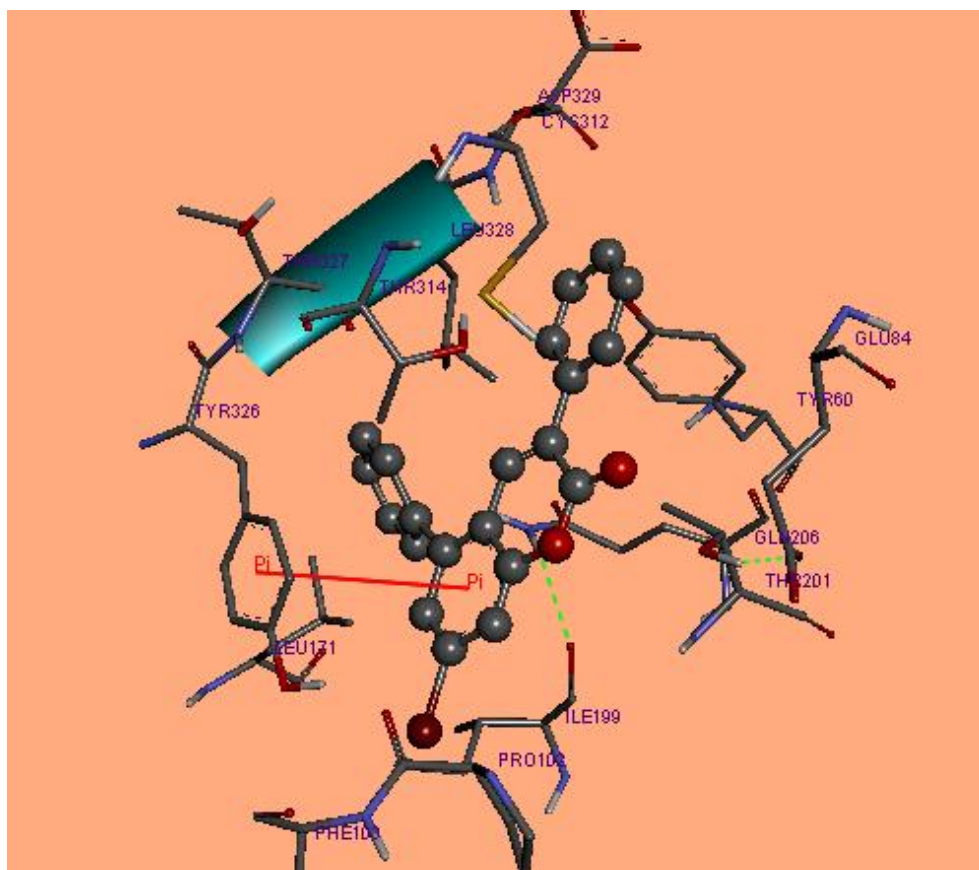


Figure 5.20: 3-D representation of M115 ligand and MAO-B enzyme binding properties. Red balls represent Oxygen atoms, grey balls are Carbon atoms and burgundy ball is Bromine atom. Green dashed lines represent polar interactions.

A strong electrostatic interaction was installed between Thr201 amino acid and phenyl ring at the 3rd position of ligand. Compound M115 and MAO-B complex has 597.98 nM Ki value and -8.49 kcal/mol free binding energy. M115 ligand is more effective 69 fold for MAO-A than MAO-B. It is the best second ligand for MAO-B enzyme in these 125 ligands. Compound M115 has a good inhibition effect for MAO-B enzyme as like being for MAO-A enzyme.

5.9 Evaluation of M118 Ligand and MAO-A Enzyme Binding Properties

Compound M118 (3-amide-5,7-diphenylcoumarin derivative) is an available inhibitor candidate for MAO-A that has two aromatic group at 5th and 7th position of coumarin scaffold which has an important role at placed in hydrophobic cavity of the enzyme. M118 ligand shows a very good settlement in MAO-A enzyme binding cavity. In the Figure 5.22, it can be seen clearly three dimensional position of compound M118. A pi-pi interaction had 3.43 Å distance was installed between Tyr407 amino acid and α -pyrone ring of coumarin nucleus. Same polar aromatic amino acid made another pi-pi interaction with benzene ring of coumarin had 4.25 Å distance. As shown in the Figure 5.21, two polar interactions were established. One of them was formed between Tyr197 amino acid and Nitrogen atom of amide group in the 3rd position, this interaction had 4.9 Å distance.

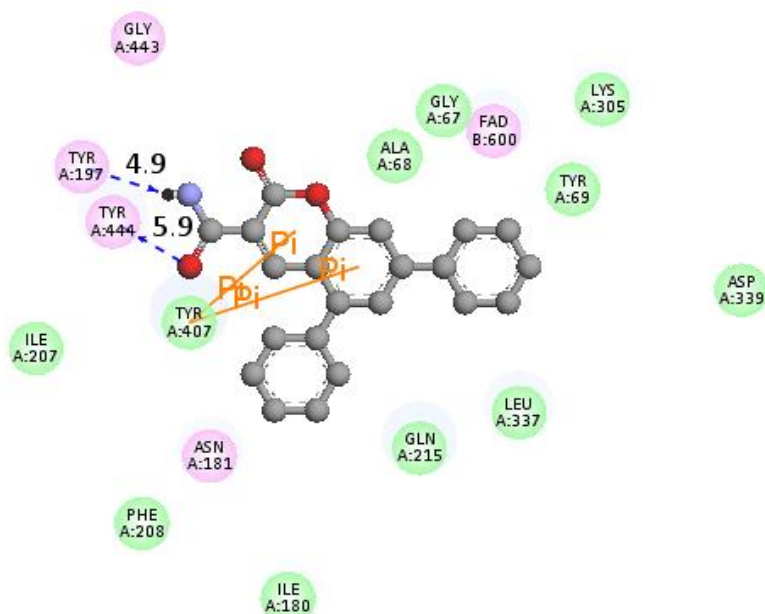


Figure 5.21: 2-D representation of ligand M118 and MAO-A enzyme active site

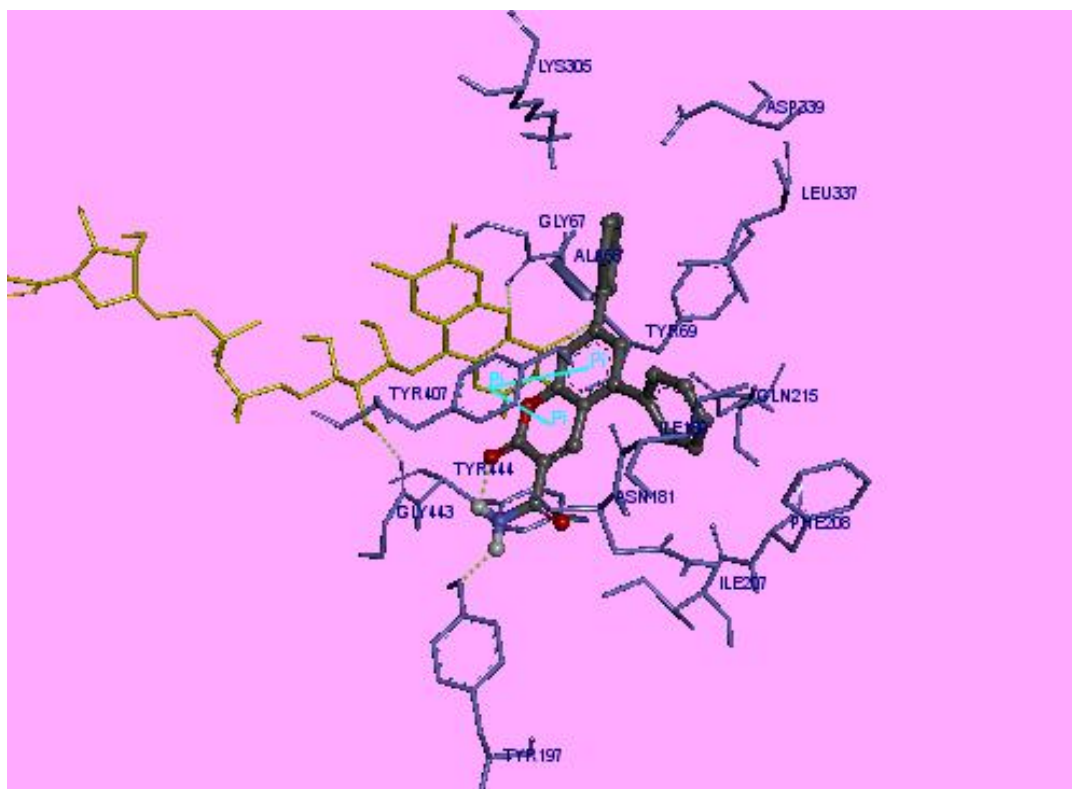


Figure 5.22: 3-D representation of M118 and MAO-A enzyme. Bold ball and stick molecule is M118 ligand, yellow large molecule is FAD, polar interactions are represented with green dashed lines, Nitrogen atom is represented with blue ball, for as Oxygen atoms are red balls and Carbon atoms are grey balls.

Another polar interaction had 5.9 Å length which was formed between Tyr444 and Oxygen atom of amide at 3rd position. Strong electrostatic interactions with FAD coenzyme were performed, and Gly443, Asn181 amino acids were performed other electrostatic interactions. Strong van der Waals forces with Tyr407 and Gln215 amino acids were formed. Leu337 made slightly strong van der Waals forces. Other van der Waals interactions were improved between compound M118 and Gly67, Ala68, Lys305, Tyr69, Ile207, Ile180, Phe208 and Asp399 amino acids.

Compound M118 (3-amide-5,7-diphenyl coumarin derivative) has an important place in this study in terms of K_i value and free binding energy.

M118 is the best ligand for MAO-A enzyme in these 125 de novo designed ligands. Corresponding to *.dlg files compound M118 was the smallest Ki value in these 125 ligand that is smaller than Ki value of Selegiline-MAO-A complex. The Ki value is 7.25 nM and free binding energy (ΔG) is -11.10 kcal/mol of M118 ligand.

5.10 Evaluation of M118 Ligand Position in the MAO-B Enzyme

Although compound M118 had not got any pi interaction with MAO-B active site, it had lots of interactions with particularly aromatic amino acids. As can be seen in Figure 5.23 a strong van der Waals force was formed with Thr314 amino acid.

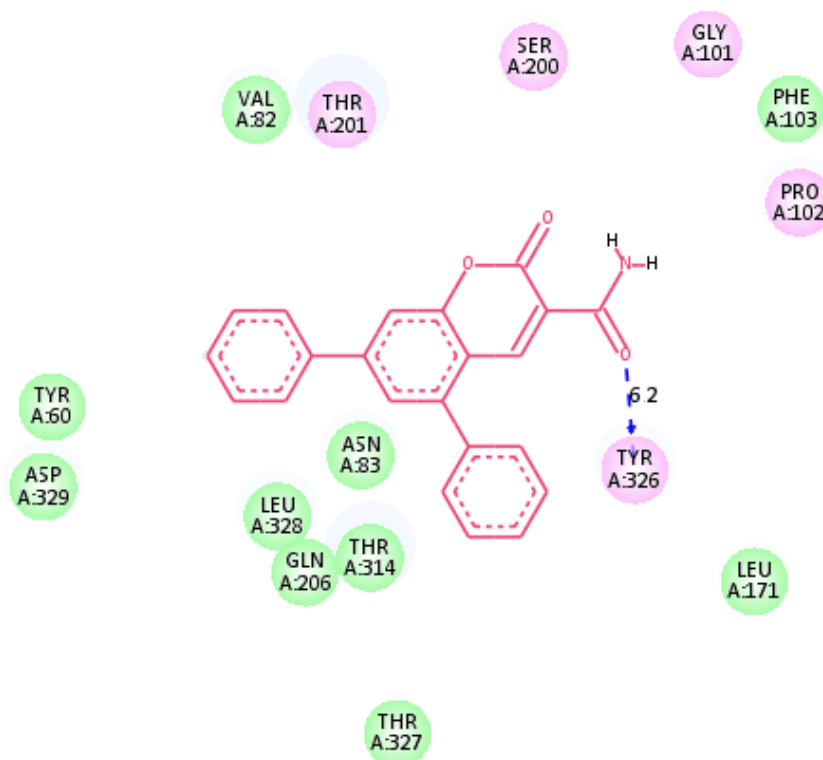


Figure 5.23: 2-D representation of M118 ligand and MAO-B's amino acids in the active site

Also some van der Waals forces were occurred between Tyr60, Asp329, Thr327, Leu171, Gln206, Phe103, Val82 amino acids and atoms belonged to ligand molecules. As shown Figure 5.24, side chain of Thr314 was very near to ligand's atoms. Another threonine amino acid, Thr201 played a role at installing strong electrostatic interactions with ligand.

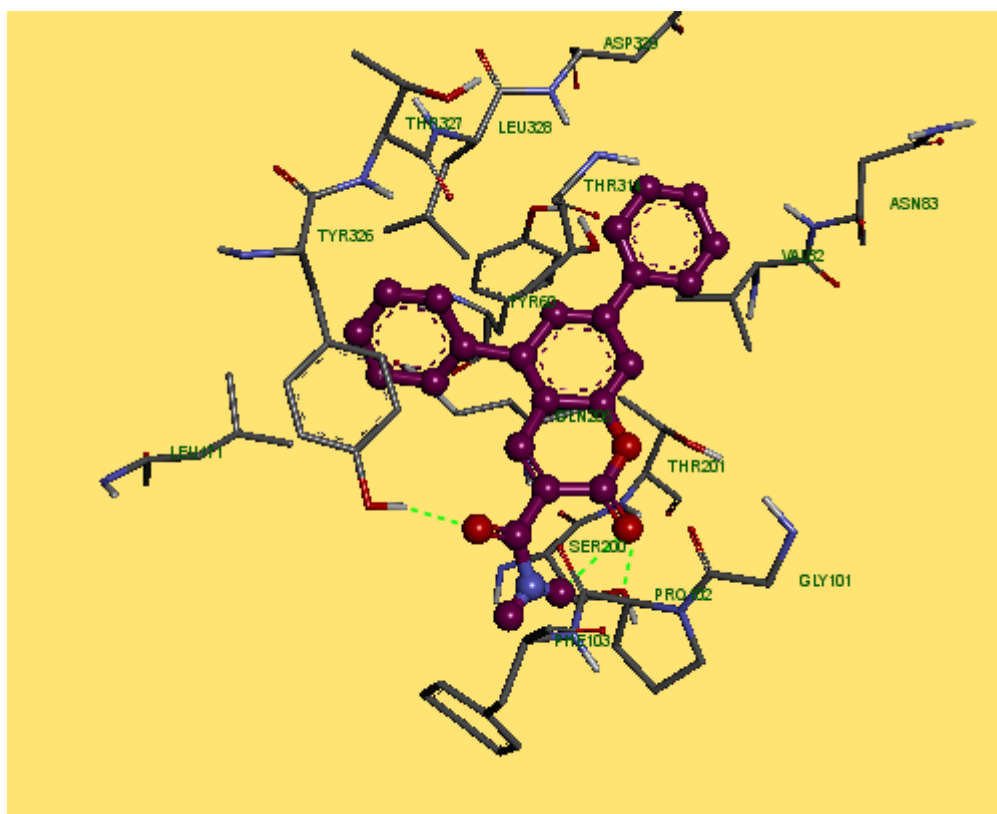


Figure 5.24: 3-D representation of compound M118 and MAO-B active site. Pink ball and stick molecule represents M118 ligand, blue ball is Nitrogen atom, red balls are Oxygen atoms, purple balls are Carbon atoms, green dashed lines are polar interactions.

Gly101, Pro102 and Ser200 amino acids are other amino acids who achieved electrostatic interactions with M118 ligand. Amino acids made slightly strong van der Waals interactions are Leu328 and Asn83.

A polar interaction had 6.2 Å distance was observed between Tyr326 and Oxygen atom of amide of compound M118.

Figure 5.25 shows valence electrons of compound M118 and atoms of amino acids in the MAO-B enzyme active site.

M118 is the best second ligand in terms of selectivity to MAO-A enzyme. K_i value is 1.60 μM and $\Delta G = -7.91$ kcal/mol for MAO-B enzyme. M118 (3-amide-5,7-diphenyl coumarin derivative) is more potent for MAO-A enzyme about 190 fold than MAO-B enzyme. Hence according to in vitro experiment, compound M118 can be valuable inhibitor candidate in cure of depression.

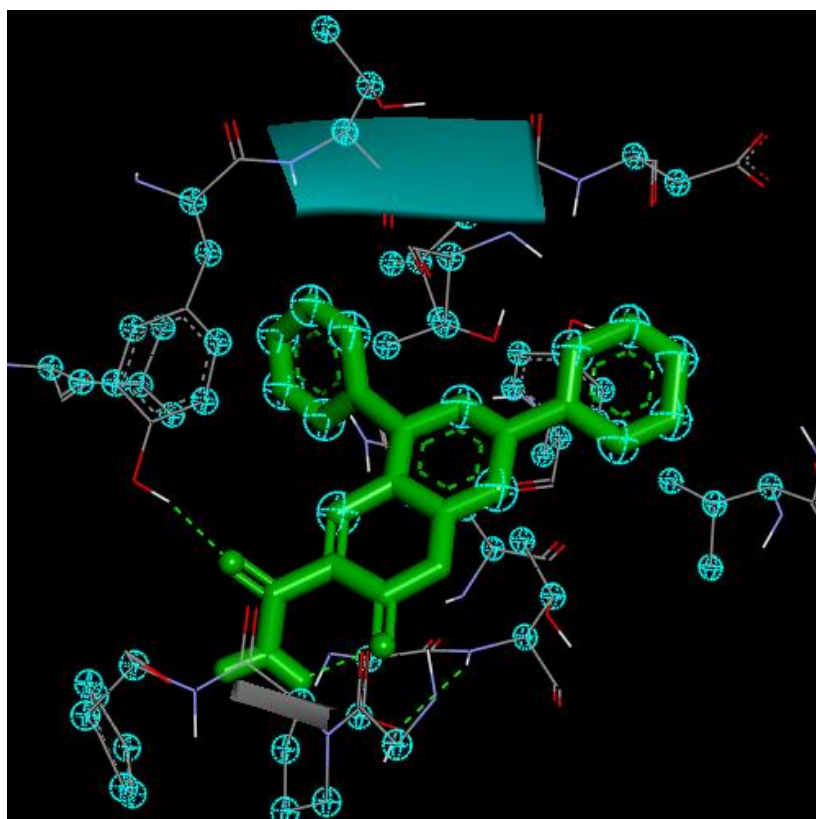


Figure 5.25: 3-D representation of valence electrons of M118 with MAO-B active site

5.11 Evaluation of Ligand M123 and MAO-A Enzyme Binding Properties

Compound M123 (3,5,7-triphenylcoumarin derivative) has a lot of pi interactions with amino acids which are in the MAO-A enzyme binding site. As shown in Figure 5.26 and Figure 5.27, a pi-cation interaction was formed that had 4.9 Å distance between Nitrogen atom of Lys:305:NZ and phenyl ring at the 7th position of ligand. Tyr407 amino acid installed three pi-pi interactions with ligand. One of them was occurred with benzene ring of coumarin nucleus had 5.1 Å distance, other interaction was formed with α -pyrone ring of coumarin nucleus had 3.7 Å distance, and the last pi-pi interaction had 4.6 Å distance was formed with phenyl ring at the 3rd position of ligand.

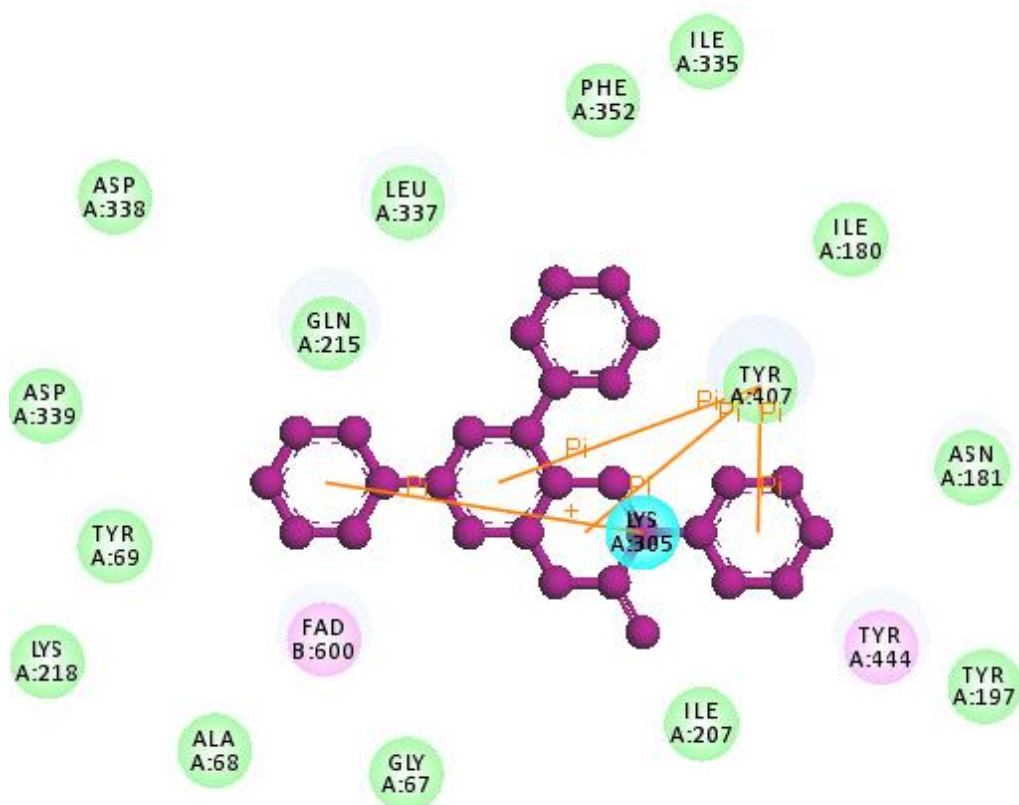


Figure 5.26: 2-D representation of M123 ligand and MAO-A enzyme

FAD coenzyme and Tyr444 amino acid had electrostatic interactions with the ligand. Gly215 and Leu337 amino acid made strong van der Waals interactions with M123.

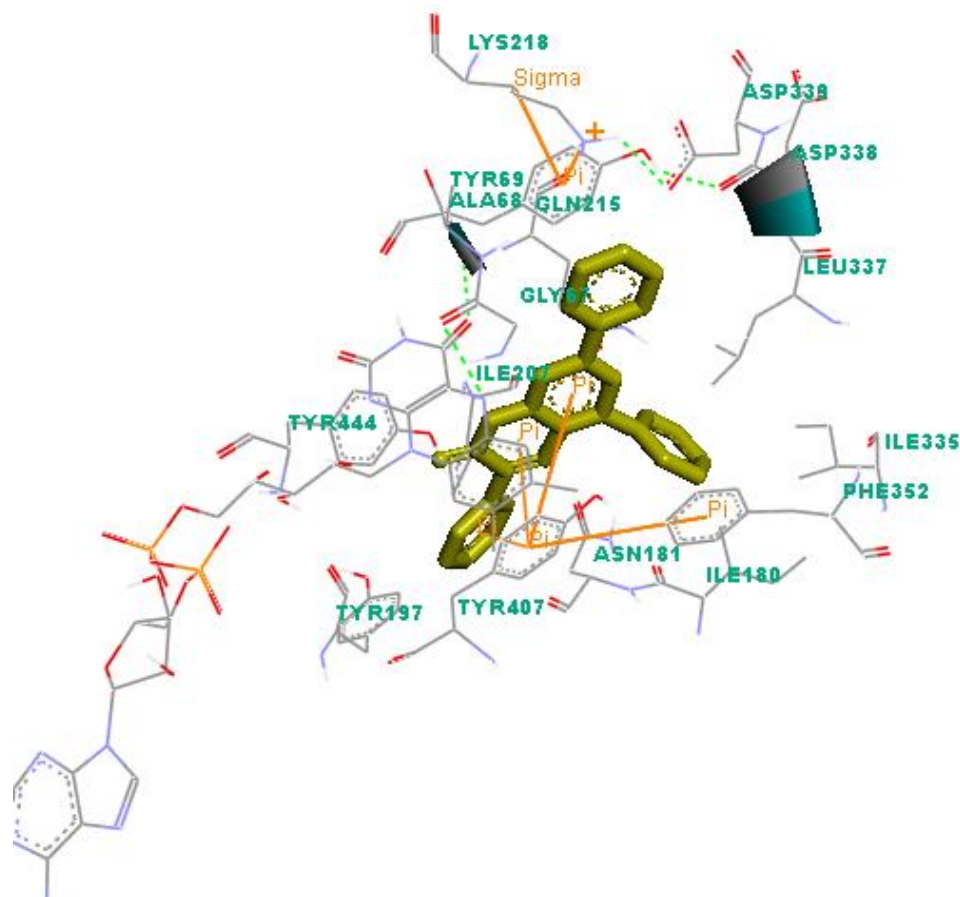


Figure 5.27: 3-D representation of M123 ligand and MAO-A enzyme's active site. Yellow bold molecule represents M123 ligand.

M123 (3,5,7-triphenyl coumarin derivative) is the best second inhibitor for MAO-A enzyme in these 125 ligands. Seeing docking result belonging to MAO-A and MAO-B, M123 is the best selective ligand for MAO-A. K_i value is 12.01 nM and $\Delta G = -10.81$ kcal/mol. Compound M123 209 fold more effective to MAO-A than MAO-B enzyme. Corresponding to this in vitro study, compound M123 (3,5,7-triphenyl coumarin derivative) is a hopeful inhibitor candidate for cure of depression. Hence it must be tried in vivo.

5.12 Evaluation of Compound M123 and MAO-B Binding Properties

As being at other binding properties of MAO-B and the best five coumarin derivatives for MAO-A enzyme, also M123 ligand has double pi-pi interactions and electrostatic interactions with Tyr326 amino acid. One of them had 6.68 Å distance was installed between benzene ring of ligand and Tyr326 amino acid, and other had 4.75 Å distance was formed with α -pyron of coumarin nucleus. Two other electrostatic interactions were occurred with Ile199 and Gln206. As shown Figure 5.28 and Figure 5.29, Thr201 had strong van der Waals force because it is nearest amino acid to ligand.

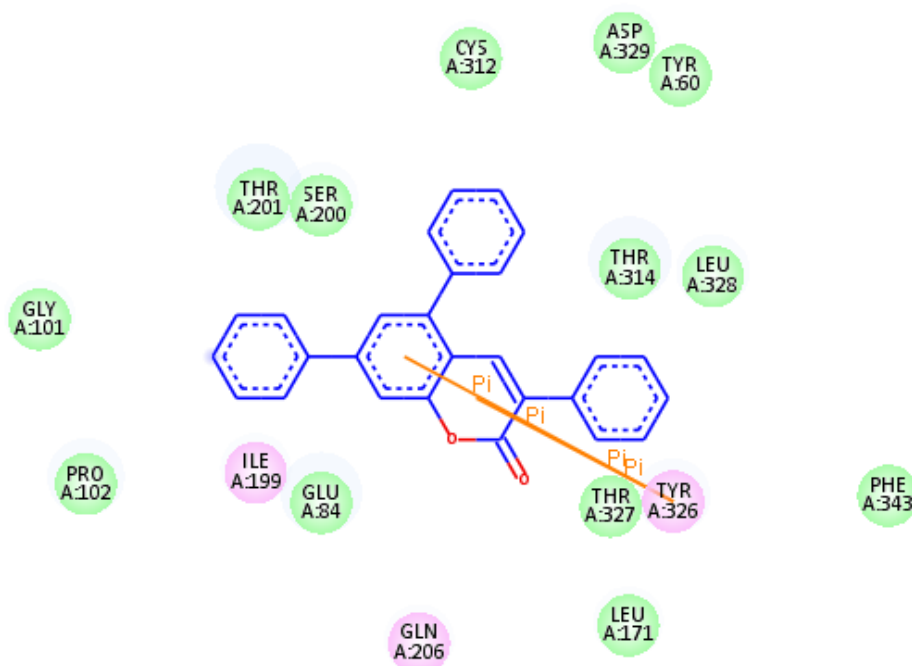


Figure 5.28: 2-D representation of M123 ligand and MAO-B enzyme's related amino acids

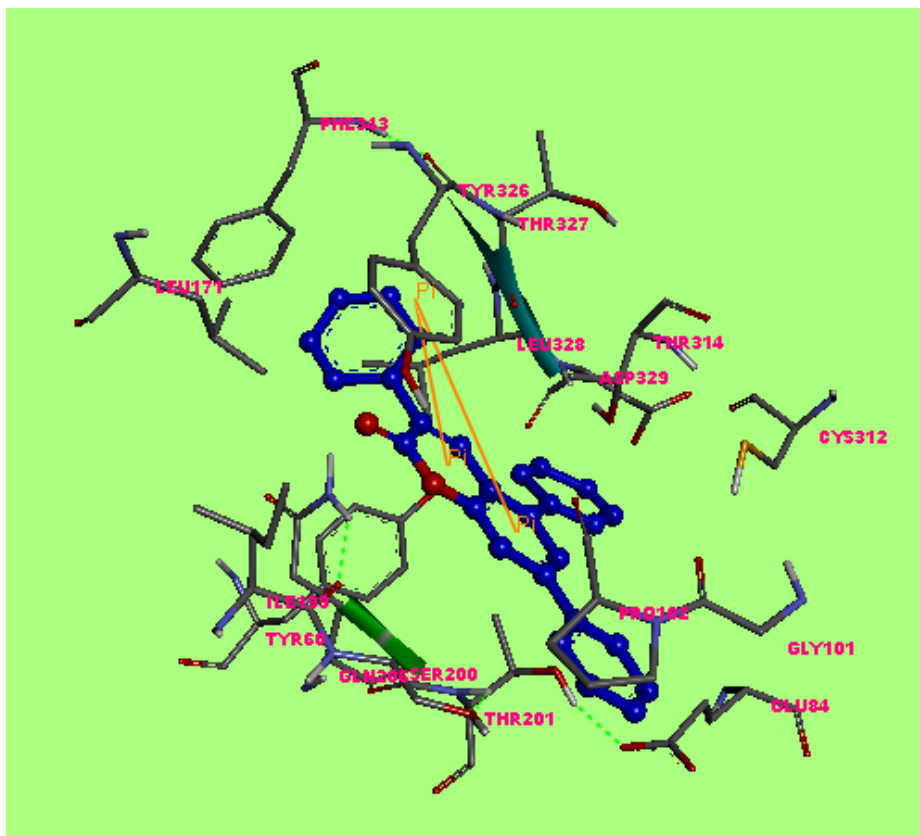


Figure 5.29: 3-D representation of M123 ligand and MAO-B enzyme positions. Oxygen atoms are being shown with red balls, blue ball and stick molecule represents compound M123

Numerous amino acids have van der Waals forces with compound M123. Strong van der Waals forces installed with Thr314 amino acid. Leu171, Thr327, Pro102, Gly101, Tyr60, Ser200, Tyr327, Cys312, Asp329, Leu328, Glu84 and Phe343 were other installed van der Waals interactions. As can be seen in Figure 5.29, particularly Glu84 interacted with aromatic ring at 7th position of ligand. It can be seen that aromatic ring of Phe343 amino acid was perpendicular to ligand. K_i value of M123 and MAO-B complex is 2.52 μM and free binding energy is -7.64 kcal/mol. Actually M123 (3,5,7-triphenylcoumarin derivative) has a good docking result for MAO-B enzyme, however it is the best selective ligand for MAO-A in these 125 coumarin derivatives in vitro and it has 209 fold more affinity to MAO-A.

5.13 Evaluation of M106 Ligand with MAO-B Enzyme Complex

As can be seen Figure 5.30 and Figure 5.32 a pi-pi interaction was performed α -pyrone ring of coumarin nucleus and Tyr326, which had 6.04 Å distance, this amino acid had van der Waals forces with atoms of ligand. Thr201 amino acid installed strong electrostatic interactions with this ligand. Gln206 and Ile199 have weaker electrostatic interactions since they were a little far away than ligand.

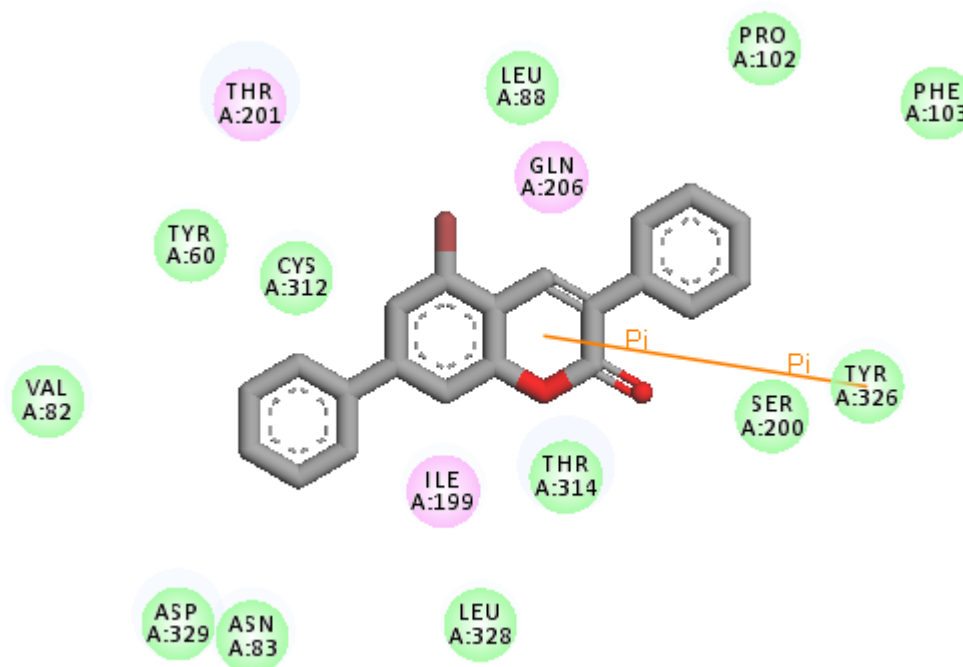


Figure 5.30: 2D representation of M106 ligand and MAO-B binding site. Burgundy stick represents Bromine atom, red sticks are Oxygen atoms and grey sticks are Carbon atoms.

Thr314 had large van der Waals forces with M106 ligand. Other amino acids had van der Waals interactions with ligand were Val82, Tyr60, Cys312, Asp329, Asn83, Leu328, Thr314, Ser200, Phe103, Pro102 and Leu88.

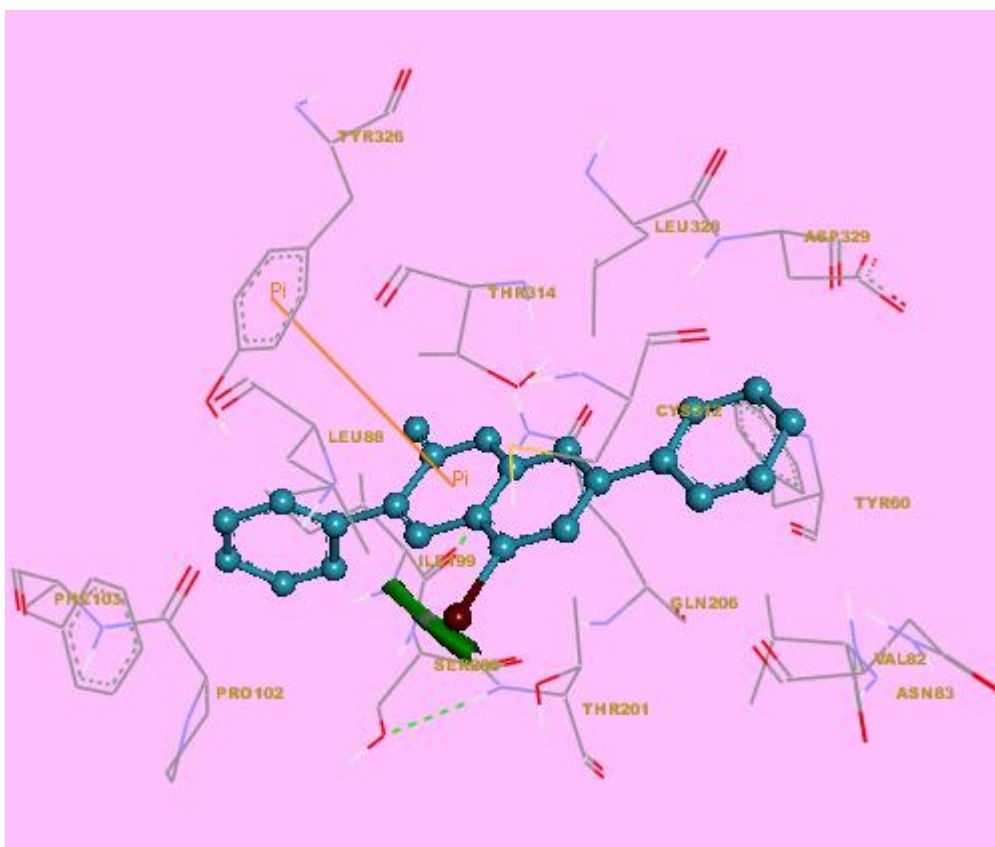


Figure 5.31: 3-D representation of compound M106 and MAO-B enzyme's binding site amino acids. Blue ball and stick molecule represents M106 ligand, burgundy ball represents Bromine atom.

Although M106 is the best 5th ligand for MAO-B enzyme in these 125 ligands, this ligand is not a reliable inhibitor candidate as like other the best five ligands for MAO-B. Because any ligands are not selective for MAO-B they showed more effective score for MAO-A enzyme. Therefore in this study a good inhibitor candidate could not be found for treatment of Parkinson's disease.

Ki value of M106 ligand with MAO-B is 784.65 nM, free energy of binding (ΔG) is -8.33 kcal/mol. Ki value of M106 ligand with MAO-A is 69.16 nM, $\Delta G = -9.67$ kcal/mol.

5.14 Evaluation of M061 Ligand with MAO-B Enzyme Active Site

M061 (5,7-diphenyl-3-methoxycoumarin derivative) has lots of van der Waals interactions with MAO-B enzyme's active site amino acids' atoms. Ligand M061 had only one pi-pi interaction. This pi-pi interaction was formed between Tyr326 amino acid and benzene ring of ligand. This pi-pi interaction being seen in Figure 5.32 and Figure 5.33 had 5.18 Å distance. Gln206 and Tyr60 stood near to ligand and they had van der Waals forces with ligand's atoms.

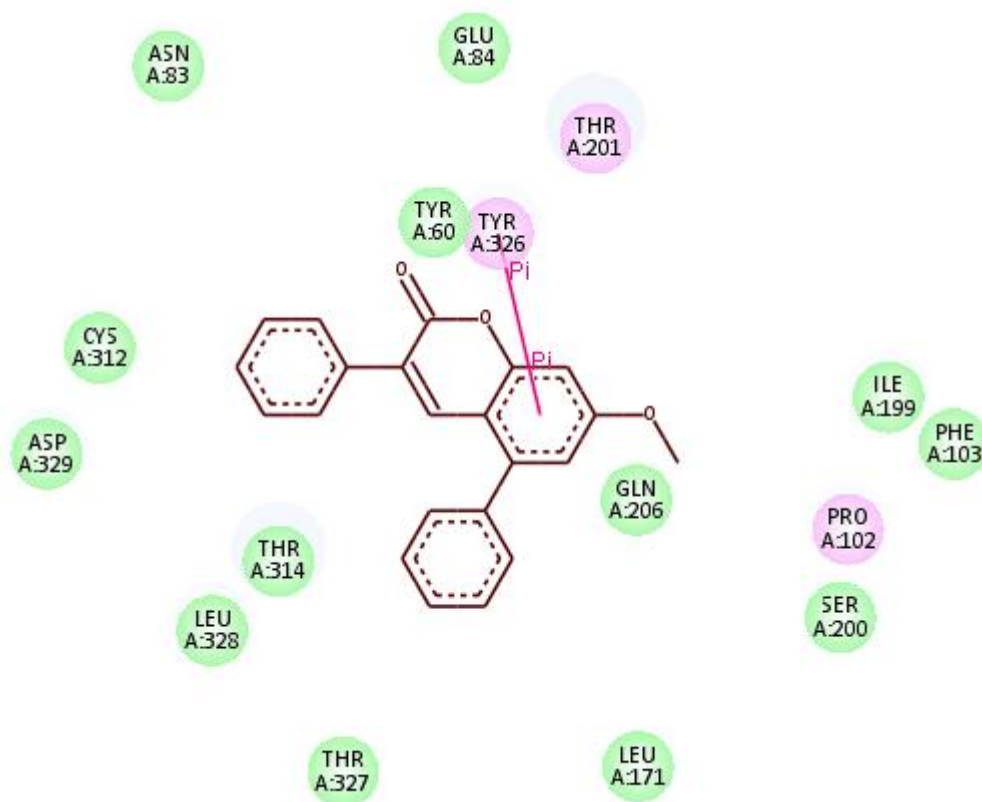


Figure 5.32 : 2-D representation of M061 ligand and MAO-B enzyme

Electrostatic interactions were observed between Thr201, Pro102 amino acids and ligand.

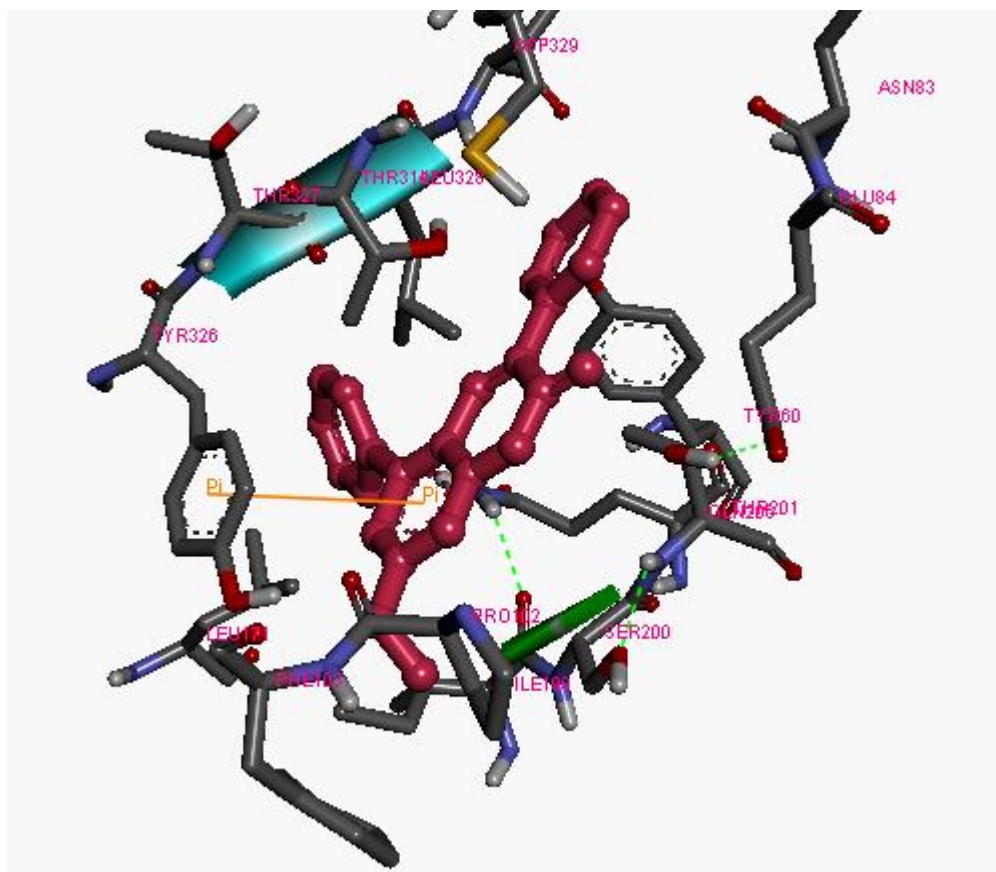


Figure 5.33 : 3-D representation of M061 ligand and MAO-B enzyme

Ile199, Thr314, Asp329, Cys312, Asn83, Glu84 achieved van der Waals interactions.

M061 ligand and MAO-B enzyme complex had 623.52 nM K_i value and -8.47 kcal/mol free energy of binding. As for MAO-A enzyme, M061 ligand had 37.39 nM K_i value and -10.15 kcal/mol free energy of binding. While considering docking results, it can be said that although compound M061 is the best 3rd ligand in these 125 ligand for MAO-B enzyme, it is not a true inhibitor candidate neither MAO-B nor MAO-A enzymes.

5.15 Evaluation of M101 Ligand and MAO-B Enzyme Binding Properties

Compound M101 (3,5-dibromo-7-phenylcoumarin derivative) shows that to care Bromine or phenyl at 5th position increase the potency for MAO-B enzyme.

As can be seen Figure 5.34 and Figure 5.35 only one pi-pi interaction did not have short distance was occurred. This interaction had 5.35 Å range and it was between Tyr326 amino acid and benzene ring of coumarin nucleus.

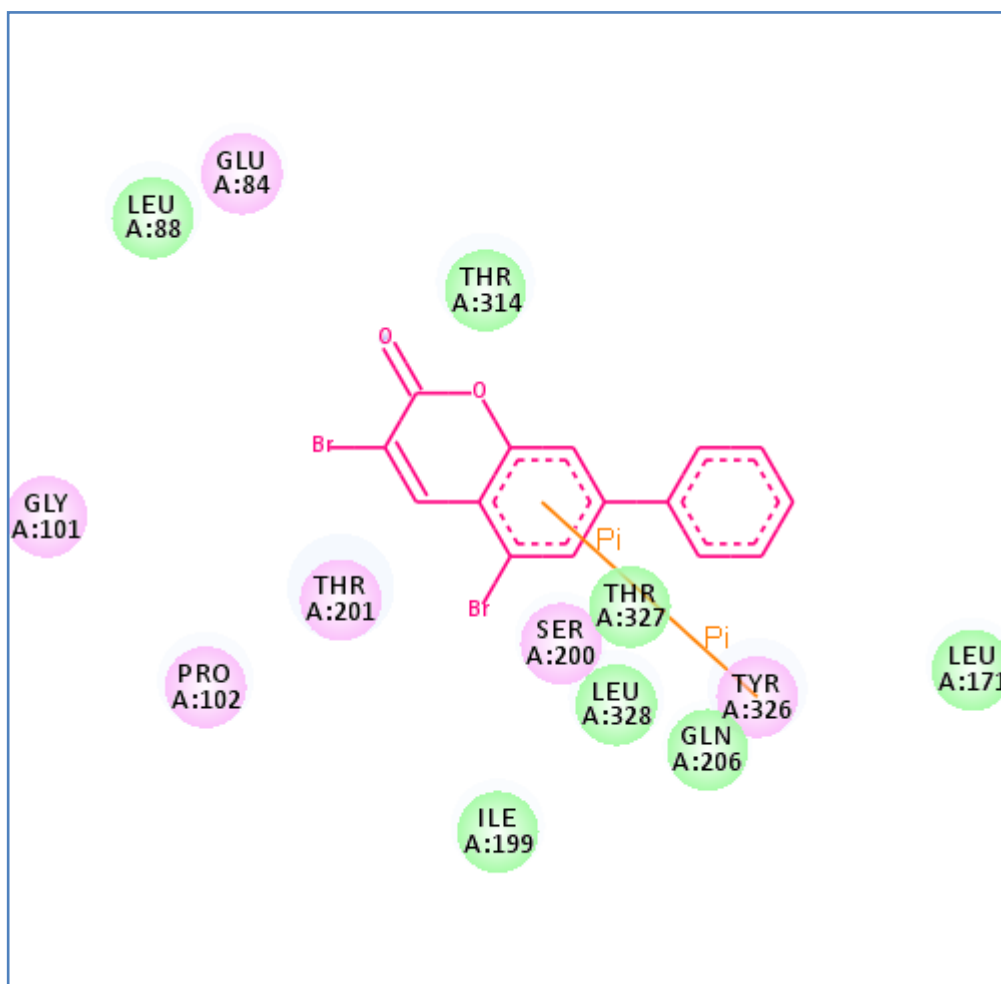


Figure 5.34 : 2-D representation of compound M101 and MAO-B enzyme
A powerful electrostatic interaction was installed between α -pyrone nucleus of

coumarin and Thr201 amino acid. Other electrostatic interactions were performed with Glu84, Gly101, Pro102 amino acids. Strong van der Waals forces were occurred with Thr314, Leu88 amino acids. Thr327, Gln206, Ile199 achieved slightly strong van der Waals interactions with M101 ligand.

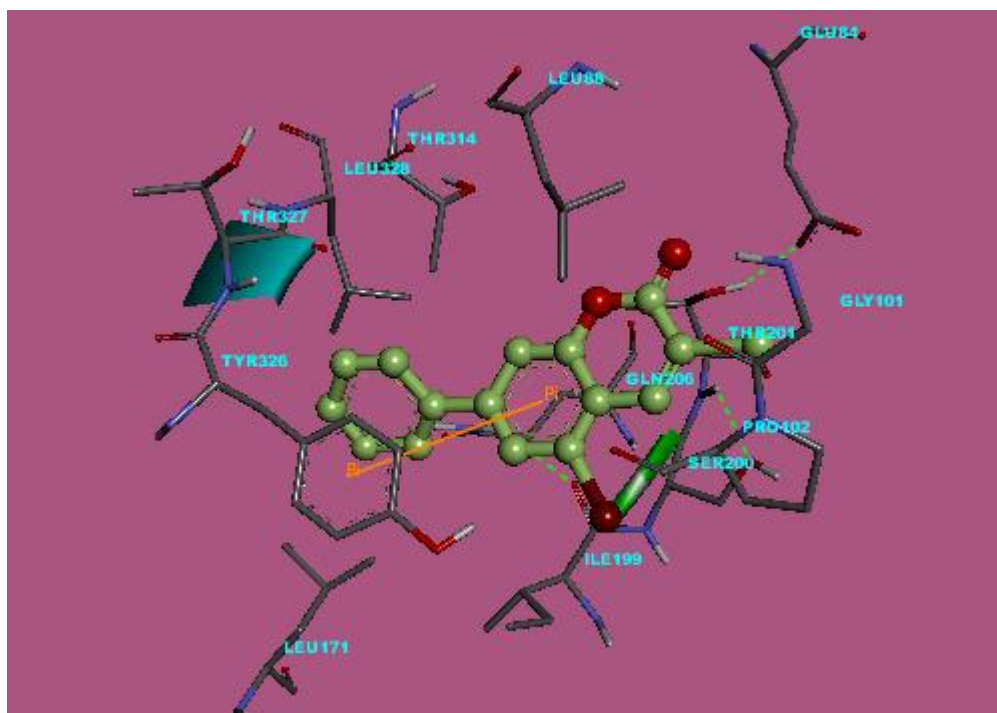


Figure 5.35: M101 ligand and MAO-B binding position 3-D representation

Consequently compound M101 had 586.16 nM K_i value for MAO-B and free energy of binding is -8.50 kcal/mol with MAO-B enzyme. Also this ligand has more effective score for MAO-A enzyme. M101 ligand had 251.81 nM K_i value and -9.00 kcal/mol ΔG for MAO-A enzyme. Therefore although M101 is the best ligand for MAO-B with these results in these 125 ligands, M101 has about two fold more affinity to MAO-A enzyme. Hence M101 ligand is not an ideal medicine candidate neither MAO-B nor MAO-A enzymes.

5.16 Evaluation of M122 Ligand and MAO-B Enzyme Binding Properties

M122 ligand (7-amide-3,5-diphenylcoumarin derivative) is an inhibitor making every kind of interaction with its surrounding amino acids' atoms and particularly aromatic side chains.

As with all other ligands, compound M122 achieved a pi-pi interaction with Tyr326 amino acid, it was also installed with the benzene ring of the coumarin nucleus. M122 ligand had a slightly strong electrostatic interaction with this amino acid as can be seen in Figure 5.36.

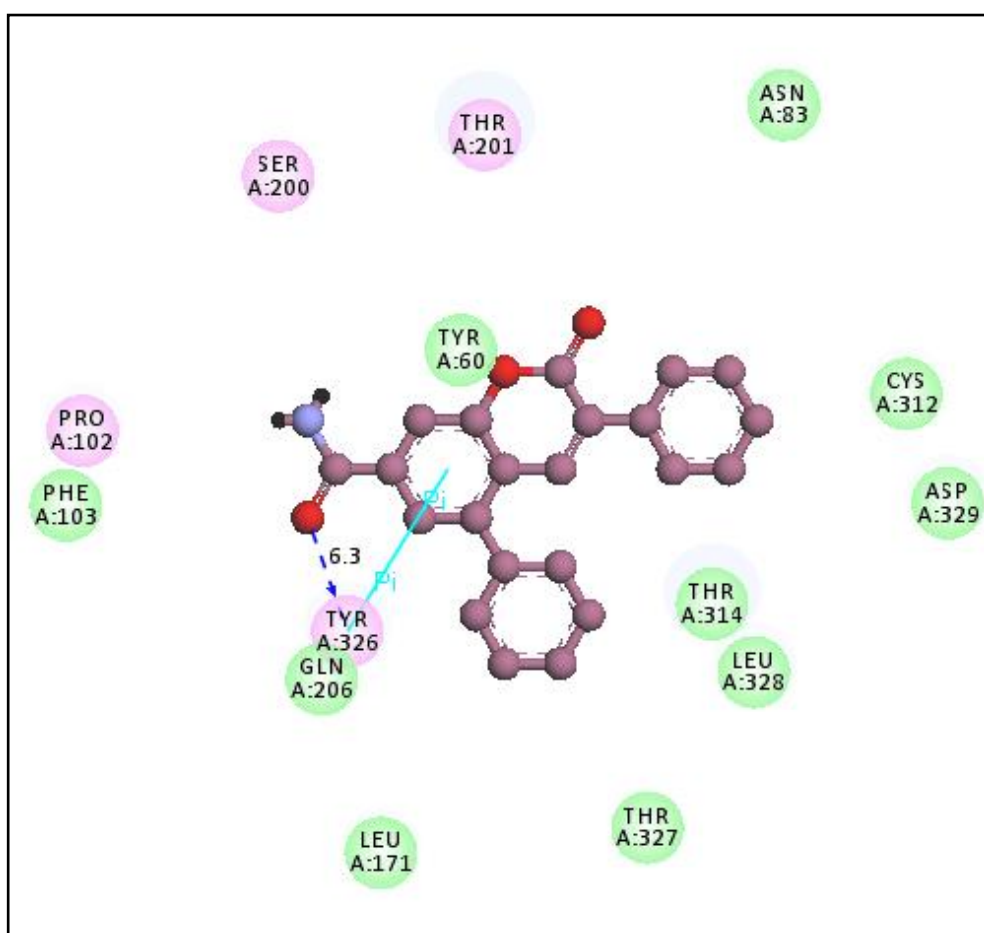


Figure 5.36: M122 ligand and MAO-B enzyme binding properties 2-D representation

It was very strong electrostatic interactions with Thr201 amino acid. Weaker electrostatic interactions were formed with Pro102 and Ser200 amino acids.

As shown Figure 5.37 a hydrogen bond had 6.3 Å length was occurred between hydroxyl group of Tyr326 amino acid and Oxygen atom of amide group at the 7th position.

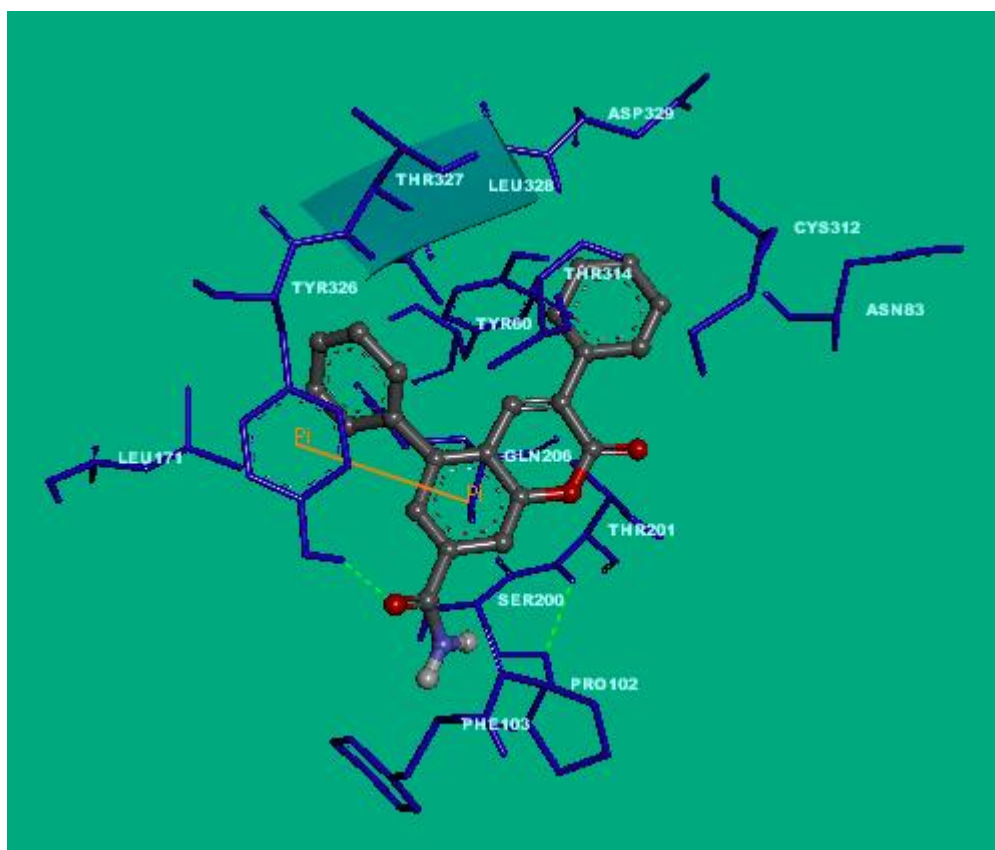


Figure 5.37: 3-D representation of compound M122 and MAO-B enzyme. Red balls represent Oxygen atoms, blue ball represent Nitrogen atom, grey atoms are Carbon atoms in ball and stick seeming ligand molecule.

Tyr60, Asn83, Phe103, Leu171, Thr327, Leu328 amino acids achieved van der Waals interactions with compound M122's atoms. Strong van der Waals interactions were occurred with Thr314 amino acid. Weaker van der Waals forces were formed with

Cys312, Asp329 amino acids.

M122 ligand has 640.62 nM K_i value and -8.45 kcal/mol free energy of binding for MAO-B enzyme and M122 ligand complex. But also M122 ligand has more potent and smaller results in terms of K_i and ΔG because K_i value for MAO-A enzyme-M122 ligand complex is 35.07 nM and free binding energy is -10.17 kcal/mol. Thus M122 ligand is the best 4th ligand in these ligands but it is not available for treatment neither Parkinson's disease nor depression.

Chapter 6

Conclusion

The result of researching inhibition properties of designed 125 ligands' with MAO-A and MAO-B enzymes via using computational methods in silico environment and comparing of results demonstrated that 125 coumarin derivatives interacted with MAO-A enzyme infinitely.

Benzene and α -pyrone ring of coumarin nucleus were important to perform effective pi-pi interactions with aromatic cage of MAO-A and MAO-B enzymes. Additionally this nucleus interacted with also FAD and at the end inhibition constants were found at nanomolar and micromolar levels. In the comparison with Moclobemide, compound M123 had more effective binding ability than Moclobemide. At the same time M123 was the most selective compound in these ligands and it had 209 fold better inhibition constant for MAO-A than MAO-B.

Also coumarin derivatives can be synthesized easily artificially and exist in nature with more than 1300 kinds, they are used in treatment of hypertension which is a serious side effect of MAO-A inhibitors. While coumarins have a large usage area in terms of medical, they make aroma therapy effect in treatment of depression by means of their pleasant perfume.

In the result of this study, it was observed that coumarin derivatives interacted with Tyr407 and Tyr444 amino acids also by coumarin nucleus in 5 ligands which were examined comprehensively. Additionally Gly67, Tyr69, Ile180, Asn181, Phe208, Gln215 and Lys305 are other important amino acids existed MAO-A active site. In these 125 derivatives, M118 was inhibitor had the highest affinity against MAO-A. This case demonstrated to us that it was important if an amide group was at the 3rd position in terms of hydrogen bond quality and number made with aromatic cage.

Another observation was occurred about MAO-B active site's amino acids by examining interactions with 10 coumarin derivatives which contain the best 5 ligands for MAO-A and other 5 ligands were the best ligands for MAO-B enzyme. According to binding results of MAO-B enzyme active site by utilizing Discovery Studio Accelrys software, pi-pi interaction particularly with Tyr326 was observed on all examined ligands. Additionally Ser200, Tyr326, Thr327, Pro102, Thr201, Tyr60, Asn83, Leu328, Ile199, Cys312, Gln 206, Thr314, Glu84 and Phe103 amino acids were existent in active site and interacted most frequently with coumarin derivatives.

Apparently it can be said about QSAR design of particularly first five compounds which had bound well and at the same time the most selective to MAO-A, the case of being bulky group at the 5th and 7th position, which was phenyl for our study, was increasing the effect to MAO-A. But when phenyl was at the 5th position, it was making aromatic interactions with also MAO-B. Although this condition decreased the selectivity, being phenyl at the 5th position is important in terms of being found high score for MAO enzymes.

We assessed results of the best 50 ones in the 125 ligands which had been screened at the end of this study. Since in these 50 ligands, 5 ligands (M123, M118, M109, M029, M115) were inhibitor candidates had high potential, it will lead to direction about MAO-A inhibition to synthesis of them.

REFERENCES

- [1] Toprakçı, M., Yelekçi K.; Docking Studies on Monoamine Oxidase-B Inhibitors: Estimation of Inhibition Constants (K_i) of a Series of Experimentally Tested Compounds; *Bioorganic & Medicinal Chemistry Letters* 15 (2005) 4438–4446
- [2] Geldenhuys, J.,W., Funk, M., O., Schyf, C., J., V., Carroll, R., T.; A Scaffold Hopping Approach to Identify Novel Monoamine Oxidase B Inhibitors; *Bioorganic & Medicinal Chemistry Letters*, 2012, Volume 22, Issue 3,1; 1380-1383
- [3] Edmondson, D. E., Binda, C., Wang, J., Upandhyay, A. K., Mattevi, A.; Molecular and mechanistic properties of the membrane-bound mitochondrial monoamine oxidase; *Biochemistry* 48 (2009) 4220-4230.
- [4] Singh, R., Geetanjali, Sharma, N.; Monoamine Oxidase Inhibitors for Neurological Disorders: A Review; *Chemical Biology Letters* 2014, 1, 1, 33-39
- [5] Haung, R. H., Faulkner, R.; The Role of Phospholipid in The Multiple Functional Forms of Brain Monoamine Oxidase; *Journal of Biological Chemistry*, 1981, 256, 9211-9215
- [6] Abdelhafez, O. M., Amin, K. A., Ali,H. I., Abdall,M. M., Batran, R. Z.; Monoamine Oxidase A and B Inhibiting Effect and Molecular Modeling of Some Synthesized Coumarin Derivatives; *Neurochemistry International*, 2013, Volume 62, Issue 2, 198-209
- [7] Matos, M. J., Santana, L., Janeiro, P., Qezada, E., Uriarte, E., Gonzalez-Diaz, H., Vina, D., Oralla, F.; Design, Synthesis and Pharmacological Evaluation of New Coumarin Derivatives as Monoamine Oxidase A and B Inhibitors; 12th International Electronic Conference on Synthetic Organic Chemistry (ECSOC-12) 1-30 November 2008

- [8] Matos, M. J., Viña, D., Picciau, C., Orallo, F., Santana, Uriarte, E.; Synthesis and Evaluation of 6-methyl-3-phenylcoumarins as Potent and Selective MAO-B Inhibitors; *Bioorganic & Medicinal Chemistry Letters*, 19 (2009) 5053-5055
- [9] Santana, L., González-Díaz, H., Quezada, E., Uriarte, E., Yáñez, M., Viña, D., Orallo, F.; Quantative Structure-Activity Relationship and Complex Network Approach to Monoamine Oxidase A and B Inhibitors; *J. Med. Chem.*, 51 (2008) 6740-6751
- [10] Matos, M. J., Teran, C., Perez-Castillo, Y., Uriarte, E., Santana, L., Viña D.; Synthesis and Study of A Series of 3-arylcoumarins as Potent and Selective Monoamine Oxidase B Inhibitors; *J. Med. Chem.* 2011, 54, 7127-7137
- [11] Camarena, B., Fres'an, A., Aguilar, A., Escamilla, R., Saracco, R., Palacios, J., Tovilla, A., Nicolini, H.; Monoamine Oxidase A and B Gene Polymorphisms and Negative and Positive Symptoms in Schizophrenia; *International Scholarly Research Network ISRN Psychiatry*, Volume 2012, Article ID 852949, 5 pages doi:10.5402/2012/852949
- [12] Medical-Encyclopedia, Depression, Aviva,
<http://www.aviva.co.uk/health-insurance/home-of-health/medical-centre/medical-encyclopedia/entry/depression/>
- [13] Varnali, F., Designing Inhibitors via Molecular Modelling Methods for Monoamine Oxidase Isozymes A and B, Master Thesis, Kadir Has University, 2012
- [14] AOFB_HUMAN-Protein Knowledgebase,
<http://www.uniprot.org/uniprot/P27338>
- [15] AOFA_HUMAN- Protein Knowledgebase,
<http://www.uniprot.org/uniprot/P21397>
- [16] Amino Acids Reference Chart, <http://www.sigmaaldrich.com/life-science/metabolomics/learning-center/amino-acid-reference-chart.html>
- [17] Edmondson, D. E., Binda, C., Mattevi, A.; The FAD Binding Sites of Human Monoamine Oxidases A and B; *Neurotoxicology*; 2004, 25(1-2):63-72
- [18] Legobe, L. J., Petzer, A., Petzer, J. P.; Selected C7-substituted chromone derivatives as monoamine oxidase inhibitors; *Bioorganic Chemistry* 45 (2012) 1-11

[19] Wang, J., Huo, K., Ma, L., Tang, L., Li, D., Huang, X., Yuan, Y., Li, C., Wang, W., Guan, W., Chen, H., Jin, C., Wei, J., Zhang, W., Yang, Y., Liu, Q., Zhou, Y., Zhang, C., Wu, Z., Xu, W., Zhang, Y., Liu, T., Yu, D., Zhang, Y., Chen, L., Zhu, D., Zhong, X., Kang, L., Gan, X., Yu, X., Ma, Q., Yan, J., Zhou, L., Liu, Z., Zhu, Y., Zhou, T., He, F., Yang, X.; Toward an Understanding of The Protein Interaction Network of The Human Liver; 3561 Associations Mol. Syst. Biol.; 536; 2011-10-13

[20] Karupphasamy, M., Mahapatra, M., Yabanoğlu, S., Uçar, G., Sinha, B. N., Basu, A., Mishra, N., Sharon, A., Kulandaivelu, U., Jayaprakash, V.; Development of Selective and Reversible Pyrazoline Based MAO-A Inhibitors: Synthesis, Biological Evaluation and Docking Studies; Bioorganic & Medicinal Chemistry 18 (2010) 1875–1881

[21] Yelekçi, K., Uçar, G., Kelekçi, N. G., Erdem, S., Erdem, A., Gökşen, U. S., Türkkkan, S.; Monoamin Oksidaz (MAO) İnhibitör Etkili Yeni Pirazolin Türevlerinin Moleküler Modelleme Yöntemiyle Tasarlanması, Sentezi ve İnhibisyon Kinetiklerinin Hesapsal ve Deneysel Olarak Tayini: Tübitak Project, Project number: 108T232; 2010; Istanbul

[22] ICM Brain & Spine Institute,
http://icm-institute.org/menu/research/pathologies_eng?lang=en&lang=en

[23] Ebadi, M., Srinivasan, S. K., Baxi, M. D.; Oxidative Stress and Antioxidant Therapy in Parkinson's Disease; Progress in Neurobiology, Volume 48, 1996, Elsevier Science

[24] Wang, J.; Comparative Structural and Functional Properties of Human and Rat Monoamine Oxidase, 2007, PhD. Thesis, Emory University

[25] Kaludercic, N., Carpi, A., Menabò, R., Lisa, F. D., Paolocci, N.; Monoamine Oxidases (MAO) in the Pathogenesis of Heart Failure and Ischemia/Reperfusion Injury; Biochimica et Biophysica Acta (BBA) - Molecular Cell Research, Volume 1813, Issue 7, 2011, Pages 1323–1332

[26] Chimenti, F., Secci, D., Bolasco, A., Chimenti, P., Granese, A., Carradori, S., Befani, O., Turini, P., Alcaroc, S., Ortusoc, F.; Synthesis, Molecular Modeling Studies, and Selective Inhibitory Activity Against Monoamine Oxidase of N,N0-bis[2-oxo-2H-benzopyran]-3-carboxamides; Bioorganic & Medicinal Chemistry Letters 16 (2006) 4135–4140

[27] Helguera, A. M., Garrido, A. P., Gaspar, A., Reis, J., Cogide, F., Vina, D., Borges, F., Corderio, M. N. D. S.; Combining QSAR Classification Models for

Predictive Modeling of Human Monoamine Oxidase Inhibitors; *European Journal of Medicinal Chemistry*; 59 (2013) 75-90

[28] Knudsen-Gerber, D. S.; Selegeline and Rasageline: Twins or Distant Cousins? *Guidelines; Consult Pharm*; 26 (2011) 48-51

[29] Kawai, Y., Kunitomo, J., Ohno, A.; Atropisomeric Flavoenzyme Models with a Modified Pyrimidine. *Kyoto: Institute for Chemical Research – ICR Annual Report*. 3, 1996

[30] Edmonson, D. E., Binda, C., Mattevi, A.; Structural Insights into Mechanism of Amine Oxidation by Monoamine Oxidase A and B; *Biochem. and Biophys.*, 464(2007) 269-276

[31] *Biochemistry of Neurotransmitters and Nerve Transmission*, <http://themedicalbiochemistrypage.org/nerves.html#catecholamines>

[32] Bolasco, A., Secci, D., Chimenti, P., Granese, A., Carradori, S., Yanez, M., Orallo, F., Ortuso, F., Alcaro, S.; Investigations on the 2-thiazolylylhydrazine scaffold: Synthesis and Molecular Modelling of Selective Human Monoamine Oxidase Inhibitors, *Bioorganic & Medicinal Chemistry* 18 (2010) 5715- 5723

[33] Musa, M. A., Badisa, V. L. D., Latinwo, L. M., Cooperwood, J., Sinclair, A., Abdullah, A.; Cytotoxic Activity of New Acetoxycoumarin Derivatives in Cancer Cell Lines; *Anticancer Res.* 2011; 31(6): 2017–2022.

[34] Fariello, R. G.; Sefinamide; *Neurotherapeutics*, 4 (2007), 110-116

[35] Salvati, P., Maj, R., Caccia, C., Cervini, M. A., Fornaretto, M. G., Lamberti, E., Pevarello, P., Skeen, G. A., White, H. S., Wolf, H. H., Faravelli, L., Mazzanti, M., Mancinelli, E., Varasi, M., Fariello, R. G.; Biochemical and Electrophysiological Studies on the Mechanism of Action of PNU-151774E, a novel antiepileptic compound. *J Pharmacol Exp Ther* 1999;288: 1151–1159.

[36] Bortolato, M., Shih, J. C.; Behavioral Outcomes of Monoamine Oxidase Deficiency: Preclinical and Clinical Evidence; *Int Rev Neurobiol.* 2011; 100: 13–42. doi:10.1016/B978-0-12-386467-3.00002-9.

[37] Disorders Related to MAOA-Malacards: Human Disease Database,

<http://www.malacards.org/search/results/MAOA>

[38] Disorders Related to MAOB-Malacards: Human Disease Database,
<http://www.malacards.org/search/results/MAOB>

[39] Brunner, H. G., Nelen, M., Breakefield, X. O., Ropers, H. H., Oost, B. A. Abnormal Behavior Associated with a Point Mutation in the Structural Gene for Monoamine Oxidase A; *Science* 1993; 262: 578-580.

[40] MAOA-001-Transcript-Ensemble,
http://www.ensembl.org/Homo_sapiens/Transcript/ProteinSummary?g=ENSG00000189221;r=X:43515467-43606068;t=ENST00000338702

[41] X Chromosome-Genetics Home References,
<http://ghr.nlm.nih.gov/chromosome/X> Reviewed January 2012

[42] MAOA Gene Location-Genetics Home References,
<http://ghr.nlm.nih.gov/gene/MAOA#location>

[43] MAOA Genomic Map-Genatlas sheet,
<http://genatlas.medecine.univ-paris5.fr/fiche.php?n=5050>

[44] MAOA Gene Transcription Factors-QIAGEN, Sample & Assay Technologies,
http://www.sabiosciences.com/chipqpcrsearch.php?factor=Over+200+TF&species_id=0&ninfo=n&ngene=n&nfactor=y&gene=MAOA

[45] MAOA Gene-Genecards, The GeneCards Human Gene Database,
<http://www.genecards.org/cgi-bin/carddisp.pl?gene=MAOA>

[46] Duncan, J., Johnson, S., Ou, X. M.; Monoamine Oxidases in Major Depressive Disorder and Alcoholism; *Drug. Discov. Ther.* 2012 Jun;6(3):112-22

[47] Oprea, C. I., Panait, P., Cimpoesu, F., Ferbinteanu, M., Gîrțu, M. A.; Density Functional Theory (DFT) Study of Coumarin-based Dyes Adsorbed on TiO₂ Nanoclusters—Applications to Dye-Sensitized Solar Cells; *Materials* 2013, 6(6), 2372-2392; doi:10.3390/ma6062372

[48] Cheng, A., Scott, A. L., Ladenheim, B., Chen, K., Ouyang, X., Lathia, J. D., Mughal, M., Cadet, J. L., Mattson, M. P., Shih, J. C.; Monoamine Oxidases Regulate

Telencephalic Neural Progenitors in Late Embryonic and Early Postnatal Development; *J Neurosci.* 2010 Aug 11;30(32):10752-62. doi: 10.1523/JNEUROSCI.2037-10.2010.

[49] Nedic, G., Pivac, N., Hercigonja, D. K., Jovancevic, M., Curkovic, K. D., Muck-Seler, D.; Platelet Monoamine Oxidase Activity in Children with Attention-Deficit/Hyperactivity Disorder; *Psychiatry Res.*, 2010 Feb 28;175(3):252-5. doi: 10.1016/j.psychres.2009.08.013.

[50] Newman, T. K., Syagailo, Y. V., Barr, C. S., Wendland, J. R., Champoux, M., Graessle, M., Suomi, S. J., Higley, J. D., Lesch, K. P.; Monoamine Oxidase A Gene Promoter Variation and Rearing Experience Influences Aggressive Behavior in Rhesus monkeys. *Biol Psychiatry.* 2005;57:167–72

[51] Kendler, K. S.; “A Gene for...”: The Nature of Gene Action in Psychiatric Disorders; *Am. J. Psychiatry.* 2005;162:1243–52

[52] Sabol, S. Z., Hu, S., Hamer, D.; A Functional Polymorphism in the Monoamine Oxidase A Gene Promoter; *Hum Genet.* 1998;103:273–9

[53] Lea, R., Chambers, G.; Monoamine Oxidase, Addiction, and the "Warrior" Gene Hypothesis; *Journal of the New Zealand Medical Association*, 2007, Vol 120, (1250): U2441

[54] Ibanez, A., de Castro I. P., Fernandez-Piqueras, J., Blanco, C., Saiz-Ruiz, J.; Pathological Gambling and DNA Polymorphic Markers at MAO-A and MAO-B Genes; *Mol. Psychiatry*, 2000;5:105–109

[55] Gibbons, A.; Tracking the Evolutionary History of a “Warrior” Gene; *American Association of Physical Anthropologists Meeting; Science*, 2004; 304: 818

[56] MAOB Gene-Genecards, The GeneCards Human Gene Database, <http://www.genecards.org/cgi-bin/carddisp.pl?gene=MAOB>

[57] MAOB Genomic Map-Genatlas, Genatlas Sheet <http://genatlas.medecine.univ-paris5.fr/fiche.php?n=5051>

[58] Grimsby, J., Chen, K., Wang, L. J., Lan, N. C., Shih, J. C.; Human Monoamine Oxidase A and B Genes Exhibit Identical Exon-Intron Organization; *Proc Natl Acad Sci U S A.* 1991 May 1;88(9):3637-41

[59] Costa-Mallen, P., Afsharinejad, Z., Kelada, S. N., Costa, L. G., Franklin, G. M., Swanson, P. D., Longstreth, W. T. Jr., Viernes, H. M., Farin, F. M., Smith-Weller, T., Checkoway, H.; DNA Sequence Analysis of Monoamine Oxidase B Gene Coding and Promoter Regions in Parkinson's Disease Cases and Unrelated Controls; *Mov. Disord.*, 2004 Jan;19(1):76-83

[60] Shih, J. C., Boyang, Wu., Chen, K.; Transcriptional regulation and multiple functions of MAO genes; *Journal Neural Transmission*, 2011, 118: 979-986.

[61] Ou, X. M., Chen, K., Shih, J. C.; Dual Functions of Transcription Factors, Transforming Growth Factor-Beta-Inducible Early Gene (TIEG)2 and Sp3, Are Mediated by CACCC Element and Sp1 Sites of Human Monoamine Oxidase (MAO) B Gene; *J Biol Chem.*, 2004;279(20):21021–21028

[62] MAOB Gene Transcription Factors-QIAGEN, Sample & Assay Technologies, http://www.sabiosciences.com/chipqpcrsearch.php?factor=Over+200+TF&species_id=0&ninfo=n&ngene=n&nfactor=y&gene=MAOB

[63] MAOB-001 Transcript-Ensembl, Ensembl genome browser, http://www.ensembl.org/Homo_sapiens/Transcript/ProteinSummary?g=ENSG0000069535;r=X:43625858-43741693;t=ENST00000378069

[64] Ren, Y., Jiang, H., Ma, O., Nakaso, K., Feng, J.; Parkin Degrades Estrogen-Related Receptors to Limit the Expression of Monoamine Oxidase; *Hum Mol Genet.*, 2011 Mar 15; 20(6): 1074-1083

[65] Wu, H. F., Chen, K., Shih, J. C.; Site-directed Mutagenesis of Monoamine Oxidase A and B: Role of Cysteines; *Mol. Pharmacol.*, 1993, 43:888-893

[66] Cesura, A. M., Gottowik, J., Lahm, H. W., Lang, G., Imhof, R., Malherbe, P., Roethlisberger, U., Da Prada, M.; Investigation on the Structure of the Active Site of Monoamine Oxidase-B by Affinity Labeling with the Selective Inhibitor Lazabemide and by Site-directed Mutagenesis; *Eur. J. Biochem.*, 1996, 236:996-1002

[67] Zellner, M., Baureder, M., Rappold, E., Bugert, P., Kotzailias, N., Babeluk, R., Baumgartner, R., Attems, J., Gerner, C., Jellinger, K., Roth, E., Oehler, R., Umlauf, E.; Comparative Platelet Proteome Analysis Reveals an Increase of Monoamine Oxidase-B Protein Expression in Alzheimer's Disease but not in Non-demented Parkinson's Disease Patients; *J Proteomics*. 2012 ;75(7):2080-92

[68] Jakubauskiene, E., Janaviciute, V., Peciuliene, I., Söderkvist, P., Kanopka, A.; G/A Polymorphism in Intronic Sequence Affects the Processing of MAO-B Gene in Patients with Parkinson Disease; FEBS Lett., 2013 Jan 31;587(3):302-3.

[69] Sources of Coumarin, <http://www.fragrantica.com/notes/Coumarin-259.html>

[70] Patil, P. O., Bari, S. B., Firke, S. D., Deshmunk P. K., Donda S. T., Patil, D. A.; A Comprehensive Review on Synthesis and Designing Aspects of Coumarin Derivatives as Monoamine Oxidase Inhibitors for Depression and Alzheimer's Disease; Bioorg Med Chem 2013 May 1;21 (9): 2434-2450

[71] Iranshahi, M., Askari, M., Sahebkar, A., Hadjipavlou-Litina, D.; Evaluation of Antioxidant, Anti-inflammatory and Lipoxxygenase Inhibitory Activities of the Prenylated Coumarin Umbelliprenin; DARU, 2009, 17(2):99–103.

[72] Farook, M., Ashish, P., Nida, K.; A Review on Design, Synthesis and Pharmacological Effect of Novel Coumarins Derivatives; Journal of Medical Pharmaceutical and Allied Sciences, 2013, 04:43-59

[73] Synthesis of Coumarin, <http://koti.kapsi.fi/kaviaari/homechemistry/coumarin/>

[74] Sahoo, S. S., Shukla, S., Nandy, S., Sahoo, H. B.; Synthesis of Novel Coumarin Derivatives and Its Biological Evaluations; European Journal of Experimental Biology, 2012, 2 (4):899-908

[75] Čačić, M., Pavić, V., Molnar, M., Šarkanj, B., Has-Schön, E.; Design and Synthesis of Some New 1,3,4-Thiadiazines with Coumarin Moieties and Their Antioxidative and Antifungal Activity; Molecules (Impact Factor, 2.43) 01/2014;19(1): 1163-1177 DOI: 10.3390/molecules:19011163

[76] Alipour, M., Khoobi, M., Emami, S., Fallah-Benakohal, S., Ghasemi-Niri, S. F., Abdollahi, M., Foroumadi, A., Shafiee, A.; Antinociceptive Properties of New Coumarin Derivatives Bearing Substituted 3,4-dihydro-2H-benzothiazines; Daru- Journal of Faculty of Pharmacy (Impact Factor 0.62), 01/2014; 22(1):9. DOI: 10.1186/2008-2231-22-9

[77] Darla, M. M., Krishna, B. S., Rao, K. U., Reddy, N. B., Srivash, M. K., Adeppa, K.; Synthesis and Bio-Evaluation of Novel 7-Hydroxy Coumarin Derivatives via Knoevenagel Reaction; Res Chem Intermed; 2013, DOI 10.1007/s11164-013-1258-1

- [78] Abraham, K., Wöhrlin, F., Lindther, O., Heinemeyer, G., Lampen, A.; Toxicology and Risk Assessment of Coumarin: Focus on Human Data; *Molecular Nutrition & Food Research* 2010 Feb; 54 (2): 228-239
- [79] Liu, R., Sun, Q., Sun, A., Cui, J.; Isolation and Purification of Coumarin Compounds from Cortex Fraxinus by High-Speed Counter-Current Chromatography; *Journal of Chromatography. A*, 2005, 1072(2):195-199
- [80] Potdar, M. K., Mohile, S. S., Salunkhe, M. M.; Coumarin Synthesis via Pechmann Condensation in Lewis Acidic Chloroaluminate Ionic Liquid; *Tetrahedron Lett.*, 2001, 42, 9285-9287.
- [81] Ferguson, J., Zeng, F., Alper, H.; Synthesis of Coumarins via Pd-catalyzed Oxidative Cyclocarbonylation of 2-vinylphenols; *Org. Lett.*; 2012,14, 5602-5605
- [82] Lacy, A., O’Kennedy, R.; Studies on Coumarins and Coumarin-Related Compounds to Determine their Therapeutic Role in the Treatment of Cancer; *Current Pharmaceutical Design*, 2004,10:3797-3811
- [83] Carotti, A., Altomare, C., Catto, M., Gnerre, C., Summo, L., De Marco, A., Rose, S., Jenner, P., Testa, B.; Lipophilicity Plays a Major Role in Modulating the Inhibition of Monoamine Oxidase B by 7-substituted Coumarins; *Chemistry & Biodiversity*, 2006 Feb;3(2):134-49.
- [84] Kumar, A., Jain, S., Parle, M., Jain, N., Kumar, P.; 3-Aryl-1-Phenyl-1H-Pyrazole Derivatives as New Multitarget Directed Ligands for the Treatment of Alzheimer’s Disease, with Acetylcholinesterase and Monoamine Oxidase Inhibitory Properties; *EXCLI Journal*, 2013;12:1030-1042
- [85] Binda, C., Wang, J., Pisani, L., Caccia, C., Carotti, A., Salvati, P., Edmonson, D. E., Mattevi, A.; Structures of Human Monoamine Oxidase B Complexes with Selective Noncovalent Inhibitors: Safinamide and Coumarin Analogs; *J. Med. Chem.*, 2007, 50, 5848-5852
- [86] Gacche, R. N., Jadhav, S. G.; Antioxidant Activities and Cytotoxicity of Selected Coumarin Derivatives: Preliminary Results of a Structure Activity Relationship Study Using Computational Tools; *Journal of Experimental and Clinical Medicine*, 2012;4(3):165-169

[87] Kawase, M., Sakagami, H., Hashimoto, K., Tani, S., Hauer, H., Chatterjee, S.S.; Structure Cytotoxic Activity Relationships of Simple Hydroxylated Coumarins; *Anticancer Res.*, 2003;23:3243-3246.

[88] Thornes, D., Daly, L., Lynch, G., Browne, H., Tanner, A., Keane, F., O'Loughlin, S., Corrigan, T., Daly, P., Edwards, G.; Prevention of Early Recurrence of High-Risk Malignant Melanoma by Coumarin. Irish Melanoma Group. *Eur J Surg Oncol.* 1989;15 (5):431-435

[89] Jain, P. K., Joshi, H.; Coumarin: Chemical and Pharmacological Profile; *Journal of Applied Pharmaceutical Science* 02 (06); 2012: 236-240

[90] Paramjeet, M. K., Dipak, S., Arti, D.; Comparative Study of Microwave and Conventional Synthesis and Pharmacological Activity of Coumarins : A Review; *Journal of Chemical and Pharmaceutical Research*, 2012, 4(1):822-850

[91] Soman, S. S., Soni, J. N., Inamdar, G. S., Robertson, G. P.; Synthesis and Anticancer Activity of 4-hydroxy Naphtho Coumarin Derivatives and Naphtho Coumestans; *Der Pharma Chemica*, 2013, 5(6):201-207

[92] Matos, M. J., Viña, D., Quezada, E., Picciau, C., Delogu, G., Orallo, F., Santana, L., Uriarte, E.; A New Series of 3-phenylcoumarins as potent and Selective MAO-B Inhibitors; *Bioorganic Medicinal Chemistry Letters*, 2009, 19:3268-3270

[93] Fraaije, M. W., Mattevi, A.; Flavoenzymes: Diverse Catalysis with Recurrent Feature; *TIBS* 25- March 2000; 126-132

[94] Molecular modeling-Wikipedia, the free encyclopedia,
http://en.wikipedia.org/wiki/Molecular_modelling

[95] Ramachandran, K. I., Deepa, G., Krishnan Namboori, K.; P.K. *Computational Chemistry and Molecular Modeling Principles and Applications* 2008

[96] Science-AutoDock, <http://autodock.scripps.edu/resources/science>

[97] Equations-AutoDock, <http://autodock.scripps.edu/resources/science/equations/>

[98] Ural, G.; Blind Docking Simulations of Benzothiazoles on Triosephosphate Isomerase, Master Thesis, Boğaziçi University, 2011

Curriculum Vitae

Dilara Karaman was born in Istanbul, 1987. She started her education in Nişantaşı Nilüfer Hatun primary school. She completed first education in Yeşil Bahar primary school in Göztepe, 1999. She graduated from 75. Yıl Cumhuriyet high school in Antalya, 2005. She was student of Prof. Dr. Metin Aktaş in Gazi University Biology Department. In Gazi University she achieved two searching project, one of them is “Multiple Sclerosis” with Asst. Prof. Dr. Levent Bingöl, another searching project is “Microorganisms Existent in Space and can Live in Extreme Conditions” with Prof. Dr. Güven Uraz. She graduated as Honorary Student from Gazi University in Ankara, 2009. She was accepted to Computational Biology and Bioinformatics Graduate Program in Kadir Has University in 2012.